

BEN-GURION UNIVERSITY OF THE NEGEV
THE FACULTY OF NATURAL SCIENCES
DEPARTMENT OF GEOLOGICAL AND ENVIRONMENTAL
SCIENCES

**Study of the early stage immature oil
produced from the Israeli oil shale**

THESIS SUBMITTED IN PARTIAL FULFILLMENT OF THE REQUIREMENTS
FOR THE MASTER OF SCIENCES DEGREE

By Ilya Kutuzov

<September, 2017>

BEN-GURION UNIVERSITY OF THE NEGEV
THE FACULTY OF NATURAL SCIENCES
DEPARTMENT OF GEOLOGICAL AND ENVIRONMENTAL
SCIENCES

THESIS SUBMITTED IN PARTIAL FULFILLMENT OF THE REQUIREMENTS
FOR THE MASTER OF SCIENCES DEGREE

**Study of the early stage immature oil
produced from the Israeli oil shale**

By Ilya Kutuzov

UNDER THE SUPERVISION OF:

Dr. Alexey Kamyshny

Prof. Harold Vinegar

Dr. Alon Amrani

Signature of student:  _____ Date: 6/9/2017

Signature of supervisor:  _____ Date: 03.09.2017

Signature of supervisor:  _____ Date: 03/09/2017

Signature of supervisor:  _____ Date: 6/9/2017

Signature of chairperson
Of the committee for graduate studies:  _____ Date: 28.08.2017

Abstract

This project was dedicated to study the properties of the oil produced from the Israeli oil shale of Ghareb formation. Oil shale samples from two boreholes in the Shfela basin were used for semi-open pyrolysis experiments where the oil was collected and analyzed. In addition 5 hydrocarbon samples from the Dead Sea basin that occurred from the Ghareb oil shale were analyzed.

Pyrolysis oils were analyzed for their viscosity, density, sulfur content, alkyl-thiophene content, benzothiophenes content and *n*-alkanes content. Residual post-pyrolysis rocks were analyzed by RockEval pyrolysis, LECO elemental analyzer for total sulfur and bitumen was extracted from the rocks by Soxhlet. Naturally occurring hydrocarbons and extracted bitumen were analyzed for sulfur content, fractionated into their main groups and their aromatic and saturate fraction were analyzed on GC-MS for alkyl-thiophene content, benzothiophenes content, dibenzothiophenes content, *n*-alkanes content and biomarkers.

Pyrolysis oils were found to have exceptionally high sulfur content (up to 19% wt.) in the low maturity samples. No distinctive relation was found between the oils viscosities to their alkyl-thiophenes content. Good correlation was observed between the oil densities to their *n*-alkanes content. A comparison between naturally occurring hydrocarbon that originated from the Ghareb formation to those produced in the laboratory by pyrolysis showed some resemblance mainly in the physical properties of the oils. Comparison of the biomarker ratios of the two groups of hydrocarbons revealed a large scatter of the results over various levels of thermal maturity and environments of deposition. These observations suggest that the difference of heating gradient between the laboratory and the field might be responsible for the difference observed.

A correlation of EASY%R_O to Rock-eval T_{max} was created in order to compare pyrolysis experiments to other studies. Study of the thermal maturities during the pyrolysis experiments clearly showed an early maturation of the organic matter as was suggested by previous studies.

Acknowledgements

I would like to first thank my advisors for allowing me to shape the course of work as I wanted and especially Dr. Alon Amrani for granting me unrestricted access to his laboratories at the Hebrew University.

I thank my fellow labmates at the Hebrew University of Jerusalem: Lubna Shawar, Alexander Meshulam, Guy Dror and Ward Said-Ahamed for extensive analytical help on the GC's at the lab and useful conversations.

I thank Prof. Shimon Feinstein, Dr. Yevgeni Vapnik and Rafi Shpigel from the department at the Ben Gurion University for the fruitful conversations and help on related side projects that found their way into this work.

Special thanks go to Prof. Jiwchar Ganor and Dr. Chen Gruber for introducing me to practical geochemistry and research in first place.

Dr. Yoav Rosenberg, Ms. Edna Danon and Mr. Leonardo Freitas from Israel Energy Initiatives Ltd. are thanked for providing me with samples from the company's Shfela project and for extensive support at the laboratory in the Ben Gurion University.

Special thanks go to Rami Kremien and Eli Lifshitz of ZERAH Oil & Gas Explorations for providing me oil sample from the Emunah-1 well and for providing additional data about the production on site.

I would also like to thank Mor Matzliach (TAU) and Noam Schmerler (Kinneret College) for assisting me in the field during collection of asphalt samples.

This study was supported by the Ministry of National Infrastructures, Energy and Water Resources as part of the scholarship program for B.Sc. to PhD students in the field of energy resources.

Table of Contents

| | |
|--|-----|
| Abstract..... | I |
| Acknowledgements..... | III |
| 1. Introduction..... | 1 |
| 1.1. The Israeli oil shale | 1 |
| 1.2. Thermal maturation of type IIS kerogen | 2 |
| 1.3. Associated hydrocarbon shows/observations..... | 3 |
| 1.4. The Shfela basin..... | 4 |
| 2. Research objectives and goals | 6 |
| 3. Experimental..... | 7 |
| 3.1. Samples description..... | 7 |
| 3.1.1. Rock samples | 7 |
| 3.1.2. Hydrocarbon samples..... | 7 |
| 3.2. Methods..... | 9 |
| 3.2.1. Anhydrous Pyrolysis..... | 11 |
| 3.2.2. Bitumen extraction..... | 14 |
| 3.2.3. SARA fractionation | 14 |
| 3.2.4. Gas Chromatography/Mass spectrometry (GC/MS)..... | 15 |
| 3.2.5. Quantification of molecular groups of interest | 15 |
| 3.2.6. Rock-Eval pyrolysis..... | 16 |
| 3.2.7. Sulfur content of rock and hydrocarbon samples | 19 |
| 3.2.8. Oil viscosity | 19 |
| 3.2.9. Oil density and API gravity | 19 |
| 3.2.10. Thermal maturation and environment of deposition estimation from molecular markers..... | 20 |

| | |
|--|----|
| 3.2.11. Thermal maturation modelling | 24 |
| 4. Results..... | 25 |
| 4.1 Characterization of the source rock..... | 25 |
| 4.2 Aderet experiments | 25 |
| 4.2.1. Physical properties of produced oil..... | 26 |
| 4.2.1.1. Density of oil..... | 26 |
| 4.2.1.2. Viscosity of oil..... | 27 |
| 4.2.2. Chemistry of produced oil | 28 |
| 4.2.2.1. Alkyl-thiophenes content..... | 28 |
| 4.2.2.2. Benzothiophenes content | 29 |
| 4.2.2.3. Normal alkanes content..... | 30 |
| 4.2.2.4. Sulfur content..... | 31 |
| 4.2.3. Spent rock properties | 32 |
| 4.3 Zoharim experiments..... | 33 |
| 4.3.1. Chemistry of produced bitumen and oil..... | 34 |
| 4.3.1.1. SARA..... | 34 |
| 4.3.1.2. Sulfur content of bitumen and oil | 35 |
| 4.3.1.3. Thiophenes and benzothiophenes in oil and bitumen | 37 |
| 4.3.1.4. <i>n</i> -alkanes in oil and bitumen | 39 |
| 4.3.1.5. Aromatic thiophenes in the bitumen | 41 |
| 4.3.1.6. Molecular markers in bitumen and oil | 45 |
| 4.3.2. Geochemical properties of residual rocks..... | 48 |
| 4.4 Naturally-occurring hydrocarbons | 49 |
| 5. Discussion..... | 51 |
| 5.1. Physical properties of pyrolysis oils..... | 51 |

| | |
|--|----|
| 5.1.1. Factors affecting oil density..... | 51 |
| 5.1.2. Pyrolysis oils viscosity..... | 56 |
| 5.2. Evolution of sulfur species..... | 59 |
| 5.2.1. In oil..... | 59 |
| 5.2.2. In bitumen..... | 60 |
| 5.3. Maturation of the organic matter..... | 61 |
| 5.3.1. Correlation of T_{max} to Easy $R_O\%$ | 61 |
| 5.3.2. Early maturation of the organic matter..... | 63 |
| 5.3.3. Molecular maturity and environment of deposition parameters..... | 64 |
| 6. Conclusions..... | 72 |
| 7. References..... | 74 |
| 8. Appendix..... | 81 |
| Appendix I- Well sections for Aderet and Zoharim boreholes..... | 81 |
| Appendix II- Pseudo-Van-Krevelen plot..... | 84 |
| Appendix III- Selected GC-MS chromatograms..... | 85 |
| Appendix IV- Density and Sulfur content of Dead Sea basin and Coastal Plain oils .. | 90 |
| Appendix V- Density results for Aderet oils..... | 91 |
| Appendix VI- Spreadsheet version of the EASY% R_O model (After Sweeney and Burnham, 1990)..... | 92 |
| תקציר..... | I |

List of figures

| | |
|---|----|
| Figure 1. Map of the Shfela basin | 5 |
| Figure 2. Sampling location map | 8 |
| Figure 3. Analytical procedures flowchart..... | 10 |
| Figure 4. Schematic plot of a pyrolysis experiment heating program | 12 |
| Figure 5. Dismantled pyrolysis reactor used in the experiments, main parts are marked. | 13 |
| Figure 6. GC-MS chromatograms showing the peaks of interest for estimation of thermal maturity and environment of deposition | 22 |
| Figure 7. The change in Aderet oil production (ml) as a function of thermal maturation (%Ro equ.) at different heating gradients (4°C/day and 120°C/day). | 26 |
| Figure 8. The change in Aderet oil density (°API) as a function of thermal maturation (%Ro equ.) at different heating gradients (4°C/day and 120°C/day) | 27 |
| Figure 9. The change in Aderet oil kinematic viscosity (cSt) as a function of thermal maturation (%Ro equ.) at different heating gradients (4°C/day and 120°C/day)..... | 28 |
| Figure 10. The change in alkyl-thiophenes content in the Aderet oils (mg/g oil) as a function of thermal maturation (%Ro equ.) at different heating gradients (4°C/day and 120°C/day) | 29 |
| Figure 11. The change in benzothiophenes content in the Aderet oils (mg/g oil) as a function of thermal maturation (%Ro equ.) at different heating gradients (4°C/day and 120°C/day)..... | 30 |
| Figure 12. The change in <i>n</i> -Alkanes content in the Aderet oils (mg/g oil) as a function of thermal maturation (%Ro equ.) at different heating gradients (4°C/day and 120°C/day).31 | |
| Figure 13. The change in sulfur content in the Aderet oils (Wt. %) as a function of thermal maturation (%Ro equ.) at different heating gradients (4°C/day and 120°C/day).32 | |
| Figure 14. Oil production (ml) of Zoharim Ex42 and bitumen content (mg) of the Zoharim rock samples with respect to thermal maturation (%Ro equ.) | 34 |
| Figure 15. Results of SARA fractionation of Zoharim bitumen samples for various degrees of thermal maturation. | 35 |
| Figure 16. Sulfur content (Wt. %) of oil and bitumen from the Zoharim experiments as a function of thermal maturity (%Ro equ.)..... | 37 |

| | |
|--|----|
| Figure 17. Sulfur content (Wt. %) of the Zoharim bitumen and its asphaltene and maltene fractions as a function of thermal maturity (%Ro equ.)..... | 37 |
| Figure 18. The change of thiophenes and benzothiophenes content in the Zoharim bitumen (mg/g bitumen) as a function of thermal maturation (%Ro equ.)..... | 38 |
| Figure 19. The change of thiophenes and benzothiophenes content in the Zoharim oil (mg/g oil) as a function of thermal maturation (%Ro equ.)..... | 39 |
| Figure 20. The change of <i>n</i> -alkanes content in the Zoharim oil and bitumen (mg/g hydrocarbon) as a function of thermal maturation (%Ro equ.) | 40 |
| Figure 21. The change of benzothiophene and alkyl-benzothiophene groups concentration in the Zoharim bitumens (mg/g bitumen) as a function of thermal maturation (%Ro equ.) | 43 |
| Figure 22. The change of dibenzothiophene and alkyl-dibenzothiophene groups concentration in the Zoharim bitumens (mg/g bitumen) as a function of thermal maturation (%Ro equ.)..... | 44 |
| Figure 23. Results of SARA fractionation for the naturally- occurring hydrocarbons from the Dead Sea basin analyzed in this study. | 50 |
| Figure 24. The change of <i>n</i> -alkanes content (mg/g oil) against °API gravity for the Aderet experiment at different heating gradients (4°C/day and 120°C/day)..... | 52 |
| Figure 25. The relation of sulfur (wt. %) to °API gravity of oils used in this study..... | 55 |
| Figure 26. The change of alkyl-thiophenes content (mg/g oil) against kinematic viscosity (cSt) for the Aderet experiment at different heating gradients (4°C/day and 120°C/day) | 57 |
| Figure 27. The relation of kinematic viscosity (cSt) (Logarithmic scale) to API gravity (°) of oils | 58 |
| Figure 28. Correlation between the modeled %EasyR _O to measured T _{max} (°C) for the type IIS kerogen. Gradient labels refer to the two Aderet experiments | 62 |
| Figure 29. The relation of DBT/PHE ratio to Pr/Ph ratio for hydrocarbon samples that have originated from the Ghareb source rock..... | 65 |
| Figure 30. The relation of sulfur content (wt. %) to DBT/PHE ratio for hydrocarbon samples that have originated from the Ghareb source rock | 66 |
| Figure 31. The relation of BT's/DBT's ratio as a function of thermal maturation (%Ro equ.) for the Zoharim experiments bitumens..... | 67 |

Figure 32. The relation of %Ro equ. to MDR of the hydrocarbons produced in the pyrolysis experiments of Aderet Ex35 and Zoharim. 69

Figure 33. The relation of T_{max} (°C) to MDR of various hydrocarbons. 71

Figure 34. Chromatogram of the n-alkanes (m/z=57.10) in the unheated sample (%Ro equ. = 0.32) 85

Figure 35. Chromatogram of the n-alkanes (m/z=57.10) in the Ex41 bitumen (%Ro equ. = 0.64) 85

Figure 36. Chromatogram of the n-alkanes (m/z=57.10) in the Ex41 oil (%Ro equ. = 0.64) 86

Figure 37. Chromatogram of the n-alkanes (m/z=57.10) in the Ex43 bitumen (%Ro equ. = 0.78) 86

Figure 38. Chromatogram of the n-alkanes (m/z=57.10) in the Ex43 oil (%Ro equ. = 0.78) 87

Figure 39. Chromatogram of the n-alkanes (m/z=57.10) in the Ex47 bitumen (%Ro equ. = 1.07) 87

Figure 40. Chromatogram of the n-alkanes (m/z=57.10) in the Ex47 oil (%Ro equ. = 1.07) 88

Figure 41. Chromatogram of the n-alkanes (m/z=57.10) in the Ex42 bitumen (%Ro equ. = 1.57) 88

Figure 42. Chromatogram of the n-alkanes (m/z=57.10) in the Ex42 oil (%Ro equ. = 1.57) 89

List of tables

Table I-Heating gradient and peak temperature for the different pyrolysis experiments. 12

Table II- Quantification parameters used for the selected compound groups. 16

Table III- Heating program used on the Rock-Eval 6..... 17

Table IV- Compounds of interest identified from the m/z chromatograms..... 23

Table V - Calculated parameters for maturity and environment of deposition assesment. 23

| | |
|--|----|
| Table VI- Results of Rock-Eval pyrolysis and LECO analysis for the Aderet and Zoharim rocks..... | 25 |
| Table VII- Results of Rock-Eval pyrolysis and LECO analysis for spent rock from the Aderet experiments. | 32 |
| Table VIII- Results of Soxhlet extraction of bitumen for the rock samples from Zoharim experiments. | 33 |
| Table IX- Parameters (1-13) calculated from the GC-MS chromatogram peaks of the Zoharim experiment and naturally- occurring hydrocarbons analyzed in this study..... | 47 |
| Table X- Results of Rock-Eval pyrolysis and LECO analysis for the Zoharim experiments spent rock. | 48 |

1. Introduction

1.1. The Israeli oil shale

The Upper Cretaceous sedimentary strata in Israel, Jordan and Lebanon contain a distinctive sequence of organic-rich formations (Luning & Kuss, 2014; Bou Daher et al., 2015). In Israel that sequence belongs to the Mount Scopus group sediments. Within the group, the highest organic content and hydrocarbon production potential are attributed to the Mishash and Ghareb formations (Campanian- Maastrichtian respectively), which are commonly termed the “Israeli oil shale” or “Oil shale unit” (Minster, 2009).

These formations were deposited during the Upper Cretaceous in a series of local synclinal basins which formed as a result of Turonian-Coniacian folding (The Syrian Arc structures). The oil shale deposition is directly related to a local upwelling system which led to a high primary productivity in the upper part of the water column, high rates of sedimentation and anoxic-dysoxic conditions on the basin bottoms (Schneider-Mor, et al., 2012; Meilijson, et al., 2014). This geological setting led to development of reducing conditions at the basin bottoms (Tannenbaum and Aizenshtat, 1985) which resulted in the accumulation and preservation of the organic matter in the sediment (Winter, 1988).

The organic matter in sedimentary rocks can be divided into two main components: Kerogen, which is the particulate organic matter that is insoluble both in water and organic solvents. Bitumen is defined as the organic phase within the sedimentary rock that is soluble in organic solvents (Peters et al., 2005).

There are approximately 30 known deposits of oil shale in Israel which spread from the south- east of the Negev desert to the Golan Heights. Two of the deposits were used for energy production: the Nebi-Musa deposit which was used in ancient times (Minster, 2009) and the Rotem deposit which is being mined for combustion in a local power plant since 1988 (Yoffe et al., 2007). Oil shale deposits are known to occur in neighboring countries as well: In Jordan at least 30 small basins are known with the largest being El-Lajjun (Abed, et al. 2005) and in Lebanon an asphalt-bearing oil shale deposit is known at Hasbayya (Bou Daher et al., 2015).

Petrographically the oil shale consists of an organic component of marine source with negligible terrestrial contribution (Spiro et al., 1983a; Meilijson, et al., 2014) and an

inorganic component which is mainly chalk to marly-chalk with appearances of chert, phosphorite and limestone (Minster, 2009). Several previous works (Heller-Kallai et al., 1984; Minster et al., 1992; Koopmans et al., 1998 (a); Koopmans et al., 1998 (b); Lewan and Henry, 1999; Amrani et al., 2005) noted the high sulfur content ($S/C \geq 0.04$) in the organic matter of the Ghareb and Mishash formations. These observations classify the organic matter within the oil shale as type II-S kerogen (Orr, 1986).

1.2. Thermal maturation of type IIS kerogen

When oil shale is subjected to suitable temperature in an oxygen depleted environment for a sufficient period of time, it can evolve to become a mature source rock and eventually produce hydrocarbons upon pyrolysis (Tissot and Welte, 1984). In general, during thermal maturation, kerogen which is trapped within the mineral matrix of the source rock undergoes thermal cracking of chemical bonds within its structure due to elevated temperature upon burial or artificial heating. During the initial stage of heating the hydrocarbon fraction generated from the kerogen is trapped within the source rock. This fraction is named “bitumen”. During further thermal cracking of the kerogen additional generation of bitumen occurs and the bitumen itself undergoes thermal cracking to smaller molecular compounds which under the right conditions can be expelled from the source rock. The expelled hydrocarbon fraction type (gas or oil) and properties depends on the type of kerogen in the oil shale (Peters et al., 2005).

Early oil generation from a type II-S kerogen was noted in several studies (Orr., 1986; Baskin and Peters., 1992; Burnham et al., 1992) and is attributed to cleavage of carbon-sulfur and other sulfur bonds which occurs at lower levels of thermal maturation compared to bonds with higher bond energy such as carbon-carbon bonds.

The initially released oil is sulfur rich due to preferential breaking of relatively weak carbon- sulfur bonds which in turn releases high amounts of asphaltenes, resins and aromatics that makes the initial oil dense, viscous and rich in sulfur (Orr, 1986; Baskin and Peters, 1992). An additional outcome of cleavage of relatively weak carbon-sulfur bonds is the high concentration of alkyl thiophenes in the early oils as was observed during CP-Py-GC-MS of Maastrichtian age oil shale from Lebanon (Bou Daher et al., 2015). Several studies (Waldo et al., 1990; Eglinton et al., 1990; Tomić et al., 1995)

showed a decrease in the alkyl thiophenes content during maturation of the kerogen which is followed by a decrease of benzothiophenes and dibenzothiophenes at higher levels of maturation. The mechanism responsible for this decrease is related to the thermal instability of these sulfur compounds. The variation of sulfur species concentration during thermal maturation is sometimes used for evaluating the maturity level of oils and bitumens (Orr, 1986; Radke and Willsch., 1994 Santamaria et al., 1998; Huang and Pearson., 1999). Alkyl thiophenes might play an important role in defining the viscosity of the early produced oils as they might act as solvents for the high viscosity groups in the oil and decrease the viscosity of those oils.

As the maturation progresses, alkyl thiophenes decompose, the amount of asphaltenes in the oil decreases while the aromatics, resins and saturates fraction increase. This change of composition leads to a decrease in oil density, viscosity and sulfur content (Baskin and Peters, 1992; Baskin and Jones, 1993).

1.3. Associated hydrocarbon shows/observations

All known oil shale deposits in Israel are not thermally mature enough to act as a source rock for hydrocarbons. Nonetheless, it has been suggested by many studies (Tannenbaum 1983; Spiro et al., 1983b; Tannenbaum and Aizenshtat, 1984; Tannenbaum and Aizenshtat, 1985; Rullkötter et al., 1985; Abed et al., 2005, Gardosh and Tannenbaum, 2014) that during the Miocene a deposit of Ghareb and Mishash oil shale has been buried in the Dead Sea graben to depths of up to 8 km and was covered by sediments. The burial led to the thermal maturation of the oil shale and expulsion of hydrocarbons which are found at multiple shows around the Dead Sea basin:

- a. Thermogenic gas at Zohar, Kidod and Ha-Kanaim fields.
- b. Light-medium-heavy oils on the west coast of the Dead Sea at the following wells: Zuk-Tamrur 1 and 3, Lot-1, Kidod-3, Massada-1, Gurim-3 and Emunah-1 (Nissenbaum and Goldberg, 1980)
- c. Appearance of asphalts on both coasts of the Dead Sea: Western shore- Amiaz borehole, Tamar borehole, Massada seep, Nahal Heimar seep, Wadi Tamar and eastern shore- Wadi Isal seep and Ain Hummar ozokerite seep (Nissenbaum and Aizenshtat, 1975; Beydoun et al., 1994)).

In addition, the Ghareb formation oil shale is suggested to be the source rock for heavy oil in the Ein Said-1 well in the south of the Golan Heights where Miocene-Pleistocene volcanic activity has aided local thermal maturation of the oil shale (Tannenbaum and Aizenshtat, 1984).

In Lebanon the oil shale was found to be the source of the Hasbayya asphalt (Connan and Nissenbaum, 2004).

1.4. The Shfela basin

The current study focuses on the Shfela deposit which covers an area of approximately 1400km² from Modi'in in the north to the Beer Sheva area in the south (Figure 1). It is considered to be the largest oil shale deposit in Israel (Minster, 2009) and one of the largest oil shale basins in the Levant (Meilijson et al., 2014). The basin has the structure of an asymmetrical syncline- the eastern flank dips steeply westwards (up to 45°), the western and central parts are nearly horizontal (Burg and Gersman, 2016). The deposition of the oil shale unit in the basin occurred in coincidence with its formation (Syn-tectonic deposition), as a result the oil shale unit is thickest in the basin center and thinning towards its eastern flank.

Known oil shale samples from the Shfela basin are characterized by high organic matter (Minster et al., 1992, Minster, 2009), high organic sulfur (Shirav and Ginzburg, 1983) and low vitrinite reflectance of 0.25-0.44% (Meilijson et al., 2014) which make it an immature source rock. Detailed lithology of the oil shale unit in the Shfela basin is described by Burg and Gersman (2016). Macrofauna identified by Meilijson et al. 2014 in the Aderet borehole consisted of inoceramids which occur in low-oxygen environments. Also, the authors concluded that the zones of highest total organic carbon (TOC) content within the Aderet borehole correspond to zones of anoxia in the basin bottom.

During the years 2009-2011 several sites in the Shfela deposit were continuously cored and logged by Israel Energy Initiatives Ltd. (Figure 1). Two of the boreholes are Zoharim and Aderet where the Ghareb and Mishash formations were continuously cored. Over 1,000 m of continuous core were obtained in the Shfela basin. The cores from

Zoharim and Aderet boreholes were used in this study as they were made available by Israel Energy Initiatives Ltd. and carry the thickest section of the oil shale sequence out of all drilled sites in the Shfela basin (Burg et al., 2010; Gersman et al., 2012).

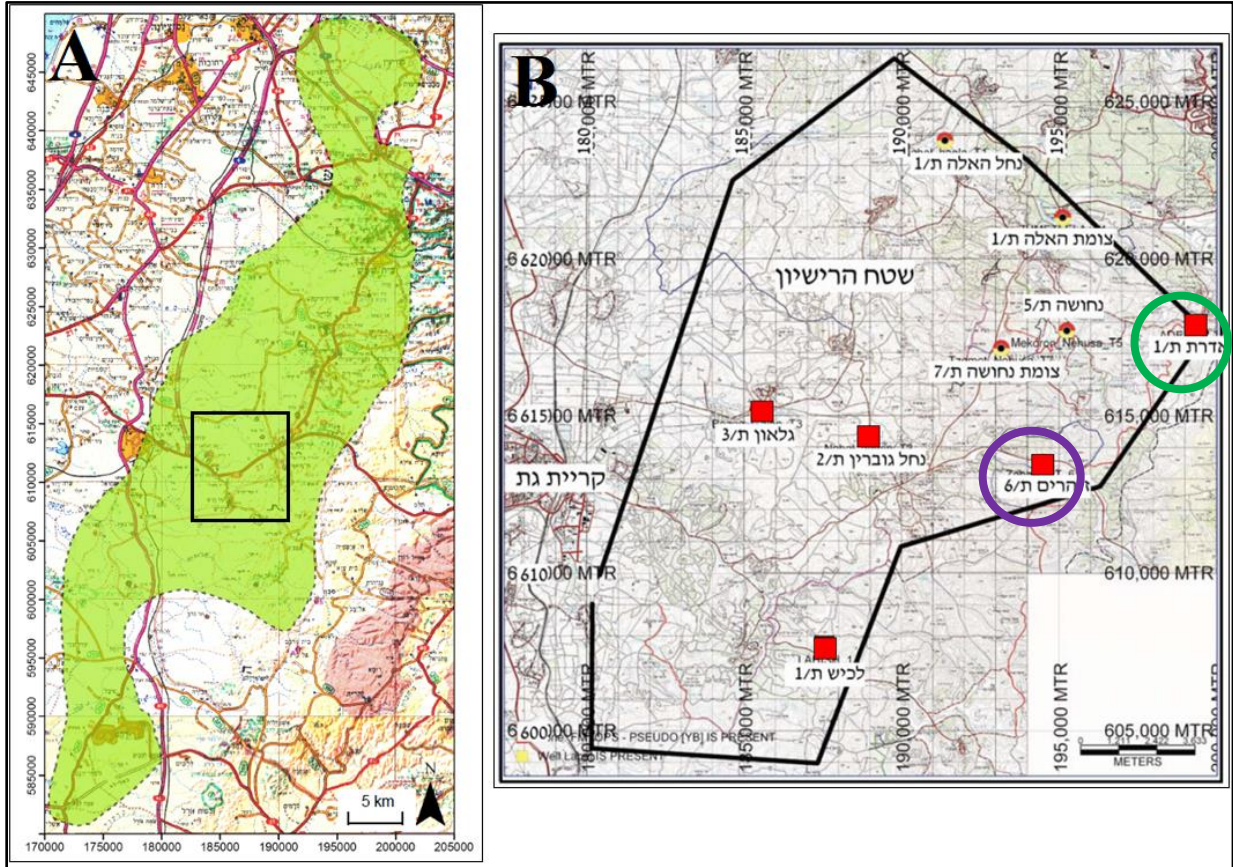


Figure 1. Map of the Shfela basin. **A.** The area of recent drills is marked with a black square (After Minster 2009). **B.** Enlarged map of the drilling area. Zoharim wellbore is marked with a purple circle; Aderet wellbore is marked with green circle. (After Gersman et al., 2012)

2. Research objectives and goals

The goals of this research are:

- a) To establish the relation between alkyl thiophene content and oil viscosity for varying level of maturation in pyrolysis oils distilled from the Israeli oil shale in the Aderet borehole.
- b) To compare the physical and chemical properties of naturally-occurring oils in the Dead Sea area to the Aderet early stage oils from pyrolysis distillation experiments. The main properties to be compared are the viscosity, density and sulfur content of the oils.
- c) To study the evolution and variation of sulfur species in the bitumen and oil produced during pyrolysis distillation experiments on the Israeli oil shale. Evaluate the applicability of aromatic compounds as markers of thermal maturation.
- d) To establish a correlation between modeled thermal maturation index “EasyRo%” (Sweeney and Burnham, 1990) to RockEval “ T_{max} ” parameter (Lafargue et al., 1998; Behar et al., 2001) for the type II-S kerogen in the Israeli oil shale. Compare the correlation to other known Type II-S kerogens.

3. Experimental

3.1. Samples description

3.1.1. Rock samples

The oil shale samples used in this study were cored from the Zoharim and Aderet boreholes in the Shfela basin (NIG 194510/613495, NIG 199263/617971 respectively; Figure 2). Both boreholes penetrated a sequence of Lower Paleogene and Upper Cretaceous sedimentary rocks (Appendix I- Well sections for Aderet and Zoharim boreholes). The oil shale unit is in the Ghareb and Mishash formations from Maastrichtian and Campanian ages respectively (Burg et al., 2010, Gersman et al., 2012).

The Zoharim rock sample is grey to brown, weakly laminated bituminous chalk with fossil fragments. The distribution of formations within the sample for the pyrolysis experiments is $\frac{1}{3}$ Mishash samples and $\frac{2}{3}$ Ghareb samples. This is done to imitate the natural distribution of the two formations within the cored section and achieve a representation of the whole source rock interval.

The Aderet rock sample was taken from the middle of the Ghareb section at approximately 356 m deep. It is petrographically identical to the Zoharim sample.

Homogeneity of the samples was ensured by crushing the sample in ball mill until fine uniform powder was available. The powdered sample was tested for several times on RockEval6 (Lafargue et al., 1998; Behar et al., 2001) to ensure homogeneity.

3.1.2. Hydrocarbon samples

Crude oil samples were received from three producing wells at the Dead Sea area:

- Zuk Tamrur-3 (NIG 231926/564405) which produces medium oil from Triassic reservoirs, exact depth is unknown (Gardosh and Tannenbaum, 2014).
- Emunah-1 (NIG 234997/587588) which produces light oil from the Triassic sandstone of the Gevanim formation at depth of 1700-1720 m (Eli Lifschitz, personal communication).
- Gurim- 4 (NIG 224047/568638) which produced heavy oil from Triassic sandstone reservoirs, exact depth is unknown (Moshe Goldberg, personal communication).

Asphalt samples were collected at two sites in the southern part of the Dead Sea basin:

- Nahal Heimar (NIG 233441/560481) where an active asphalt seep is located. The asphalt fills cracks in the Turonian limestone.
- Nahal Tamar (NIG 229777/544043) where asphalt lenses appear in cross bedded clastic sediments of the Pleistocene Lisan formation. The asphalt lenses contain a significant amount of sand which is bonded to the asphalt.

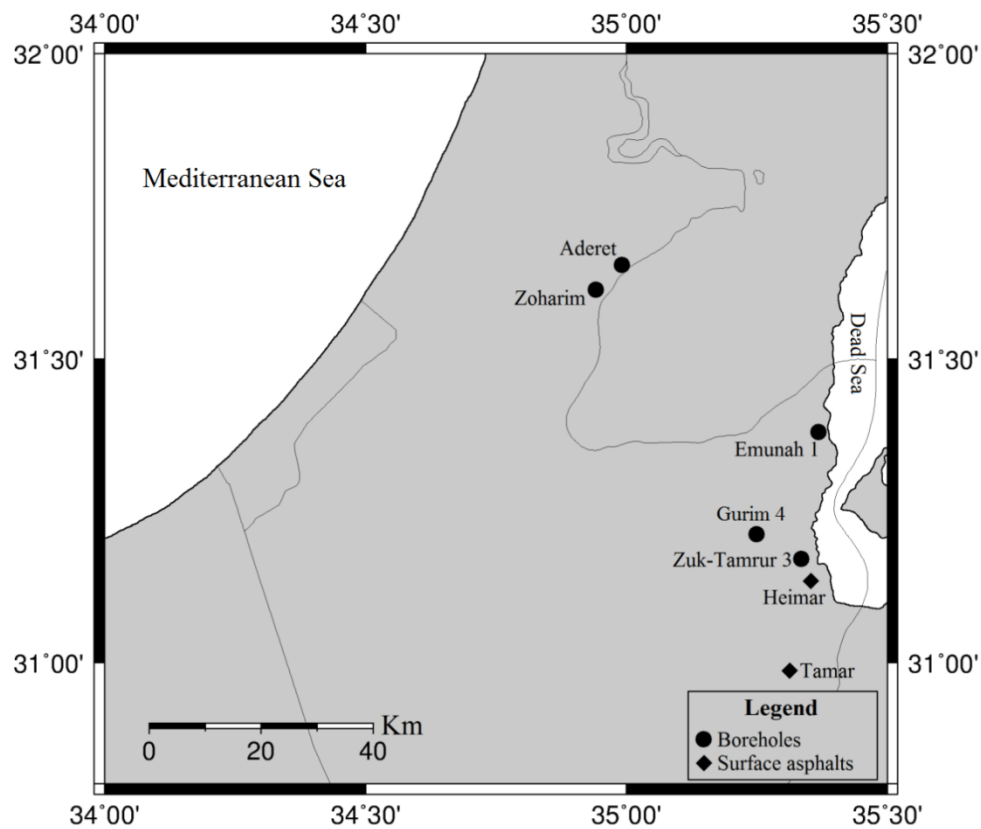


Figure 2. Sampling location map. Boreholes marked as circles. Surface asphalts marked as diamonds.

3.2. Methods

The methods implemented in this study and the order of sample analysis is shown in Figure 3. A detailed description of each method is presented in the section below.

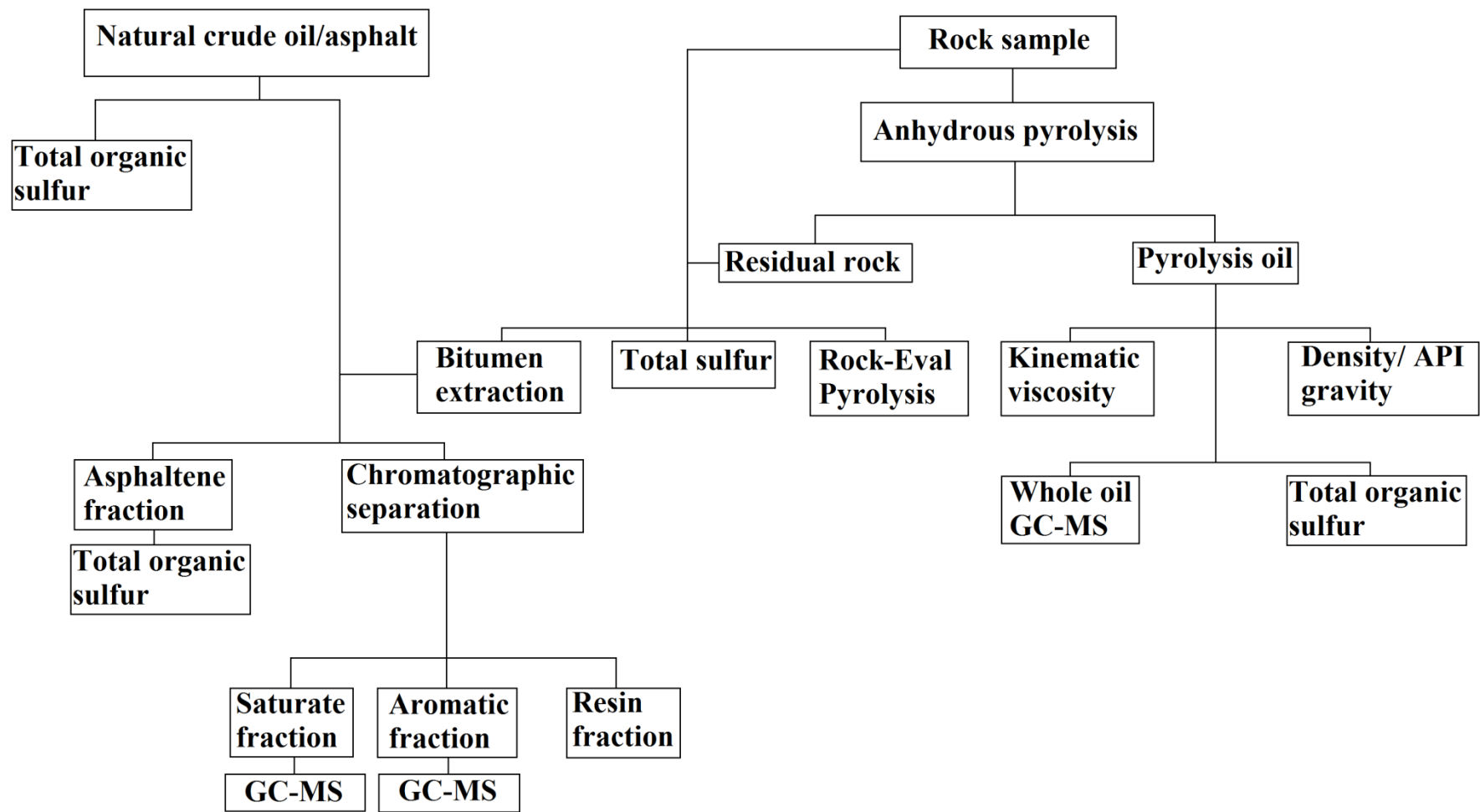


Figure 3. Analytical procedures flowchart.

3.2.1. Anhydrous Pyrolysis

Selected rock samples are ball milled and sieved, 800 g of the 1 mm – 4.75 mm particle size fraction is weighted and loaded into a 1000 ml 316 stainless steel mesh basket. This particle size is chosen for an increased surface area of the rock sample.

The basket is placed inside one of the four PARR pyrolysis reactors which are constructed of 316 stainless steel with volumes of approximately 2000 ml. All parts of the reactor are presented in Figure 5. The pyrolysis reactors are located in Prof. Shimon Feinstein's Geochemistry Laboratory in the Department of Geological and Environmental Studies at Ben-Gurion University. They are similar to those used in Shell's ICP Laboratory at the Bellaire Research Center in Houston (Ryan, 2010).

After loading the sample basket the reactor is sealed and checked for leakage by filling it with nitrogen/Freon mixture and inspecting the surroundings of the reactor with a Freon detector. Following the leakage test the reactor is pressurized with nitrogen to 150 psi and then pressure is released; this is done three times to ensure complete removal of trapped oxygen in the system. Temperature is distributed homogeneously throughout the reactor by three heating elements located in the bottom, middle and top of the reactor.

Pressure within the reactor is kept atmospheric during the whole experiment by a check valve at its upper part. Collection of fluids distilled from the top of the reactor is done by condensing their vapor in a water-cooled condenser (4°C) connected to the reactor. The operation temperature of the condenser guarantees collection of all alkanes from pentane ($n\text{-C}_5$) and higher.

Moisture and pore-water is extracted by gradually increasing the reactor temperature to 200°C and collecting the condensed water. When production of water vapor ceases (within 12-24 hours) the reactor temperature is increased according to the experiment heating program (Table I, Figure 4).

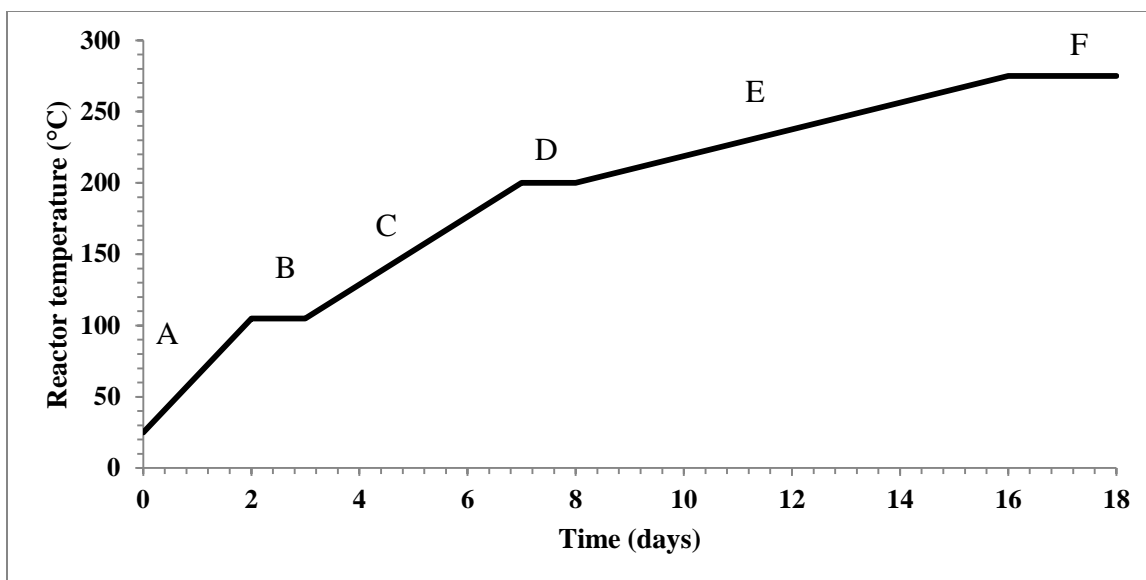


Figure 4. Schematic plot of a pyrolysis experiment heating program. A- Heating to 105°C to release all moisture, B- Hold at 105°C, C- Heating to 200°C to release all pore-water, D- Hold at 200°C, E- Pyrolysis heating ramp, F- Hold at experiment peak temperature.

Table I-Heating gradient and peak temperature for the different pyrolysis experiments

| Experiment name | Heating gradient (°C/day) | Peak temperature (°C) |
|-----------------|---------------------------|-----------------------|
| Aderet Ex15 | 4 | 399 |
| Aderet Ex35 | 120 | 427 |
| Zoharim Ex41 | 2 | 276 |
| Zoharim Ex43 | 2 | 304 |
| Zoharim Ex47 | 2 | 338 |
| Zoharim Ex42 | 2 | 377 |

The amount of distilled oil varies with reactor temperature during the pyrolysis. Sampling is performed when at least 1ml of oil has been condensed in the collector. Graduated glass test tube is connected to the condenser and purged with argon to remove all oxygen. Condenser bottom valve is opened to allow the condensed fluids to flow into the test tube. The temperature of the reactor at the point of sampling is recorded. Collected oil and associated water that is formed during pyrolysis are stored in sealed glass test tubes at room temperature under argon atmosphere until they are analyzed.

Produced gas is released through the check valve into a Ritter drum-type gas meter which records the gas flow rate and allows collection of gas samples. Uncollected gas is passed through a scrubber and released in the fume hood.

After pyrolysis is terminated, the reactor is allowed to cool down to room temperature. The reactor is opened and the sample basket is removed to record the residual rock weight. The residual rock is sampled for analysis at the top, bottom and middle of the reactor.

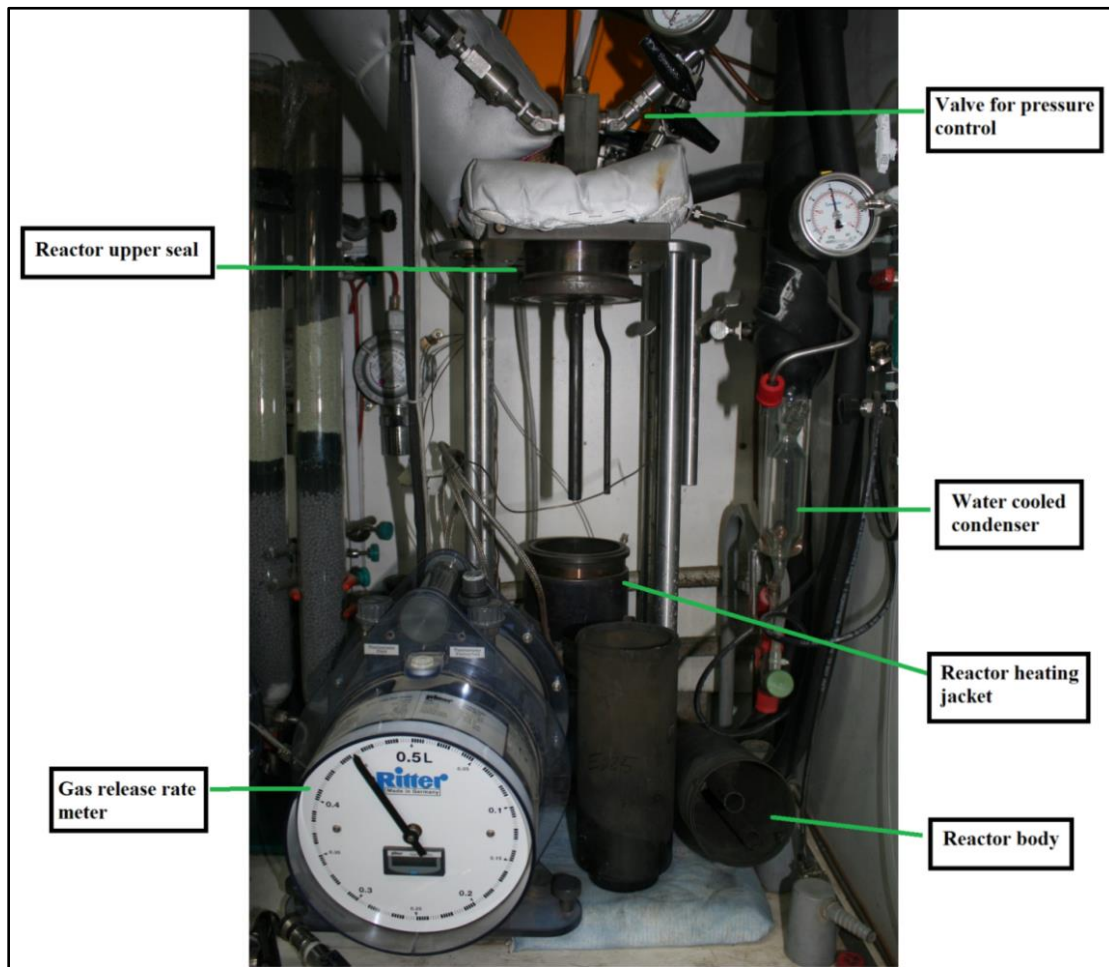


Figure 5. Dismantled pyrolysis reactor used in the experiments, main parts are marked.

3.2.2. Bitumen extraction

Bitumen is defined as the organic phase within the sedimentary rock that is soluble in organic solvents (Peters et al., 2005). Bitumen was extracted from the initial and all residual Zoharim rock samples (total 5 samples).

Approximately 100 g of crushed rock is placed inside a Soxhlet extractor and subjected to a dichloromethane/methanol (9:1 v/v) mixture for 72 hours (Amrani et al., 2005). Bitumen content is calculated by weight difference between original rock sample and residual rock after extraction.

Collected solution is evaporated under gentle flow of nitrogen until no change in sample weight was detected.

3.2.3. SARA fractionation

All bitumen and natural hydrocarbons were divided into four fractions: Saturates, Aromatics, Resins and Asphaltenes (Peters et al., 2005; Bastow et al., 2007).

Asphaltenes precipitation was performed by mixing approximately 100 mg of sample with 50 times (by weight) *n*-pentane in a clean 20 ml vial. The vial is sealed and its contents are mixed ultrasonically for 10 minutes. Following the mixing the vial was left overnight (at least 12 hours) to precipitate all asphaltenes. The remaining solution is termed the maltene solution and it contains the saturates, aromatics and resins fraction. The vial contents are filtered and the separated maltene solution is mixed with squalene and benzyl phenyl sulfide (BPS) standards for later quantification of interesting compounds and is then separated on a column of pre-activated silica gel and alumina. The column is composed of 2.5 g of silica gel in the lower part of the column and approximately 0.2 g of alumina in the upper part.

The **saturate** fraction is eluted with *n*-hexane (20ml) and contains squalene as standard. The **aromatic** fraction is eluted with *n*-hexane/dichloromethane (7:3 v/v) (20 ml) and contains benzyl phenyl sulfide as standard. The **resins** are eluted with methanol (20 ml).

Solvent of each fraction was evaporated under gentle flow of nitrogen and the fractional weight was recorded.

3.2.4. Gas Chromatography/Mass spectrometry (GC/MS)

Pyrolysates (or pyrolysis oils) and oil fractions (saturate and aromatic) were analyzed using an Agilent 7890A GC coupled with an Agilent 5975C mass selective detector. A 30 m X 250 μ m X 0.25 μ m DB-5MS fused-silica capillary column is used. Helium is used as carrier gas with flow rate of 1.2 ml/min. The injection mode used is of split ratio of 10 (i.e. one tenth of the sample that entered the GC injector is passed on to the column while the rest of the sample is vented out of the system as waste). The temperature program used is: 50°C for 5 minutes, a 5°C/min linear gradient up to 320°C, constant temperature (320°C) for 20 minutes. Detector solvent delay is set to 7 minutes. Total run time is 79 minutes. Data acquisition was performed with Agilent MSD ChemStation software.

3.2.5. Quantification of molecular groups of interest

The following groups of compounds were quantified in experiments on pyrolysis oils and bitumen: *n*-alkanes, alkyl-thiophenes, benzothiophenes and dibenzothiophenes. Quantification was performed by integration of the main fragment ions of each compound group on the GC/MS. The result of the ion fragment integration is a molar response which was calibrated to a standard. As the compound group and the standard used have a different ionization potential a suitable response factor had to be used in concentration calculations. All quantification parameters are listed in Table II.

Response factors (RF) were calculated by injecting a compound of interest with the selected standard at different concentrations to GC-MS. The produced peaks were integrated and the peak areas were used to determine the slope of calibration curve. The response factor and its uncertainty were calculated from a 6-point calibration curve by using linear regression and standard error functions in Excel by using equations 1 and 2 respectively:

$$1) \quad RF = \frac{\frac{Area_{peak\ 1} - Area_{peak\ 2}}{C_{peak\ 1} - C_{peak\ 2}}}{\frac{Area_{standard\ 1} - Area_{standard\ 2}}{C_{standard\ 1} - C_{standard\ 2}}} = \frac{Slope_{compound}}{Slope_{standard}}$$

2) *Uncertainty on RF (%) =*

$$\sqrt{\left(\frac{\text{Standard error}_{\text{compound}}}{\text{Slope}_{\text{compound}}}\right)^2 + \left(\frac{\text{Standard error}_{\text{standard}}}{\text{Slope}_{\text{standard}}}\right)^2}$$

Table II- Quantification parameters used for the selected compound groups.

| Compound group | Main fragment ions (m/z) | Standard used | Response factor | Uncertainty of response factor (%) |
|-----------------------|---------------------------------|---|--|--|
| <i>n</i> -Alkanes | 57 | Squalane | 1.73 | 1.87 |
| Alkyl-thiophenes | 97, 111, 125 | <u>Squalane</u> in whole oil and in saturate fraction | <u>For squalene:</u> 1.29 | <u>For squalene:</u> 11.27 |
| Benzothiophenes | 134, 148, 162, 176, 190 | <u>Squalane</u> in whole oil <u>BPS</u> in aromatic fraction | <u>For squalene:</u> 1.66 <u>For BPS:</u> 1.38 | <u>For squalene:</u> 5.33 <u>For BPS:</u> 4.75 |
| Dibenzothiophenes | 184, 198, 212, 226 | <u>BPS</u> in aromatic fraction | 0.75 | 2.48 |

All concentrations are presented as mg/g of fraction analyzed (i.e. mg/g_{oil} or mg/g_{bitumen}) in the C_n>10 range (i.e Decane and higher).

3.2.6. Rock-Eval pyrolysis

The Rock-Eval 6 was used to estimate the type of organic matter, degree of maturation and petroleum production potential of sedimentary rocks by heating a small amount of crushed rock (20-30mg) or oil in a pyrolysis oven under nitrogen atmosphere followed by combustion under air atmosphere (Lafargue et al., 1998; Behar et al., 2001). Each analysis was repeated 2-4 times to ensure reproducibility of the results. The Rock-

Eval 6 is located in Prof. Shimon Feinstein's Organic Geochemistry Laboratory in the Department of Geological and Environmental Studies at Ben-Gurion University.

In the pyrolysis oven the sample is subjected to gradual heating according to selected heating program (Table III) under nitrogen atmosphere. This process leads to maturation of the source rock sample and evolution of hydrocarbons which in turn are analyzed by a flame ionization detector (FID) and the evolution of CO and CO₂ are analyzed by an infrared detector (IR).

Table III- Heating program used on the Rock-Eval 6.

| Stage\Parameter | Initial temp. (°C) | Final temp (°C) | Rate (°C minute⁻¹) | Initial time (minute) | Final time (minute) |
|------------------------|---------------------------|------------------------|--------------------------------------|------------------------------|----------------------------|
| Pyrolysis | 300 | 650 | 25 | 3 | 0 |
| Oxidation | 300 | 850 | 20 | 1 | 5 |

The following parameters are obtained on the pyrolysis stage:

S1: The peak area represents the amount of free hydrocarbons (HC) present in the sample that are released in the initial stage where pyrolysis is isothermal at 300 °C. Unit of measurement is mg HC g⁻¹ rock.

S2: The peak area presents the amount of hydrocarbons released due to thermal cracking of organic matter between 300-650°C, corresponds to the hydrocarbon evolution potential of the rock during maturation. Unit of measurement is mg HC g⁻¹ rock.

S3, S3CO, S3'CO: These peaks areas represent the amount of CO₂ and CO released from organic matter and mineral phase during pyrolysis, Unit of measurement is mg CO₂ g⁻¹ rock and mg CO g⁻¹ rock respectively.

T_{max}: The T_{max} value is the temperature at which the S2 peak reaches its maximum. The T_{max} is used as a thermal maturity parameter. The unit of measurement is degrees Celsius (°C).

At the end of the pyrolysis stage the sample is transported to the oxidation oven where it is heated to 850°C under air atmosphere and the produced CO₂ is transported to the IR detector. The following parameters are obtained in the oxidation stage:

S4CO: Represents the CO evolved during the oxidation. This CO is of organic origin. mg CO g⁻¹ rock

S4CO₂: Represents the CO₂ evolved during oxidation between 300°C and temperature of minimum organic carbon. Unit of measurement is mg CO₂ g⁻¹ rock.

S5: Represents the CO₂ evolved during oxidation between the temperature of minimum organic carbon to the end of the measurement at 850°C. Unit of measurement is mg CO₂ g⁻¹ rock.

The produced parameters are used for the following calculations:

Pyrolysable organic carbon (PC) (wt %):

$$3) \quad PC = \frac{[(S1+S2) \times 0.83] + [S3 + \frac{12}{44}] + [(S3CO + \frac{S3'CO}{2}) \times \frac{12}{28}]}{10}$$

Residual organic carbon (RC) (wt %):

$$4) \quad RC = \frac{S4CO \times \frac{12}{28}}{10} + \frac{S4CO_2 \times \frac{12}{44}}{10}$$

Total organic carbon (TOC) (wt %):

$$5) \quad TOC = PC + RC$$

Hydrogen index (HI) (mg HC g⁻¹ TOC):

$$6) \quad HI = \frac{S2 \times 100}{TOC}$$

Oxygen index (OI) (mg HC g⁻¹ TOC):

$$7) \quad OI = \frac{S3 \times 100}{TOC}$$

Production index (PI):

$$8) \quad PI = \frac{S1}{(S1+S2)}$$

The complete analysis described above will be termed RockEval analysis henceforth.

3.2.7. Sulfur content of rock and hydrocarbon samples

Total sulfur and carbon were analyzed for all rock and hydrocarbon samples. Rock samples consisted of approximately 60mg crushed rock; oil and asphalt samples consisted of approximately 20mg hydrocarbons. Analyzed samples were placed in a porcelain crucible and combusted in a pure oxygen atmosphere at 1350°C in a LECO SC632 Sulfur-Carbon elemental analyzer. Released sulfur dioxide was measured by an IR detector. Each analysis was repeated 2-4 times to ensure reproducibility of the results unless noted otherwise. This sulfur content analysis will be termed LECO analysis henceforth.

3.2.8. Oil viscosity

Viscosity was measured using a calibrated Zeitfuchs cross-arm viscometer (Cannon Instrument Company) according to ASTM D 445.

The viscometer was held by a round holder and immersed into a thermostatic bath at 40°C for 10 minutes to allow thermal equilibrium. Viscosity is reported as kinematic viscosity in centistokes units (cSt, cm²/sec). Each analysis was repeated 2 times to ensure reproducibility of the results.

The uncertainty in viscosity measured by viscometer is directly related to the viscosity of the sample but is less than ±1% for all measurements.

The sample of Zuk Tamrur 3 oil is too viscous to be measured in a viscometer and therefore was measured on HAAKE viscotester iQ Rheometer. The reported accuracy of the rheometer measurement is ±2%.

3.2.9. Oil density and API gravity

Oil density was measured using a calibrated 2ml Gay-Lussac pycnometer. The pycnometer was placed in a thermostatic bath at 15.6 and 40°C for 10 minutes to allow thermal equilibrium prior to analysis. Measurements at 15.5°C were used to calculate the oil sample API gravity. Each analysis was repeated 2-4 times to ensure reproducibility of the results.

API gravity is a unit of measurement for crude oil density. It has an inverse relation to the oil specific gravity (i.e. API gravity is increasing with specific gravity decreasing).

API gravity is calculated according to following equation:

$$9) \text{ } ^\circ\text{API gravity} = \frac{141.5}{\text{Specific gravity at } 15.6^\circ\text{C}} - 131.5$$

The uncertainty in measured density is less than $\pm 0.5\%$ for all measurements.

3.2.10. Thermal maturation and environment of deposition estimation from molecular markers

The thermal stability of methyl dibenzothiophenes (MDBT) and methyl phenanthrenes (MP) varies with the position of the alkyl group. Out of the MDBT's the 1-methyl isomer is the least thermally stable and 4-methyl is the most thermally stable. In the MP group the 1-methyl and 9-methyl isomers are the least thermally stable and the 2-methyl and 3-methyl are the most thermally stable. Consequently the relative abundance of alkylated isomers of DBT and phenanthrene can be used as an indicator for level of maturation of oil and bitumen (Radke, 1988; Radke and Willsch., 1994; Huang and Pearson., 1999; Li et al., 2014a). Moreover, the concentration of MDBT's in oil is usually much higher than that of biomarkers used for maturity assessment. This feature makes maturity parameters based on MDBT useful in cases of high level of maturity or in situations where biomarkers are not present or are insufficient in concentration for maturity assessment (Chakhmakhchev et al., 1997; Li et al., 2014b). Estimation of thermal maturity based on MDBT is done by calculating the methyl dibenzothiophene ratio (MDR) based on the following equation from Radke (1988):

$$10) \text{ } MDR = \frac{4\text{-MDBT}}{1\text{-MDBT}}$$

Calculation of the equivalent vitrinite reflectance and T_{max} is done using the following equations:

$$11) R_c(\%) = 0.4 + 0.3 \cdot MDR - 0.094 \cdot MDR^2 + 0.011 \cdot MDR^3$$

$$12) T_{\max(\text{equiv.})} = 419 + 10.9 \cdot MDR - 1.74 \cdot MDR^2 + 0.13 \cdot MDR^3$$

Estimation of thermal maturity based on MP is done by calculating the methylphenanthrene index (MPI) and the methylphenanthrene ratio (MPR) by the following equations from Radke (1988):

$$13) MPI = 1.5 \cdot \frac{((3-MP)+(2-MP))}{(Phenanthrene+(9-MP)+(1-MP))}$$

$$14) MPR = \frac{(2-MP)}{(1-MP)}$$

Calculation of the equivalent vitrinite reflectance is done by the following equations:

$$15) R_c(\%) = 0.38 + 0.61 * MPI \text{ for } 0.65 \leq R_c(\%) \leq 1.35$$

$$16) R_c(\%) = 2.59 - 0.59 * MPI \text{ for } 1.35 \leq R_c(\%) \leq 2$$

$$17) R_c(\%) = 0.95 + 1.1 \cdot \log(MPR)$$

DBT to phenanthrene ratio (DBT/PHE) is used in combination with pristane/phytane ratio (pr/ph) and sulfur content of hydrocarbons for the assessment of depositional environment, lithology of the source rock and oxidation conditions during deposition (Hughes, 1995; Chakhmakhchev and Suzuki., 1995a). Since all hydrocarbon samples used in this study originated from the Ghareb formation source rock it is worth testing the applicability of these relations for oils produced by pyrolysis.

An additional thermal maturity marker is the ratio between benzothiophenes (BT's) concentration and DBT's concentration. The rationale behind this marker is that thermal stability of BT's is lower than that of DBT's. The ratio between the two groups was shown to decrease with the increase in vitrinite reflectance due the difference in their thermal stabilities (Santamaria et al., 1998).

Peaks of pristane, phytane, benzothiophene, phenanthrene, dibenzothiophene, alkylated DBT and phenanthrenes were identified on GC/MS by monitoring the ions with a mass-to-charge ratio (m/z) of 134, 178, 183, 184, 192 and 198.

The following figures illustrate the peaks that were identified on the chromatograms and the tables below them provide a short description of each peak (See Figure 6 and Table IV).

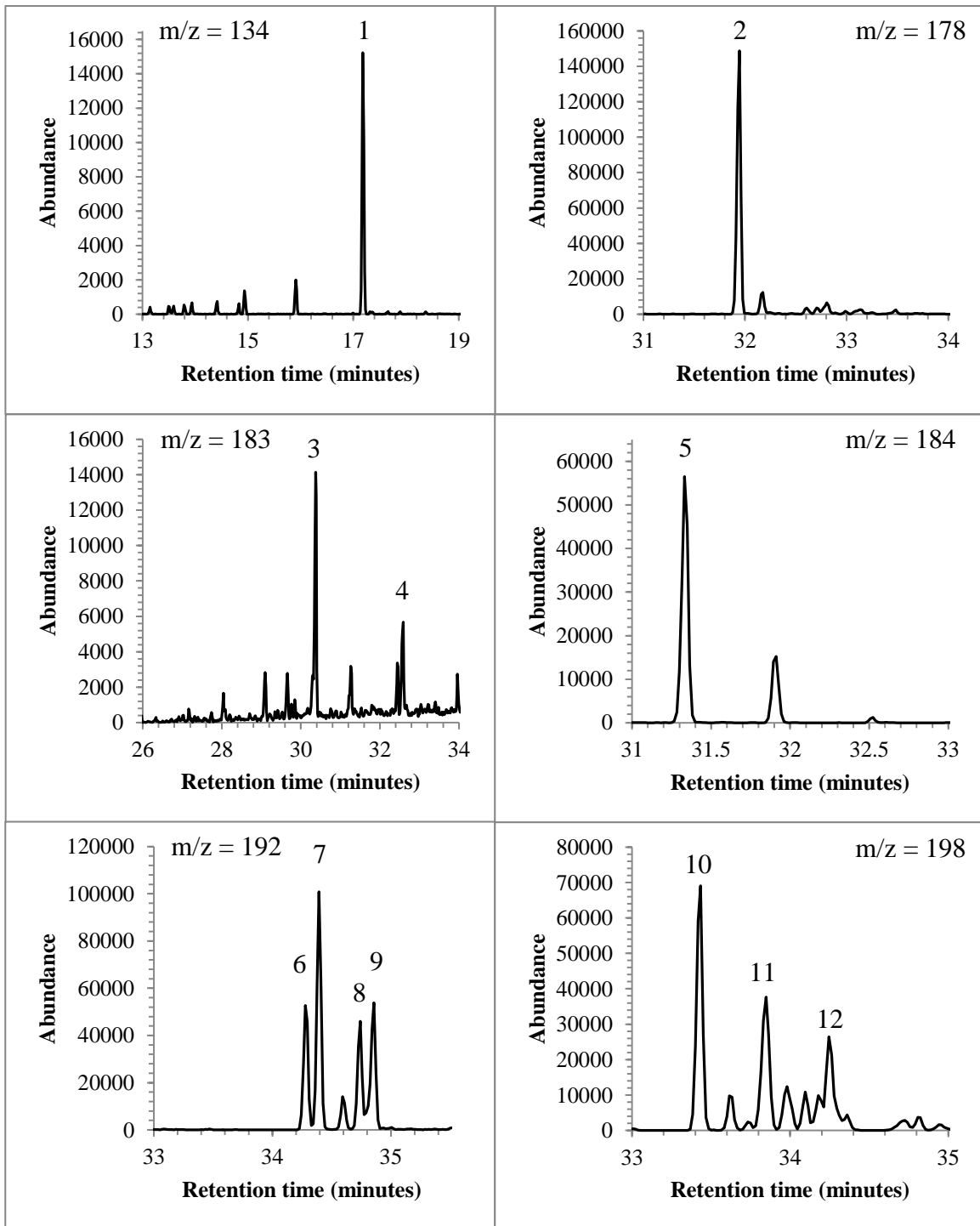


Figure 6. GC-MS chromatograms showing the peaks of interest for estimation of thermal maturity and environment of deposition. See Table IV for identification of peaks.

Table IV- Compounds of interest identified from the m/z chromatograms.

| Peak | Compound |
|-------------|---|
| 1 | Benzothiophene |
| 2 | Phenanthrene |
| 3 | Pristane (2,6,10,14-Tetramethylpentadecane) |
| 4 | Phytane (2,6,10,14-Tetramethylhexadecane) |
| 5 | Dibenzothiophene |
| 6 | 3- methylphenanthrene |
| 7 | 2- methylphenanthrene |
| 8 | 9- methylphenanthrene |
| 9 | 1- methylphenanthrene |
| 10 | 4- methyl dibenzothiophene |
| 11 | 2/3- methyl dibenzothiophene |
| 12 | 1- methyl dibenzothiophene |

The following parameters were calculated by using the area of the peaks described above:

Table V - Calculated parameters for maturity and environment of deposition assesment.

| Abbreviation | Identification | Reference |
|---------------------|---|-------------------------|
| DBT/PHE | DBT/Phenanthrene | Radke et al., 1991 |
| MDBT/MP | MDBT/Methyl phenanthrenes | Hughes et al., 1995 |
| BT/DBT | Benzothiophenes/ Dibenzothiophenes | Santamaria et al., 1998 |
| MPI 1 | Methylphenanthrene index 1 | Radke, 1988 |
| R _{c1} (%) | Calculated vitrinite reflectance based on MPI 1 | Radke, 1988 |
| MPR | Methylphenanthrene ratio | Radke, 1988 |
| R _{c2} (%) | Calculated vitrinite reflectance based on MPR | Radke, 1988 |
| MDR | Methyldibenzothiophene ratio | Radke, 1988 |
| R _{c3} (%) | Calculated vitrinite reflectance based on MDR | Radke, 1988 |
| R _{c3} (%) | Calculated T _{max} based on MDR | Radke, 1988 |

| | | |
|-------|--------------------------------|----------------------------|
| MDR' | Modified Methylthiophene ratio | Radke and Willsch, 1994 |
| Pr/Ph | Pristane/Phytane | Tissot and Welte 1984 |

3.2.11. Thermal maturation modelling

Thermal maturation modeling allows the comparison pyrolysis experiments with different heating rates and the comparison of laboratory heating rates to those occurring naturally in geological basins.

Thermal maturation of pyrolysis oils and residual rocks was estimated from the heating time-temperature program by using the EASY% Ro model which is based on an Arrhenius first-order parallel-reaction approach with a distribution of activation energies (Sweeney and Burnham, 1990). The value predicted by the model is represented as vitrinite reflectance equivalent (%Ro equ.). For a detailed spreadsheet of the model see Appendix VI.

4. Results

4.1 Characterization of the source rock

Samples of rocks from the Aderet and Zoharim boreholes were analyzed by Rock-Eval and LECO to determine their geochemical characteristics. The results are presented in Table VI.

Both samples are rich with organic matter (TOC>4%, Peters et al., 2005) which makes them excellent source rocks. The low T_{max} and production index (PI) coupled with high hydrogen index (HI) classify the rocks as immature and oil-prone. High S2 values of both rocks indicate their high hydrocarbon production potential. The low OI coupled with the high HI imply a marine source for the organic matter in the rocks (Appendix 2.1). Both rocks have high sulfur content.

Table VI- Results of Rock-Eval pyrolysis and LECO analysis for the Aderet and Zoharim rocks.

| | SI $(\frac{mg_{HC}}{g_{rock}})$ | $S2$ $(\frac{mg_{HC}}{g_{rock}})$ | T_{max} (°C) | TOC (wt. %) | HI $(\frac{mg_{HC}}{g_{TOC}})$ | OI $(\frac{mg_{HC}}{g_{TOC}})$ | PI | Sulfur (Wt. %) |
|---------|--------------------------------------|--------------------------------------|-------------------|----------------|-----------------------------------|-----------------------------------|------|-------------------|
| Aderet | 2.1 | 113.9 | 406 | 15.8 | 720 | 25 | 0.02 | 2.8 |
| Zoharim | 1.9 | 73.6 | 412 | 11.3 | 652 | 15 | 0.02 | 2.2 |

4.2 Aderet experiments

Two pyrolysis experiments with different heating gradients were performed on the Aderet rock samples: low heating gradient Ex15 (4°C/day) and high heating gradient Ex35 (120°C/day) (Table I). The difference in heating gradient leads to a difference of the thermal maturation degree: The low heating gradient Ex15 (4°C/day) reaches thermal maturity of %Ro equ. = 1.95 while the high heating gradient Ex35 (120°C/day) reaches thermal maturity of %Ro equ. = 1.29.

Oil production started earlier at the high heating gradient experiment (%Ro equ. = 0.43) and increased steadily whereas oil production at the low heating gradient experiment started at %Ro equ. = 0.52 and started to increase only after %Ro equ. = 0.56 (Figure 7). Both experiments reach peak production (“peak of oil window”) at a similar

level of maturation (%Ro equ. = 0.86-0.87) and then followed by decline in production. Oil production in both experiments continues until pyrolysis termination but the decline of production in the low heating gradient experiment is less significant than that of the high heating gradient experiment. Total oil production is 44.5 ml during the whole length of the low heating gradient experiment and 84.3 ml during the whole length of the high heating gradient experiment.

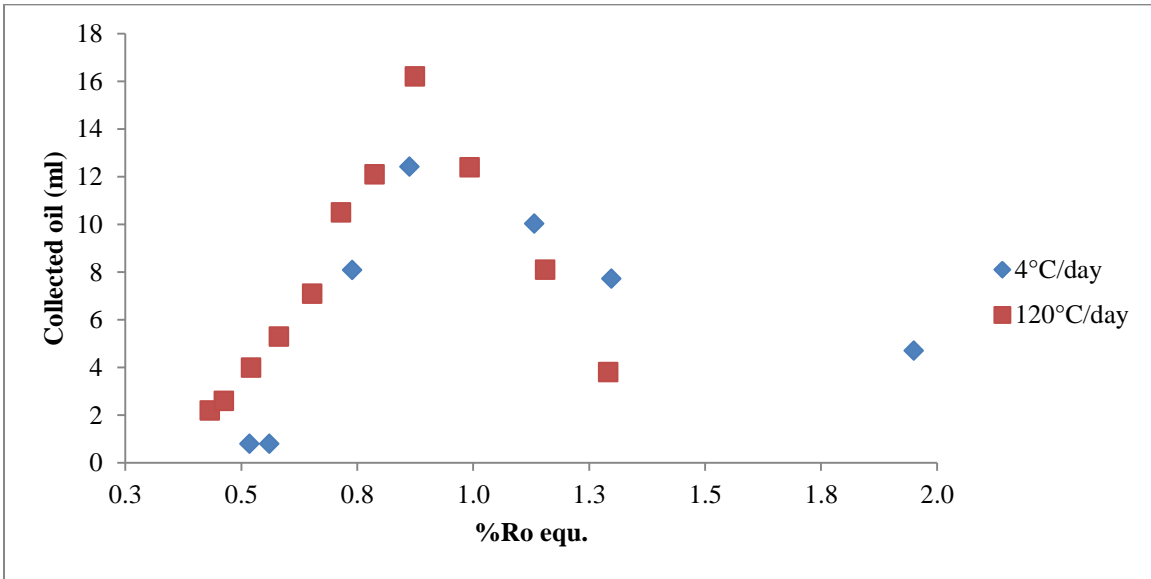


Figure 7. The change in Aderet oil production (ml) as a function of thermal maturation (%Ro equ.) at different heating gradients (4°C/day and 120°C/day).

4.2.1. Physical properties of produced oil

4.2.1.1. Density of oil

The change of oil density (reported as °API gravity) as a function of thermal maturity is presented in Figure 8, the complete set of measurements at 15.5°C and 40°C is reported in appendix V. Both experiments show an increase of the °API with increasing maturity in the range of %Ro equ. = 0.6-1.0 with the low heating gradient experiment having slightly higher API than the high heating gradient for a given level of maturity. For the high heating gradient experiment the highest API gravity of 27.18 was detected at %Ro equ. = 1.16 followed by a decrease- to a final value of 24.4 at %Ro equ. = 1.29. This behavior differs from the low heating gradient experiment where the API

gravity increases throughout the whole experiment to a final value of 37.1 at %Ro equ. = 1.30.

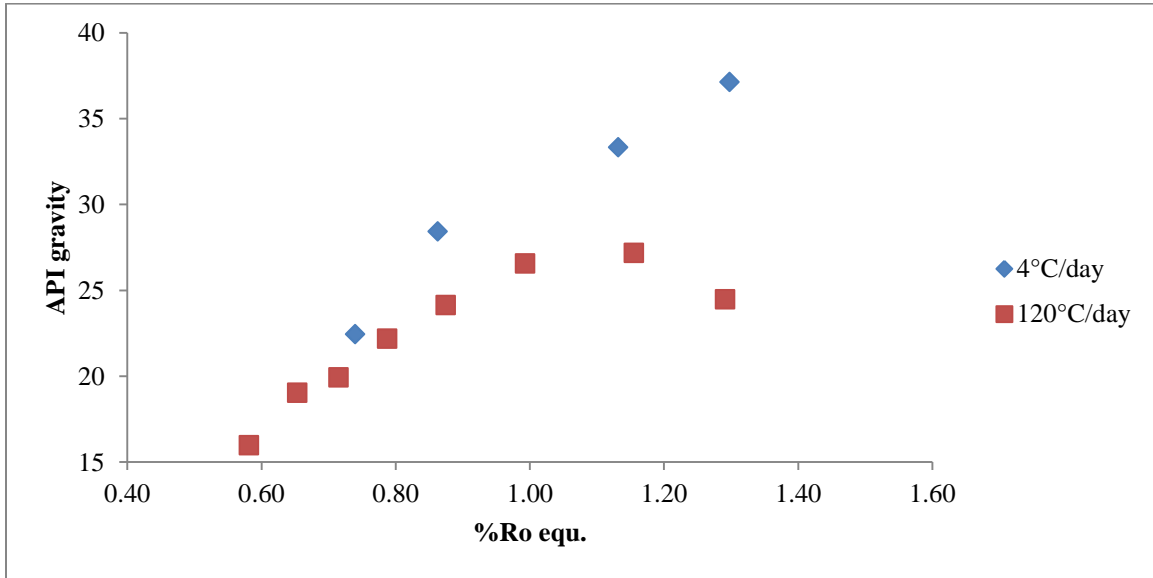


Figure 8. The change in Aderet oil density ($^{\circ}$ API) as a function of thermal maturation (%Ro equ.) at different heating gradients ($4^{\circ}\text{C}/\text{day}$ and $120^{\circ}\text{C}/\text{day}$). Error bars are smaller than the symbols.

4.2.1.2. Viscosity of oil

The change of kinematic viscosity as a function of thermal maturity is presented in Figure 9. Viscosity of the high gradient experiment changes irregularly with respect to thermal maturity with initial increase of viscosity (%Ro equ. = 0.43-0.52) followed by a decrease (%Ro equ. = 0.52-0.65), slight increase (%Ro equ. = 0.65-0.79) and then gradual decrease until the end of the experiment.

In the low gradient experiment viscosity is decreasing-increasing-decreasing with respect to thermal maturity, thus creating a zig-zag pattern for the first 4 samples (%Ro equ. = 0.74-1.30). The last sample of the experiment shows an additional slight decrease. Regardless of the heating gradient applied, the overall trend is of viscosity decreasing with thermal maturity for both experiments.

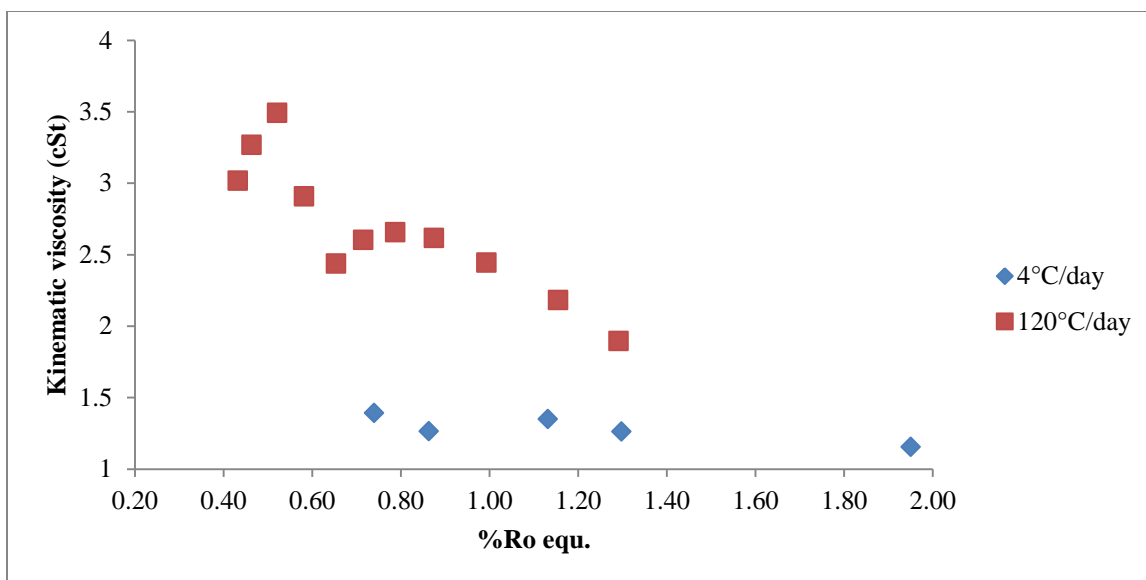


Figure 9. The change in Aderet oil kinematic viscosity (cSt) as a function of thermal maturation (%Ro equ.) at different heating gradients (4°C/day and 120°C/day). Error bars are smaller than the symbols.

4.2.2. Chemistry of produced oil

4.2.2.1. Alkyl-thiophenes content

Alkyl-thiophenes were present in all the oil samples of both experiments (Figure 10). The high gradient experiment starts with constant concentration (within error) at the range of %Ro equ. = 0.43-0.72. The concentration is then gradually declining to the end of the experiment at %Ro equ. = 1.16. The low gradient has a trend of concentration increase from the start of the experiment to the peak concentration at %Ro equ. = 0.74, as the level of maturity increases the concentration is declining gradually until the end of the experiment at %Ro equ. = 1.95. The peak concentration of the low gradient experiment (%Ro = 0.74) is 1.75 times higher than that of the high gradient experiment (%Ro = 0.58). The low gradient experiment has concentration of at least 2 times higher compared to the high gradient experiment in the maturity range of %Ro equ. = 0.74-1.16. By the end of the experiments the concentration of alkyl-thiophenes is 5-10 times lower than that of the first samples. Nevertheless, a detectable amount of alkyl-thiophenes is present at the last point of the low gradient experiment which is at the highest level of thermal maturity.

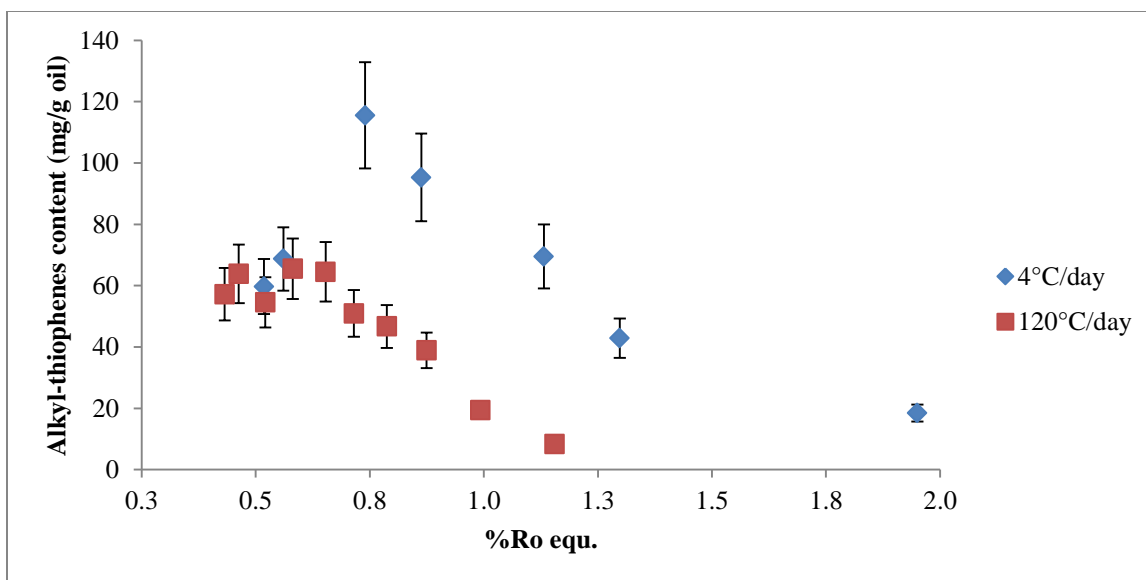


Figure 10. The change in alkyl-thiophenes content in the Aderet oils (mg/g oil) as a function of thermal maturation (%Ro equ.) at different heating gradients (4°C/day and 120°C/day). Data of the 120°C/day experiment is from Amrani et al., in preparation.

4.2.2.2. Benzothiophenes content

Benzothiophenes were present in all oil samples of both experiments (Figure 11). The heating low gradient experiment exhibits a trend of increase from the start of the experiment to peak concentration at %Ro equ. = 0.74. The high heating gradient experiment has two peak concentrations: Initial peak at %Ro equ. = 0.65 followed by a decrease to minimum at %Ro equ. = 0.79 and increase until the end of the experiment. Peak concentration of the low heating gradient experiment is almost 1.5 times higher than the highest concentration reached in the high heating gradient experiment. Benzothiophene concentration of the high heating gradient experiment shows continues increase at the maturity range of %Ro equ. = 0.79-1.16 in contrast with the low heating gradient experiment where decline of concentration is observed during the whole length of the experiment. The last point of the low heating gradient experiment is at a high level of maturation (%Ro equ. = 1.95) but still contains a detectable amount of benzothiophenes.

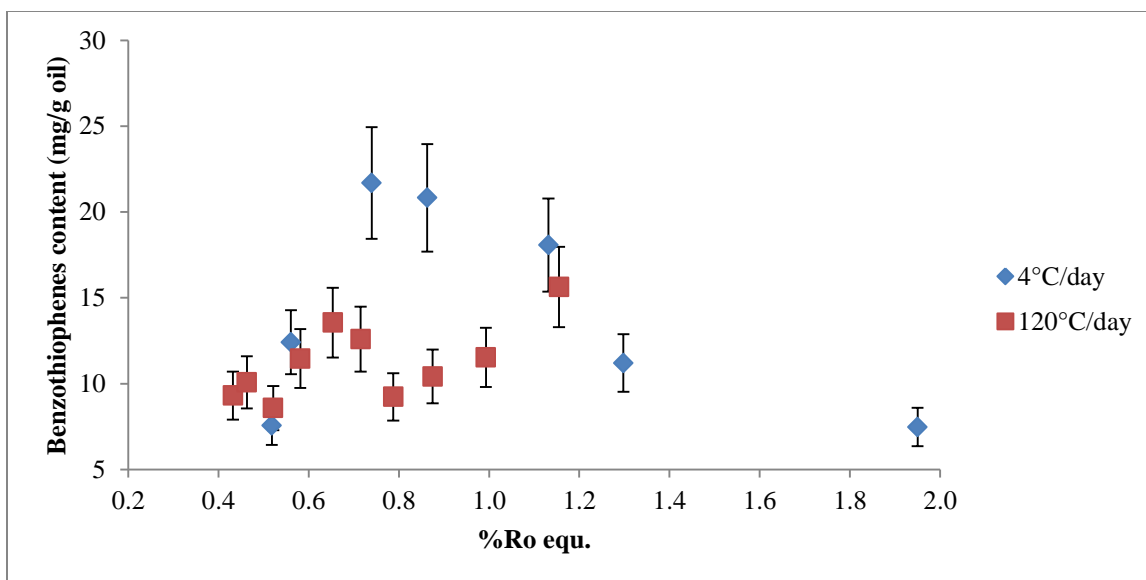


Figure 11. The change in benzothiophenes content in the Aderet oils (mg/g oil) as a function of thermal maturation (%Ro equ.) at different heating gradients (4°C/day and 120°C/day). Data of the 120°C/day experiment is from Amrani et al., in preparation.

4.2.2.3. Normal alkanes content

Normal alkanes concentration in the high gradient experiment shows an initial slight decline pattern for the low maturity samples (%Ro equ. = 0.43-0.52) followed by a steady increase until the end of the experiment (Figure 12). The low heating gradient experiment shows a steady increase during the whole experiment. Both experiments behave similarly from their start to %Ro equ. = 1.13-1.16 where *n*-alkanes in the low heating gradient experiment increases compared to the high heating gradient experiment; at the next sampling point, the concentration is 1.3 times the low heating gradient experiment. The last sampling point of the low heating gradient experiment has approximately 20% by weight of *n*-alkanes.

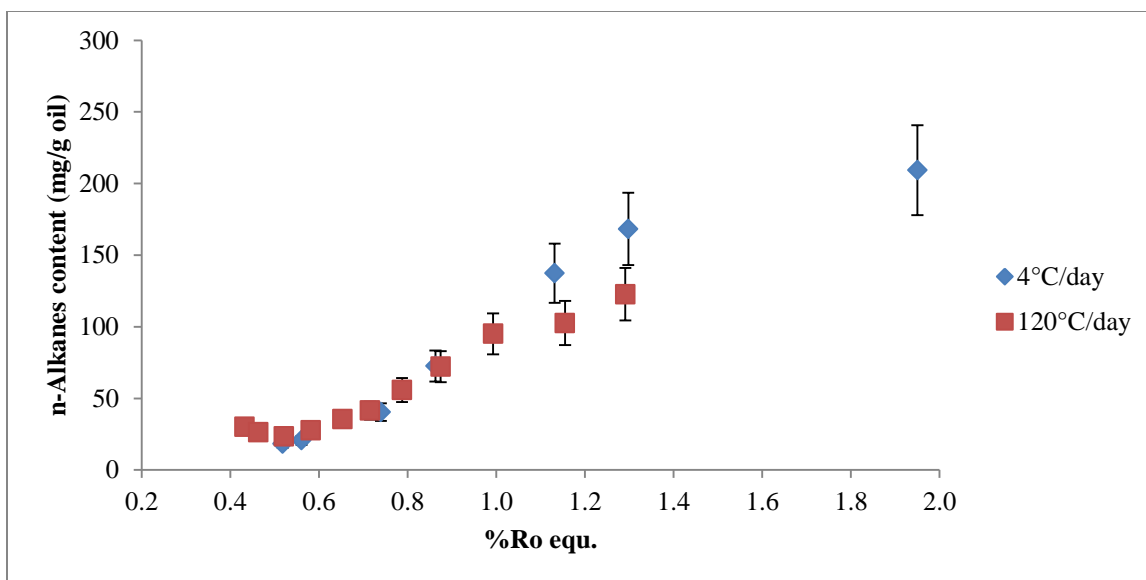


Figure 12. The change in *n*-Alkanes content in the Aderet oils (mg/g oil) as a function of thermal maturation (%Ro equ.) at different heating gradients (4°C/day and 120°C/day).

4.2.2.4. Sulfur content

The sulfur content of oils in both experiments declines with increasing level of maturity (Figure 13). Both experiments show abnormally high sulfur content in low maturity samples: in the high gradient experiment the first sample has 19.2% sulfur while the first sample of the low gradient experiment has 15% sulfur. The sulfur content of the low gradient experiment oils is higher than that of the high gradient experiment for the maturity increment of %Ro. Equ. = 0.52-1.13, followed by similar sulfur content for %Ro equ. =1.30 where the high gradient experiment is terminated. The last sample of the low gradient experiment has the highest maturity reported in this study but still contains a relatively high sulfur concentration of 1.95%.

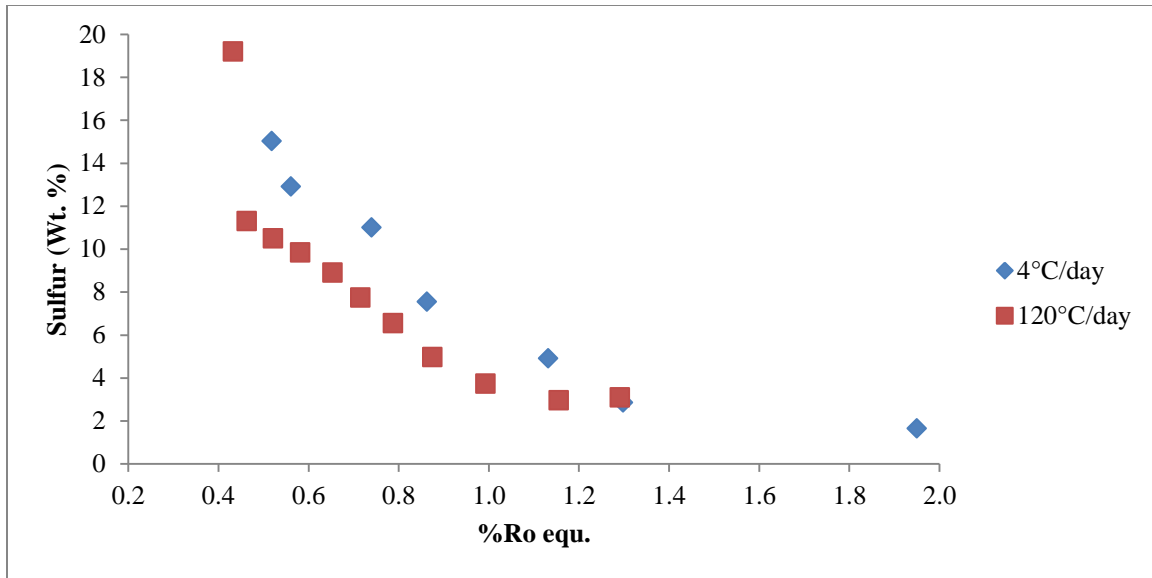


Figure 13. The change in sulfur content in the Aderet oils (Wt. %) as a function of thermal maturation (%Ro equ.) at different heating gradients (4°C/day and 120°C/day). Error bars are smaller than the symbols.

4.2.3. Spent rock properties

Spent rocks from both experiments were analyzed by Rock-Eval and LECO to determine their geochemical parameters. The results are presented in Table VII. The very high T_{max} values of both rocks indicate they have overmatured. As expected, the low hydrogen index values and the high production index indicate these spent rocks have a very poor hydrocarbon production potential (Appendix 2.1).

Table VII- Results of Rock-Eval pyrolysis and LECO analysis for spent rock from the Aderet experiments.

| | $S1$ $\left(\frac{mg_{HC}}{g_{rock}}\right)$ | $S2$ $\left(\frac{mg_{HC}}{g_{rock}}\right)$ | T_{max} (°C) | TOC (wt. %) | HI $\left(\frac{mg_{HC}}{g_{TOC}}\right)$ | OI $\left(\frac{mg_{HC}}{g_{TOC}}\right)$ | PI | Sulfur (Wt. %) |
|-----------|---|---|-------------------|----------------|--|--|------|-------------------|
| 4°C/day | 0.8 | 3.4 | 547 | 11.7 | 29 | 11.5 | 0.16 | 0.71 |
| 120°C/day | 0.5 | 4.6 | 515 | 11.4 | 40.75 | 15.5 | 0.1 | 0.68 |

4.3 Zoharim experiments

Four pyrolysis experiments were conducted on the Zoharim rock sample (Table I). Each experiment produced rock, which has a higher level of maturity compared to his preceding experiment in order to study the residual rock and the bitumen it contains at various stages of thermal maturation. The highest pyrolysis temperature, calculated level of maturity and the bitumen content of the unheated and residual rocks of the Zoharim experiments are presented in Table VIII. The level of maturation shown for the unheated sample is an actual %Ro measurement of the immature kerogen in the Shfela basin from Meilijson et al., (2014).

Table VIII- Results of Soxhlet extraction of bitumen for the rock samples from Zoharim experiments.

| Sample | Pyrolysis peak temperature (°C) | %Ro equivalent | Bitumen extracted (g) | Bitumen extracted (g/ kg rock) |
|---------------|--|-----------------------|------------------------------|---------------------------------------|
| Unheated rock | ----- | 0.32 | 0.73 | 7.64 |
| Ex41 | 275.81 | 0.64 | 4.12 | 41.15 |
| Ex43 | 304.16 | 0.78 | 4.93 | 51.13 |
| Ex47 | 338.18 | 1.07 | 4.53 | 46.58 |
| Ex42 | 376.53 | 1.57 | 1.42 | 14.65 |

Figure 14 illustrates the production of bitumen and oil with respect to thermal maturity. The oil production data presented is from Ex42 since it was the only experiment to pass beyond the peak of oil production. Bitumen content is presented for all of samples in the Zoharim experiment.

Bitumen is present in all samples including the initial unheated sample. Bitumen content increases with increasing maturation until reaching the peak of production at %Ro equ. = 0.78 which is followed by a decrease of bitumen content to the highest level of maturity measured.

Oil production starts at %Ro equ. = 0.43, it increases with level of maturity to peak of production at %Ro equ. = 0.94 - 1.08 and it then decreases in production until the end of the experiment.

Oil samples from each experiment were mixed together in order to create a single sample which represents the whole duration of the experiment. The mixing was done in such a way that the relative proportion of each sampling is represented.

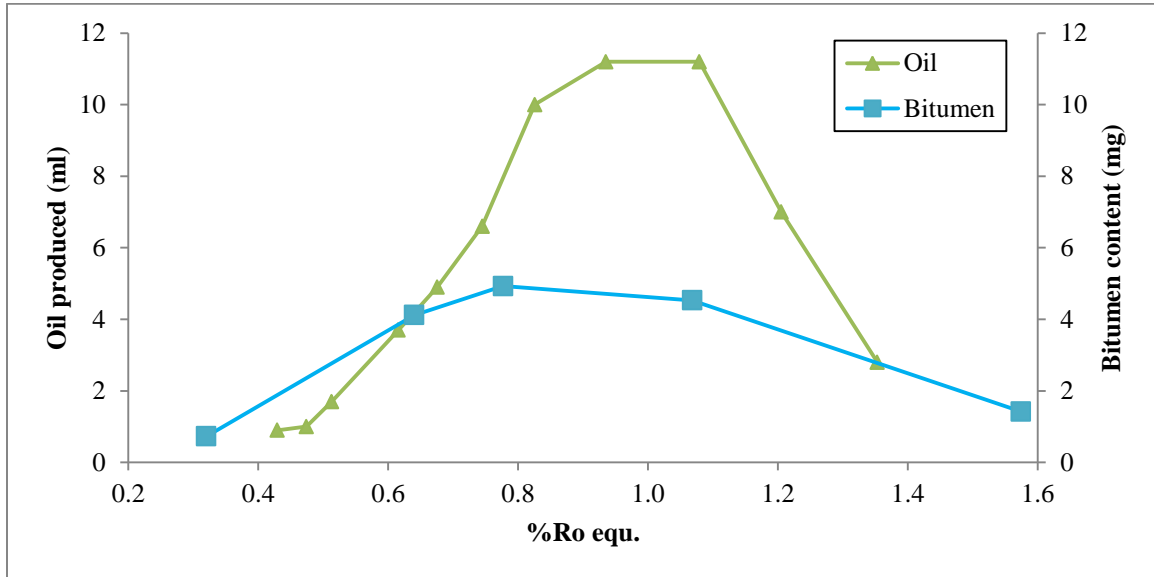


Figure 14. Oil production (ml) of Zoharim Ex42 and bitumen content (mg) of the Zoharim rock samples with respect to thermal maturation (%Ro equ.)

4.3.1. Chemistry of produced bitumen and oil

4.3.1.1. SARA

The results of SARA fractionation of the bitumen samples is presented in Figure 15. The relative proportions of the saturated and aromatic hydrocarbons of the bulk bitumen extracted follow a general trend of an increase with increasing thermal maturation. In the early stages of maturation the portion of saturates and aromatics increases dramatically from 10% combined to 30% combined in %Ro equ. = 0.32-0.64 respectively. The portion then decreases to 27-28% combined at %Ro equ. = 0.78 and 1.07. The decreasing trend continues with a combined portion of 23% at %Ro equ. = 1.57.

The resin fraction is relatively constant in the range of %Ro equ. = 0.32- 0.78; it then decreases and then increases slightly. The general trend during maturation is a decrease in the relative proportion of the resin fraction.

The amount of asphaltenes generated decreases in the first pyrolysis step between %Ro equ. = 0.32-0.64 from 76% to 58% respectively but then increases gradually to 68% at %Ro equ. = 1.07 and is kept at the same proportion at the last pyrolysis experiment.

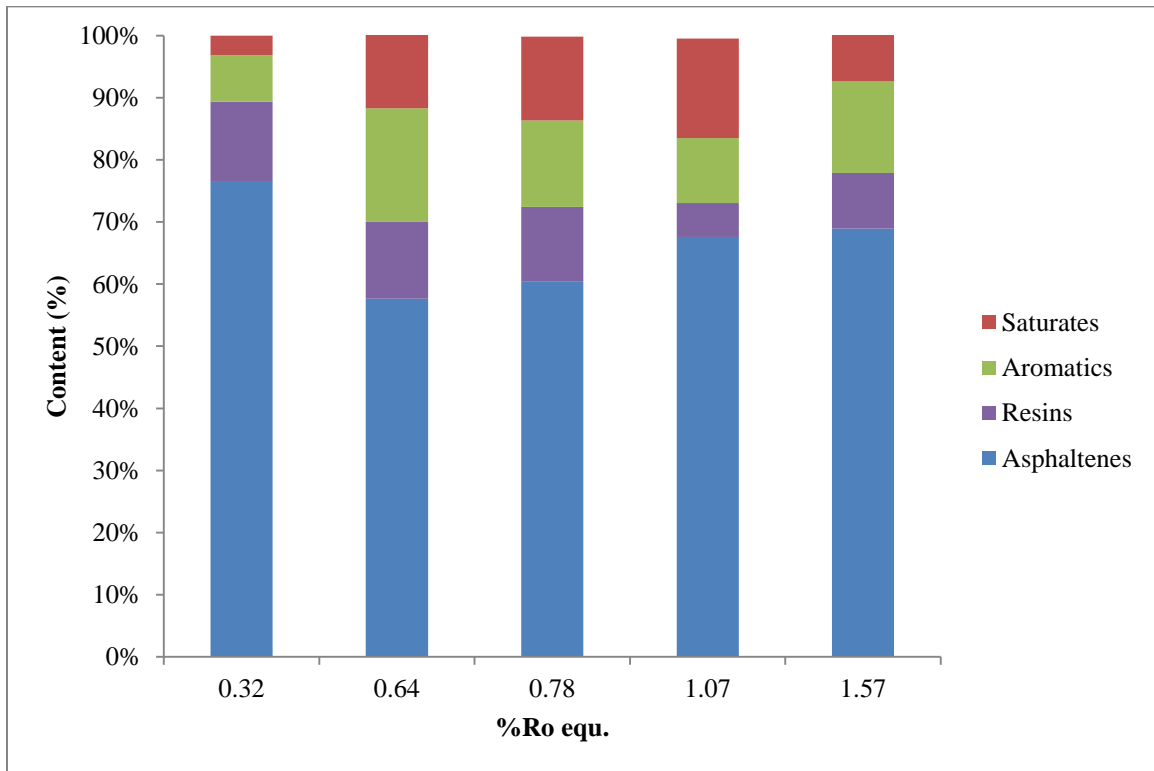


Figure 15. Results of SARA fractionation of Zoharim bitumen samples for various degrees of thermal maturation.

4.3.1.2. Sulfur content of bitumen and oil

Figure 16 shows the variation of the sulfur content in the oil and bitumen with increasing thermal maturity. The sulfur content of the oil is initially very high (14.5%) and it declines with increasing thermal maturity. The sulfur content is 6.5% at the highest level of thermal maturity reached in the experiment (%Ro equ. = 1.57).

The initial sulfur content of the bitumen is 7.2% at %Ro equ. = 0.32. As thermal maturity increases the sulfur content decreases as was observed for the oil fraction.

Increase of thermal maturity from %Ro equ. = 1.07 to 1.57 shows a sudden increase of the sulfur content of the bitumen to a final value of 4.3%.

Further examination of the sulfur content variation was achieved by observing the sulfur content of the bitumens asphaltene and maltene fractions (Figure 17). The asphaltene sulfur content was measured directly. The maltene sulfur content was calculated based on mass balance by the following equation:

$$18) \%S_{Maltene} = \frac{\%S_{bitumen} - (\%S_{asphaltene} \times fraction_{asphaltene})}{fraction_{maltene}}$$

The distribution of sulfur between the bitumen fractions is initially that of high sulfur content in the asphaltene fraction and low sulfur content in the maltene fraction (with respect to the bitumen itself). This trend continues with the bitumen decreasing in sulfur content in the maturity range of %Ro equ. = 0.32 – 0.78. When the level of maturity reaches %Ro eq. = 1.07 the sulfur content of the asphaltene and maltene fractions are practically identical. This is also the thermal maturity at which the sulfur content of the bitumen is at the lowest point of the entire experiment.

At the highest thermal maturity reached in the Zoharim experiment (%Ro equ. = 1.57) the sulfur content distribution is inverted: the maltene fraction has the high sulfur content and the asphaltene has the low sulfur content.

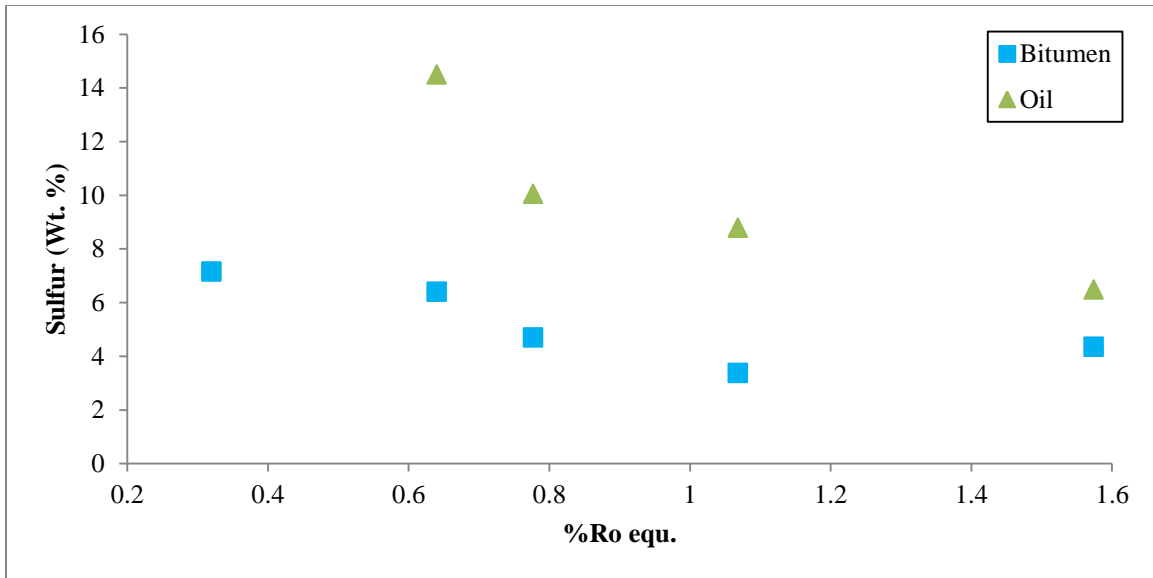


Figure 16. Sulfur content (Wt. %) of oil and bitumen from the Zoharim experiments as a function of thermal maturity (%Ro equ.).

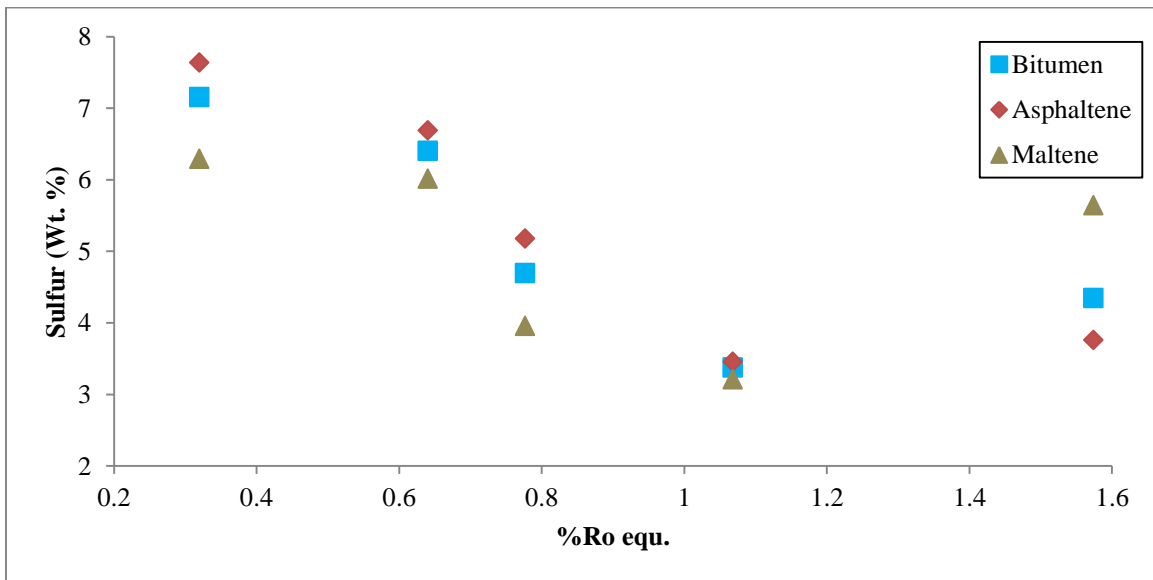


Figure 17. Sulfur content (Wt. %) of the Zoharim bitumen and its asphaltene and maltene fractions as a function of thermal maturity (%Ro equ.).

4.3.1.3. Thiophenes and benzothiophenes in oil and bitumen

Figure 18 shows the relation of the alkyl-thiophenes and benzothiophenes concentration in the bitumen samples to the level of thermal maturation. The unheated sample contains low concentration of benzothiophenes and alkyl-thiophenes which

increases with increasing thermal maturity in the range of %Ro equ. = 0.32- 0.78. The increase of alkyl-thiophenes is relatively constant with increasing thermal maturity. The behavior of benzothiophenes in the same maturity range is that of a more significant increase with increasing thermal maturity.

At the maturities range of %Ro equ. = 0.78- 1.06, the concentration of both groups of compounds decreases. In higher maturity samples the concentration of alkyl-thiophenes stays constant but the concentration of benzothiophenes increases significantly. In general, alkyl-thiophenes trend reaches peak concentration of 0.5 mg/g bitumen at %Ro equ. = 0.78. The benzothiophenes concentration trend has two peaks: first at %Ro equ. = 0.78 with 0.51 mg/g bitumen and second at the end of the experiment at %Ro equ. = 1.57 with 1.78 mg/g bitumen. The concentration of benzothiophenes in the bitumen is lower than that of alkyl-thiophenes during the whole experiment except the final sampling point.

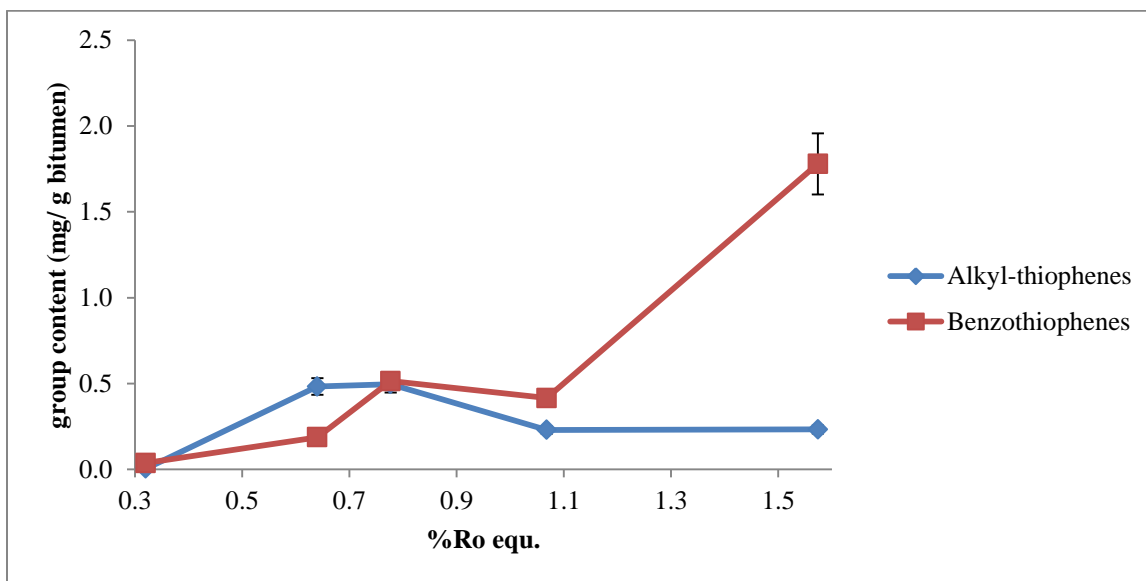


Figure 18. The change of thiophenes and benzothiophenes content in the Zoharim bitumen (mg/g bitumen) as a function of thermal maturation (%Ro equ.). Error bars are smaller than the symbols.

Figure 19 shows the relation of the alkyl-thiophenes and benzothiophenes concentration in the oil samples to the level of thermal maturation. Initial oil sample at %Ro equ. = 0.64 has an alkyl-thiophenes concentration of 67 mg/g oil and

benzothiophenes concentration of 12 mg/g_{oil}. The concentrations of both groups reach a peak at %Ro_{equ.} = 0.78. At higher thermal maturity the concentrations of both groups decrease: alkyl-thiophenes concentration decrease to 54 mg/g_{oil} and stay constant until the end of the experiment while the concentration of benzothiophenes first decreases to 17 mg/g_{oil} and then further declines until the end of the experiment.

The trend of alkyl-thiophenes is similar in both oil and bitumen but the concentrations are significantly higher in the oil phase (up to 2 orders of magnitude difference). The benzothiophenes concentration trend starts with a similar trend in both oil and bitumen- it reached a peak at %Ro_{equ.} = 0.78 which is followed by a decline of concentration to %Ro_{equ.} = 1.07. At the maturities range of %Ro_{equ.} = 1.07- 1.57 benzothiophenes concentration has inverse relation between oil and bitumen- it is increasing significantly in the bitumen fraction while the concentration in the oil phase is decreasing.

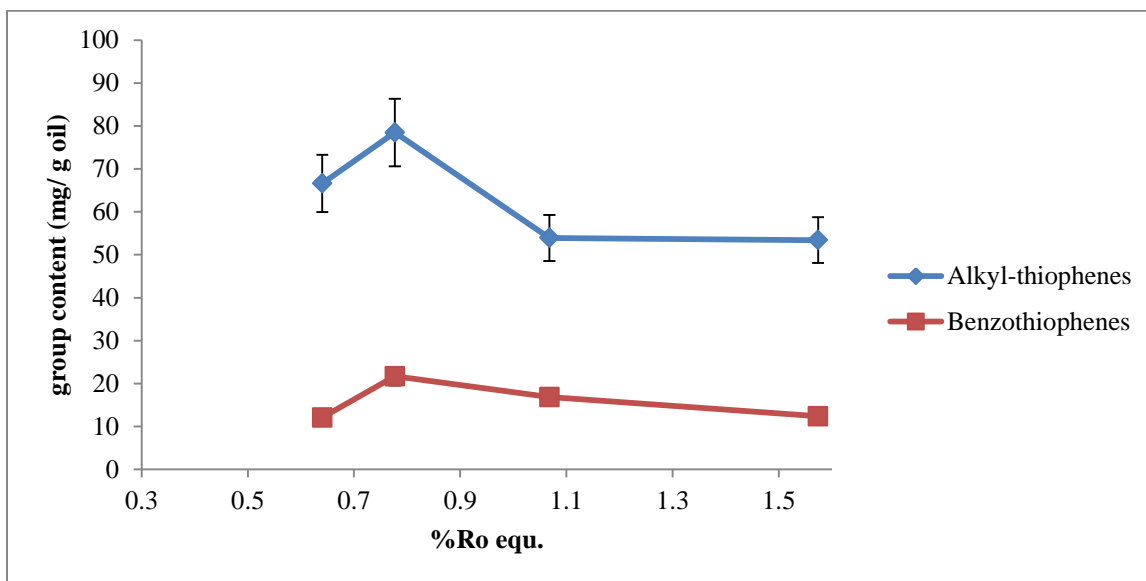


Figure 19. The change of thiophenes and benzothiophenes content in the Zoharim oil (mg/g oil) as a function of thermal maturation (%Ro_{equ.}). Error bars are smaller than the symbols.

4.3.1.4. *n*-alkanes in oil and bitumen

The *n*-alkanes concentration has a general trend of increase with increasing thermal maturity in both bitumen and oil until %Ro_{equ.} = 1.07 where the concentration in

bitumen then decreases until the end of the experiment (Figure 20). The main difference between the concentrations of *n*-alkanes in the oil fraction compared to the bitumen fraction is the significantly higher concentration in the oil (about an order of magnitude) during the experiment.

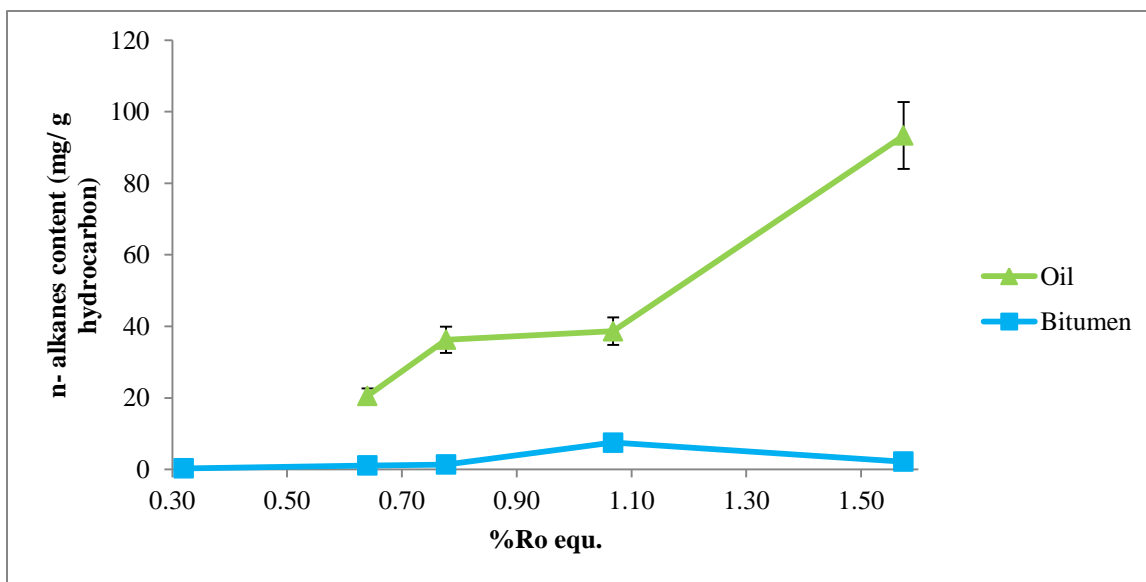


Figure 20. The change of *n*-alkanes content in the Zoharim oil and bitumen (mg/g hydrocarbon) as a function of thermal maturation (%Ro equ.). Error bars are smaller than the symbols.

The distribution of *n*-alkanes in each sample was analyzed by monitoring the ion with a mass-to-charge ratio (*m/z*) of 57.10 in the saturate fraction and is described below:

Unheated bitumen (%Ro equ. = 0.32): The chromatogram of this sample shows *n*-alkanes in the range of C₁₂-C₃₁ (Appendix III- Selected GC-MS chromatograms). The chromatogram shows a multimodal distribution with *n*-C₁₇ being the dominant peak. Prominent odd- over- even predominance is observed in the C₂₃-C₃₀ range.

Ex 41 oil and bitumen (%Ro equ. = 0.64): The chromatogram of the oil sample shows *n*-alkanes in the range of C₉-C₂₄ with unimodal distribution around C₁₅ dominant peak (Appendix III- Selected GC-MS chromatograms). The chromatogram of the bitumen sample shows *n*-alkanes in the range of C₁₁-C₃₈. The distribution of *n*-alkanes is multimodal with highest peak at C₃₀. Prominent even over odd predominance is observed in the C₂₃-C₃₀ range.

Ex 43 oil and bitumen (%Ro equ. = 0.78): The chromatogram of the oil sample shows *n*-alkanes in the range of C₉-C₂₆ with unimodal distribution around C₁₅ dominant peak (Appendix III- Selected GC-MS chromatograms). The chromatogram of the bitumen sample shows *n*-alkanes in the range of C₁₂-C₃₈. The distribution of *n*-alkanes is multimodal with highest peak at C₃₀. Prominent even over odd predominance is observed in the C₂₃-C₃₀ range. The content of the short chained *n*-alkanes (C_n<20) is highly reduced compared to the longer chains *n*-alkanes.

Ex 47 oil and bitumen (%Ro equ. = 1.07): The chromatogram of the oil sample shows *n*-alkanes in the range of C₉-C₂₂ with unimodal distribution around C₁₅ dominant peak (Appendix III- Selected GC-MS chromatograms). The chromatogram of the bitumen sample shows *n*-alkanes in the range of C₁₃-C₃₆, highest peak is the C₂₂. The distribution of *n*-alkanes is irregular: the content of *n*-alkanes with chains shorter than C₂₁ is significantly reduced compared to longer chains *n*-alkanes. Also, the transformation between the *n*C₂₁ to *n*C₂₂ distinctively irregular.

Ex 42 oil and bitumen (%Ro equ. = 1.57): The chromatogram of the oil sample shows *n*-alkanes in the range of C₉-C₂₆ with unimodal distribution around C₁₄ dominant peak (Appendix III- Selected GC-MS chromatograms). The chromatogram of the bitumen sample shows *n*-alkanes in the range of C₉-C₃₀. The distribution of *n*-alkanes is smooth and unimodal with highest peak at C₁₂, followed by a continuous and steep decrease to C₃₀.

4.3.1.5. Aromatic thiophenes in the bitumen

Figure 21 shows the change of benzothiophene and alkyl-benzothiophenes groups concentration with thermal maturity. The initial unheated bitumen sample contains very low concentration of benzothiophene and alkyl-benzothiophenes groups. The highest concentration is that of the C3-benzothiophenes (0.021 mg/g bitumen) followed by C4-benzothiophenes (0.007 mg/g bitumen), C2-benzothiophenes (0.009 mg/g bitumen), C1-benzothiophenes (0.001 mg/g bitumen) and benzothiophene (0.00004 mg/g bitumen). This distribution pattern is kept with increasing maturation which leads to an increase of concentration in all groups. The C2, C3, C4 benzothiophenes reach peak concentration at %Ro equ. = 0.78 and their concentrations then decrease until %Ro equ. = 1.07. In

contrast, the concentration of benzothiophene and C1-benzothiophenes increases in the same range of thermal maturity. During the final maturity section of the experiment, the concentration of all observed groups increases (%Ro equ. = 1.07- 1.57). At the end of the experiment (%Ro equ. = 1.57) the highest concentration is that of the C2-benzothiophenes (0.665 mg/g bitumen) which is followed by C1-benzothiophenes (0.46 mg/g bitumen), C3-benzothiophenes (0.391 mg/g bitumen), C4-benzothiophenes (0.203 mg/g bitumen) and benzothiophene (0.061 mg/g bitumen).

Figure 22 shows the change of the dibenzothiophene and alkyl-dibenzothiophenes groups concentration with thermal maturity. The initial unheated bitumen has low concentration of C1-dibenzothiophenes (0.006 mg/g bitumen), C2-dibenzothiophenes (0.004 mg/g bitumen) and dibenzothiophene (0.005 mg/g bitumen). No C3-dibenzothiophenes were detected in the unheated bitumen sample. Concentrations of all groups except C1-dibenzothiophenes increase with increasing thermal maturity in the range of %Ro equ. = 0.32 – 0.78. The C1-dibenzothiophenes concentration initially increases to %Ro equ. = 0.64 and is followed by slight decrease to %Ro equ. = 0.78. At thermal maturities between %Ro equ. = 0.78 to the end of the experiment at %Ro equ. = 1.57, the concentrations of all observed groups are increasing. At the end of the experiment, the highest concentration is that of C2-dibenzothiophene (0.91 mg/g bitumen) followed by C1-dibenzothiophenes (0.73 mg/g bitumen), C3-dibenzothiophenes (0.36 mg/g bitumen) and dibenzothiophene (0.17 mg/g bitumen).

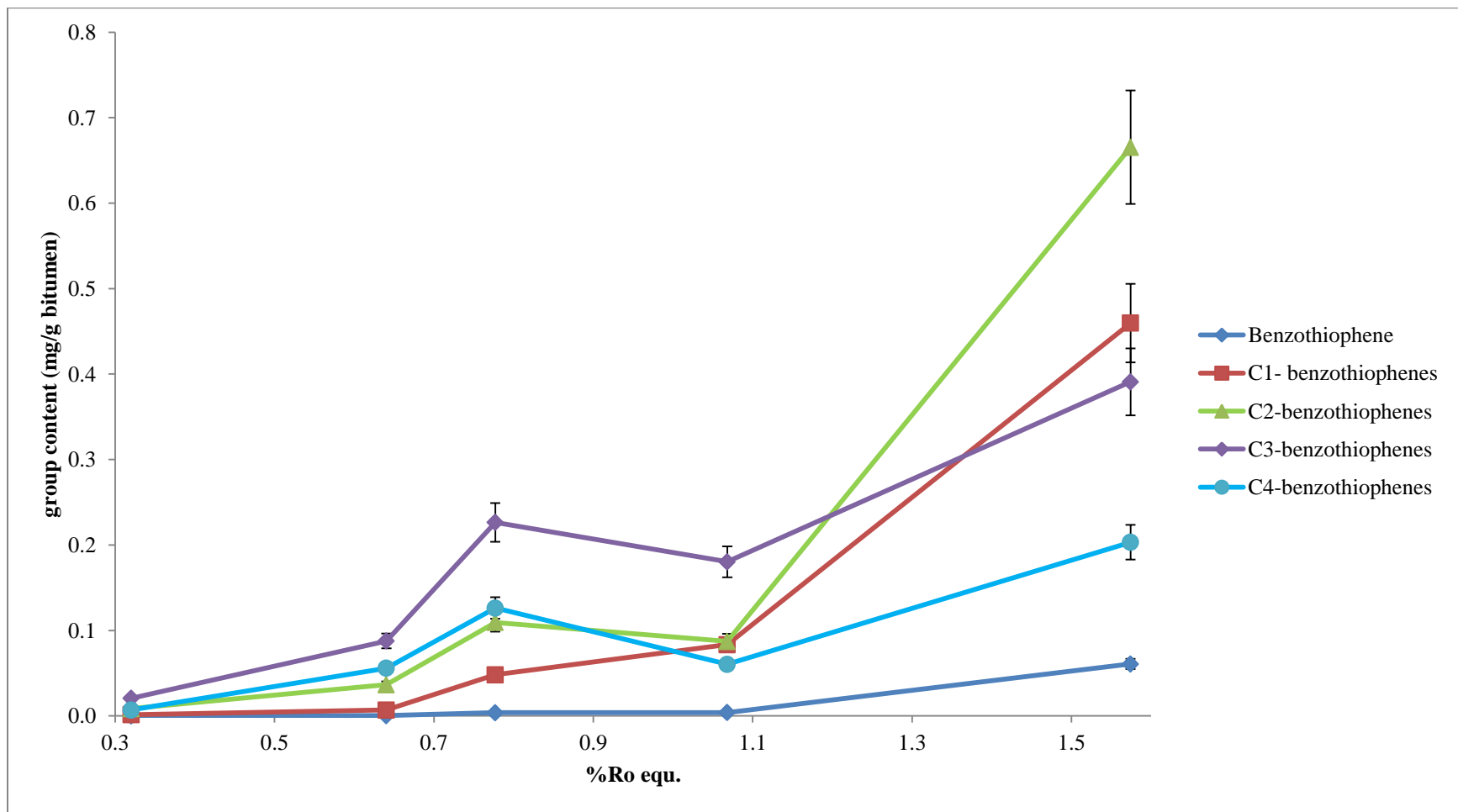


Figure 21. The change of benzothiophene and alkyl-benzothiophene groups concentration in the Zoharim bitumens (mg/g bitumen) as a function of thermal maturation (%Ro equ.). Error bars are smaller than the symbols.

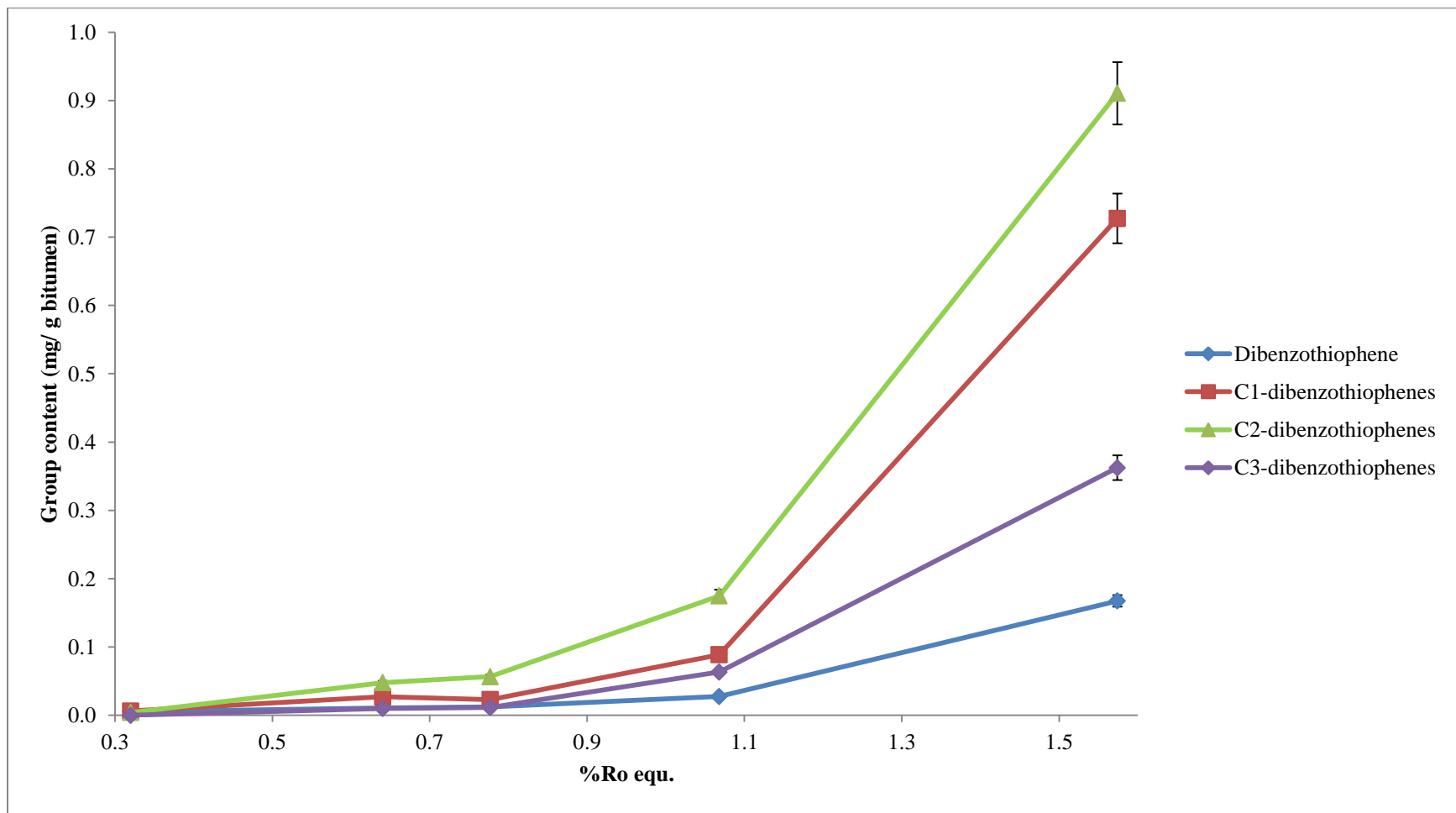


Figure 22. The change of dibenzothiophene and alkyl-dibenzothiophene groups concentration in the Zoharim bitumens (mg/g bitumen) as a function of thermal maturation (%Ro equ.). Error bars are smaller than the symbols.

4.3.1.6. Molecular markers in bitumen and oil

Maturity and facies parameters were calculated based on ratios between selected peaks as described in section 3.2.10. The calculated parameters are presented in Table IX.

In the bitumen samples of Zoharim the ratios of DBT/Phenanthrene and MDBTs/Methyl phenanthrenes exhibit a similar trend of initial increase between %Ro equ. 0.32 - 0.64 and then gradually decrease with increasing thermal maturity. At %Ro equ. = 1.57 the DBT/Phenanthrene value is 0.47 and the MDBTs/Methyl phenanthrenes value is 0.45.

The BT's/DBT's ratio value is 2.4 at the lowest maturity level. The ratio value initially decreases to 2.0 (%Ro equ. = 0.64) and then increases to peak value of 5.0 (%Ro equ. = 0.78). At higher maturities the ratio sharply increases to 1.2 (%Ro equ. = 1.07) and to 0.8 (%Ro. equ. = 1.57).

Pristane/Phytane ratio is 0.64 in the unheated sample. Upon thermal maturation the ratio increases to 2.56 (%Ro equ. = 0.64) and to peak value of 3.06 (%Ro equ. = 0.78). The Pristane/Phytane ratio then decreases to 2.7 (%Ro equ. = 1.07). No Pristane or Phytane were detected in the highest maturity sample at %Ro equ. = 1.57.

Maturity was estimated based on three parameters: methyl phenanthrene index "MPI 1", methyl phenanthrene ratio "MPR" and methyl dibenzothiophenes ratio "MDR" (Radke, 1988). The MPR values calculated start with 2.37 at %Ro equ. of 0.32, the value then decreases to 1.8 (%Ro equ. = 0.64), increases to 2.1 (%Ro equ. = 0.78), decreases to 1.95 (%Ro equ. = 1.07) and then decreases to a final value of 1.66 at %Ro equ. of 1.57. The MPR values are linearly related to calculated vitrinite reflectance. This relationship leads to identical pattern of increase and decrease of this maturity parameter.

The MPI values start with 0.77 (%Ro equ. = 0.32) and then increase to 1.04 (%Ro equ. = 0.64) and to peak value of 1.31 at %Ro equ. = 0.78. The MPI ratio then decreases to 1.21 (%Ro equ. = 1.07) and 0.87 (%Ro equ. = 1.57). The MPI ratio increases with mean vitrinite reflectance in the range of 0.65-1.35 and then decreases in the range of 1.35-2.00 (Radke, 1988). This leads to a consistent increase of the calculated vitrinite reflectance values.

The MDR value of the unheated sample is 1.33 (%Ro equ. = 0.32). With increasing thermal maturity the MDR value sharply decreases to 0.75 (%Ro equ. = 0.64) and then gradually increases to 0.78 (%Ro equ. = 0.78), 0.91 (%Ro equ. = 1.07) and finally to 2.13 (%Ro equ. = 1.57). The MDR is value is linearly related to calculated vitrinite reflectance and to calculated T_{max} . Therefore the calculated maturities are exhibiting the same trend as the MDR. The MDR' parameter is presenting the same trend as MDR.

For the Zoharim oil samples the peak area for DBT and phenanthrene could not be calculated due to co-elution. In addition, the initial sample (% Ro equ. = 0.64) does not contain a detectable amount of benzothiophenes, methyl dibenzothiophenes or any methylphenanthrenes. The pristane/phytane ratio in the initial sample is 2.31. This ratio increases with thermal maturity to 3.55 (%Ro equ. = 0.78) and then to peak value of 5.31 at (%Ro equ. = 1.07). The ratio then decreases to a final value of 3.74 at %Ro equ. = 1.57.

The MDBTs/methyl phenanthrenes ratio value at Ro equ. = 0.78 is 1.40. The ratio exhibits a trend of a gradual decrease with increasing thermal maturity. At %Ro. equ. = 1.07 the MDBTs/methyl phenanthrenes ratio is 0.91. At %Ro. equ. = 1.57 the MDBTs/methyl phenanthrenes ratio is 0.86.

The MPR ratios calculated start with 3.57 at %Ro equ. of 0.78. The ratio then decreases to 2.17 (%Ro equ. = 1.07) and then decreases to a final ratio of 1.97 at %Ro equ. of 1.57.

The MPI ratios start with 1.23 (%Ro equ. = 0.78) and then decrease to 1.09 (%Ro equ. = 1.07) and to the minimum ratio of 1.03 at %Ro equ. = 1.57.

The MDR ratios start with 0.76 (%Ro equ. = 0.78) and then increases to 0.92 (%Ro equ. = 1.07) and to a final ratio of 1.13 (%Ro equ. = 1.57). The MDR' parameter shows the same trend as MDR.

Table IX- Parameters (1-13) calculated from the GC-MS chromatogram peaks of the Zoharim experiment and naturally- occurring hydrocarbons analyzed in this study. See section 3.2.10 for description of each parameter.

| | Sample | %Ro equ. | DBT/PHE | MDBT/MP | BT's/DBT's | MPI 1 | Rc ₁ (%) | MPR | Rc ₂ (%) | MDR | Rc ₃ (%) | Tmax _{calc.} (°C) | MDR' | Pr/Ph |
|-------------------------------|--------------|----------|---------|---------|------------|-------|---------------------|-------|---------------------|-------|---------------------|----------------------------|-------|-------|
| Zoharim Bitumen | Unheated | 0.32 | 0.96 | 1.17 | 2.4 | 0.77 | 0.85 | 2.37 | 1.36 | 1.33 | 0.66 | 431 | 0.57 | 0.64 |
| | Ex41 | 0.64 | 2.30 | 1.20 | 2.0 | 1.04 | 1.01 | 1.80 | 1.23 | 0.75 | 0.58 | 426 | 0.43 | 2.56 |
| | Ex43 | 0.78 | 1.87 | 0.85 | 5.0 | 1.31 | 1.18 | 2.10 | 1.30 | 0.78 | 0.58 | 426 | 0.44 | 3.06 |
| | Ex47 | 1.07 | 0.78 | 0.67 | 1.2 | 1.21 | 1.88 | 1.95 | 1.27 | 0.91 | 0.60 | 428 | 0.48 | 2.70 |
| | Ex42 | 1.57 | 0.47 | 0.45 | 0.8 | 0.87 | 2.08 | 1.66 | 1.19 | 2.13 | 0.72 | 436 | 0.68 | ----- |
| Zoharim oil | Ex41 | 0.64 | ----- | ----- | ----- | ----- | ----- | ----- | ----- | ----- | ----- | ----- | ----- | 2.31 |
| | Ex43 | 0.78 | ----- | 1.40 | ----- | 1.23 | 1.13 | 3.57 | 1.56 | 0.76 | 0.58 | 426 | 0.43 | 3.55 |
| | Ex47 | 1.07 | ----- | 0.91 | ----- | 1.09 | 1.95 | 2.17 | 1.32 | 0.92 | 0.60 | 428 | 0.48 | 5.31 |
| | Ex42 | 1.57 | ----- | 0.86 | ----- | 1.03 | 1.98 | 1.97 | 1.27 | 1.13 | 0.63 | 429 | 0.53 | 3.74 |
| Dead Sea Basin samples | Emunah 1 | ----- | 1.16 | 1.51 | ---- | 0.87 | 0.91 | 1.52 | 1.15 | 2.54 | 0.74 | 438 | 0.72 | 1.11 |
| | Zuk Tamrur 3 | ----- | 1.06 | 1.69 | ---- | 0.75 | 0.84 | 1.52 | 1.15 | 1.82 | 0.70 | 434 | 0.65 | 1.78 |
| | Gurim 4 | ----- | 0.77 | 1.58 | ---- | 0.87 | 0.91 | 1.38 | 1.10 | 2.11 | 0.72 | 435 | 0.68 | 1.26 |
| | Heimar | ----- | 0.19 | 1.81 | ---- | 0.84 | 0.89 | 1.28 | 1.07 | 0.16 | 0.44 | 421 | 0.14 | 0.48 |

4.3.2. Geochemical properties of residual rocks

Spent rocks from the Zoharim experiments were analyzed by Rock-Eval and LECO to determine their geochemical parameters. The results are presented in Table X.

The *SI* value reaches its peak at %Ro equ. = 0.78 and then declines with increasing thermal maturity in agreement with peak bitumen content (Figure 14). The *S2* value, which represents the rock's potential to produce hydrocarbons upon maturation declines from an initial 79.6 mg_{HC}/g_{rock} to final 4.6 mg_{HC}/g_{rock} as thermal maturation increases. The Hydrogen Index decreases with increasing thermal maturity from an initial 650.5 mg_{HC}/g_{TOC} to final mg_{HC}/g_{TOC}. The Oxygen Index is low during the whole experiment with values below 8 mg_{HC}/g_{TOC}. Total Organic Carbon (TOC) decreases from an initial 12.2% to final 8.3%. A similar trend is observed for the total sulfur which decreases from an initial 1.56% to final 0.89%.

T_{max} increases from early maturity (421°C) at %Ro equ. = 0.64 to overmature (496°C) at %Ro equ. = 1.57. The Production Index increases with thermal maturity from an initially low value of 0.06 to 0.19 at %Ro equ. = 1.07. Production Index then decreases to 0.15 at %Ro equ. = 1.57. The final high Production Index indicates the rock's declining hydrocarbon production potential.

Table X- Results of Rock-Eval pyrolysis and LECO analysis for the Zoharim experiments spent rock.

| | %Ro equivalent | <i>SI</i> ($\frac{mg_{HC}}{g_{rock}}$) | <i>S2</i> ($\frac{mg_{HC}}{g_{rock}}$) | <i>T_{max}</i> (°C) | TOC (wt. %) | HI ($\frac{mg_{HC}}{g_{TOC}}$) | OI ($\frac{mg_{HC}}{g_{TOC}}$) | PI | Sulfur (Wt. %) |
|------|---------------------------|--|--|--|------------------------|--|--|-----------|---------------------------|
| Ex41 | 0.64 | 5.5 | 79.6 | 421 | 12.2 | 650.5 | 6 | 0.06 | 1.56 |
| Ex43 | 0.78 | 8.5 | 67.9 | 432 | 12.3 | 550 | 4.5 | 0.11 | 1.47 |
| Ex47 | 1.07 | 7.5 | 31.7 | 445 | 10.1 | 313.5 | 5 | 0.19 | 1.03 |
| Ex42 | 1.57 | 0.8 | 4.6 | 496 | 8.3 | 55 | 7.5 | 0.15 | 0.89 |

4.4 Naturally-occurring hydrocarbons

Five samples of naturally-occurring hydrocarbons were analyzed for sulfur content, API gravity, viscosity, SARA fractionation and molecular markers.

Emunah 1: This oil sample has sulfur content of 2.19%, API gravity of 31.4 and kinematic viscosity (at 40°C) of 6.85 cSt. The sample has saturate fraction of 69%, aromatic fraction of 19%, resin fraction of 4% and asphaltene fraction of 8% (Figure 23). The DBT/Phenanthrene ratio of the sample is 1.16 which is the highest value measured in the naturally occurring samples group. The MDBT/Methyl phenanthrene ratio is 1.51 which is the lowest value measured in the group. The calculated vitrinite reflectance based on MPI, MPR and MDR is 0.91, 1.15 and 0.74 respectively. The calculated T_{\max} is 438°C. The Pristane/Phytane ratio of the sample is 1.11.

Gurim 4: This oil sample has sulfur content of 4.41%, API gravity of 17 (Tippee, 2001). Its kinematic viscosity was not measured due to very limited sample availability. The sample has a saturate fraction of 67%, aromatic fraction of 18%, resin fraction of 6% and asphaltene fraction of 12% (Figure 23). The DBT/Phenanthrene ratio of the sample is 0.77. The MDBT/Methyl phenanthrene ratio is 1.58. The calculated vitrinite reflectances based on MPI, MPR and MDR are 0.91, 1.10 and 0.72 respectively. The calculated T_{\max} is 435°C. The Pristane/Phytane ratio of the sample is 1.26.

Zuk Tamrur 3: This oil sample has sulfur content of 3.75%, API gravity of 21.5 and kinematic viscosity (at 40°C) of 124.92 cSt. The sample has saturates fraction of 41%, aromatic fraction of 25%, resin fraction of 16% and asphaltene fraction of 17% (Figure 23). The DBT/phenanthrene ratio of the sample is 1.06. The MDBT/methyl phenanthrene ratio is 1.69. The calculated vitrinite reflectance based on MPI, MPR and MDR is 0.84, 1.15 and 0.70 respectively. The calculated T_{\max} is 434°C. The pristane/phytane ratio of the sample is 1.78.

The sample provided contained water which could be seen on the bottom of the container, thus suggesting the oil might have been produced as an emulsion or degraded by water washing.

Nahal Heimar asphalt: This asphalt sample has sulfur content of 8.69%. The sample has saturate fraction of 7%, aromatic fraction of 6%, resin fraction of 15% and asphaltene fraction of 72% (Figure 23). The DBT/Phenanthrene ratio is 0.19 which is the

lowest value measured in the naturally occurring samples group. The MDBT/Methyl phenanthrene ratio is 1.81 which is the highest value measured in the group. The calculated vitrinite reflectance based on MPI, MPR and MDR are 0.89, 1.07 and 0.44 respectively. The calculated T_{max} value is 421°C. The pristane/phytane ratio is 0.48.

Tamar asphalt: This asphalt sample was obtained from asphalt lenses that appear in cross bedded clastic sediments of the Pleistocene Lisan formation. The asphalt was separated from the sand grains it covered by dissolving a lens of asphalt in dichloromethane and then filtering the sand out of solution. The sample was determined to contain 17.4% (by weight) of organic matter and 82.4% of sand and clay, recovery was 99.8%. The recovered asphalt has sulfur content of 6.08%. Further attempts to separate the maltene fraction from the asphalt sample proved to be unsuccessful as none of it dissolved in the *n*-pentane (Figure 23).

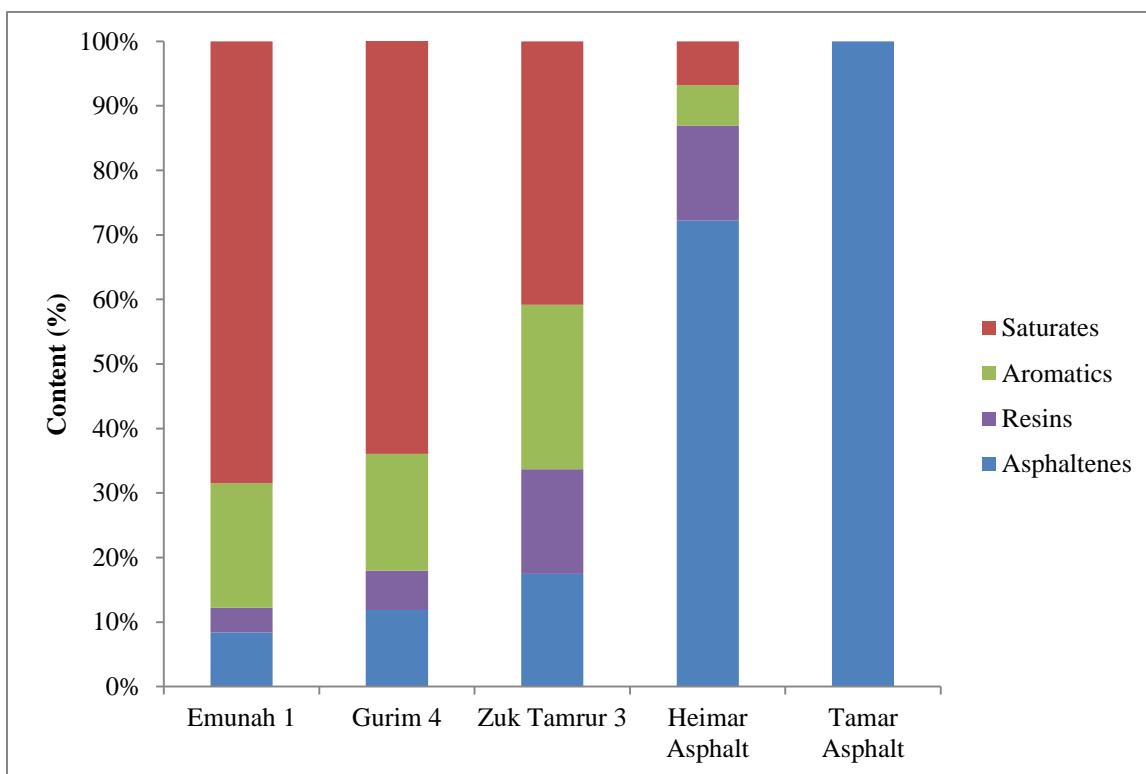


Figure 23. Results of SARA fractionation for the naturally- occurring hydrocarbons from the Dead Sea basin analyzed in this study.

5. Discussion

5.1. Physical properties of pyrolysis oils

5.1.1. Factors affecting oil density

The API gravity of oils produced in the Aderet experiment increases with thermal maturation. Chemically, the main changes that occur within the oil as the level of maturity increases are a decrease of asphaltenes and resins with an increase of aromatic and saturate compounds. The length of saturate molecules shortens with increasing maturation due to thermal cracking of bonds (Ryan et al., 2010). The chain length shortening leads to a density decrease which in turn leads to an overall decrease of oil density and an increase in API gravity (Tissot and Welte, 1984). The relation between *n*-alkanes and API gravity in the Aderet experiments (Figure 24) is in agreement with the expected trend for all samples except the highest maturity sample of the high gradient experiment. That deviation from the expected trend is probably due to degradation of the oil sample by oxidation.

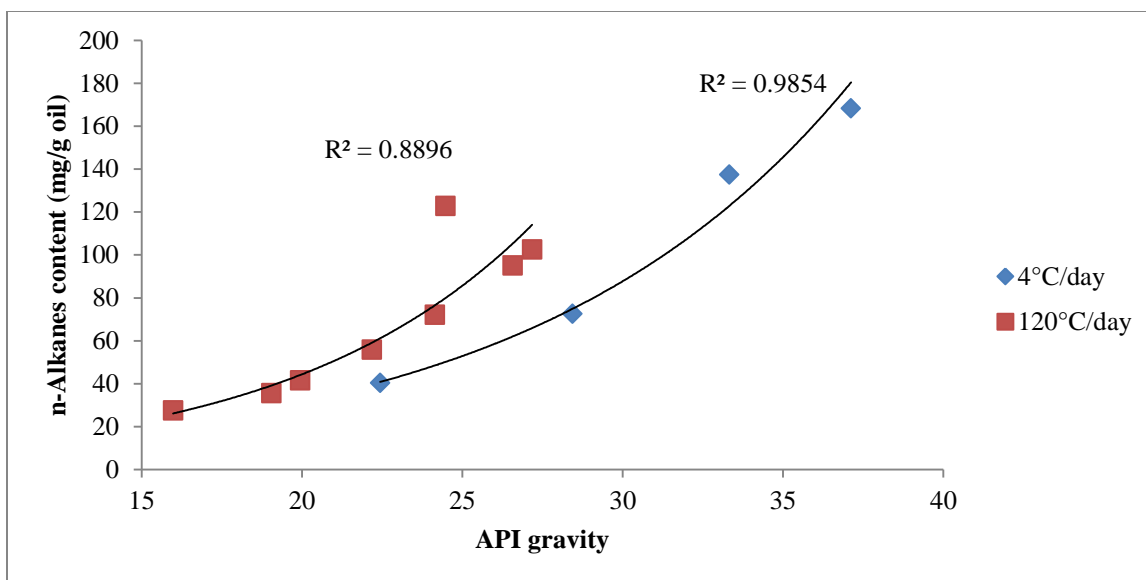


Figure 24. The change of *n*-alkanes content (mg/g oil) against °API gravity for the Aderet experiment at different heating gradients (4°C/day and 120°C/day). Black curves represent exponential trend lines, the R^2 values are 0.9854 for 4°C/day gradient and 0.8896 for 120°C/day gradient. Error bars are smaller than the symbols.

Ryan et al., (2010) have demonstrated that heating gradient applied in the pyrolysis processes had an inverse relation to the API gravity of the oil produced: lower heating gradient led to the production of high API gravity oils. The results of the Aderet experiments are in an agreement with the observations made by Ryan et al., (2010). In addition, the API gravities reached in the Aderet low heating gradient experiment are similar to those observed by Ryan et al., (2010) for semi-open anhydrous pyrolysis experiments performed on the Green River Mahogany shale under a similar heating gradient.

An additional outcome of the *n*-alkanes enrichment in the oil is a decrease of the oil sulfur content since the saturate fraction is sulfur-poor. Figure 25 shows the decrease of the Aderet oils sulfur content with an increase of their density. A similar trend of sulfur content decreasing with increasing level of maturity was observed for oils sourced from a type IIS kerogen of the Monterey formation in the work of Baskin and Peters (1992), Baskin and Jones (1993) and Ryan et al, (2010).

A plot of oil sulfur content vs. oil API gravity can be used to distinguish between oils that originated from type IIS kerogen to those originated from sulfur-poor type II kerogen, as was demonstrated by Orr (2001). As expected, the oils from both Aderet experiments fall within the type IIS kerogen region (Figure 25). Likewise, oils of the Dead Sea basin that originated from the same source rock and oils from California that were generated from the Monterey formation (Orr, 1986) fall within the type IIS kerogen region. The pyrolysis oils differ from the Dead Sea basin oils by having significantly higher sulfur content for all of the API gravity range except the highest API values in each experiment. The anomalously high sulfur content of the pyrolysis oils is the result of preferential break of relatively weak carbon - sulfur bonds which in turn lead to high alkyl-thiophene content in the oil. As thermal maturation progresses cracking of carbon bonds and alkyl-thiophenes leads to an increase of API gravity with a decrease of sulfur content. In the Aderet experiments the end of sulfur- cracking zone can be regarded as %Ro equ. = 1.13-1.16. Indeed oil generated at maturity higher than %Ro equ. = 1.16 has properties similar to naturally-occurring oils.

A similar trend of API gravity vs. sulfur content is observed for oils from the Santa Maria basin that were generated from the Monterey formation (Orr, 1986) and oils from the Dead Sea basin. The two formations have distinctively different lithology- the Monterey formation is siliceous shale (Behl, 1999) while the Ghareb formation is a bituminous chalk. Nevertheless, both formations are rich with organic matter that was deposited during upwelling event in a basin with highly reducing conditions which led to the accumulation of type IIS kerogen in both formations. The fact that a similar trend of API gravity to sulfur content is observed for both oil groups suggests the physical properties of the oils depend mostly on the type of kerogen that they have originated from and not on the lithology of the source rock.

Baskin and Jones (1993) noted that sulfur content versus oil API gravity relation is affected by degradation. They stated that during degradation the sulfur content of offshore California oils is increasing and the API gravities are decreasing. The explanation for this observation is that during degradation by either water washing or biological processes the aromatic and saturate fractions are being consumed. The

degradation leads to oil enrichment with asphaltenes and resins which are sulfur rich and have low API gravity (Price, 1980). The Dead Sea oils are known to be degraded to some extent (Tannenbaum, 1983) and present a trend of degradation as expected (Figure 25). The highest maturity sample of the high gradient experiment has lower API gravity and higher sulfur content than that expected by trend observed during the experiment. The observed deviation suggests this sample has undergone degradation.

Although it is not the intent of this research to study the origin of the oils from the Heletz and Kokhav fields, several observations for oil density and sulfur content are interesting enough to be discussed in some detail.

The geochemistry of the Heletz oils was described by Bein and Sofer (1987) who suggested the Jurassic Barnea formation (Bajocian- Bathonian) was the source rock for the oils. In their work they analyzed the elemental composition of the kerogen in the Barnea formation and showed the S/C ratio to be higher than 0.04 in some parts of the section. The oil properties presented in Figure 25 show that the Heletz and Kokhav oils have very high sulfur content relative to their API gravity.

The high S/C ratio of the Barnea kerogen and the properties of the oils produced at the Heletz and Kokhav fields suggest the Barnea formation kerogen is a type IIS (Orr, 1986; Orr, 2001).

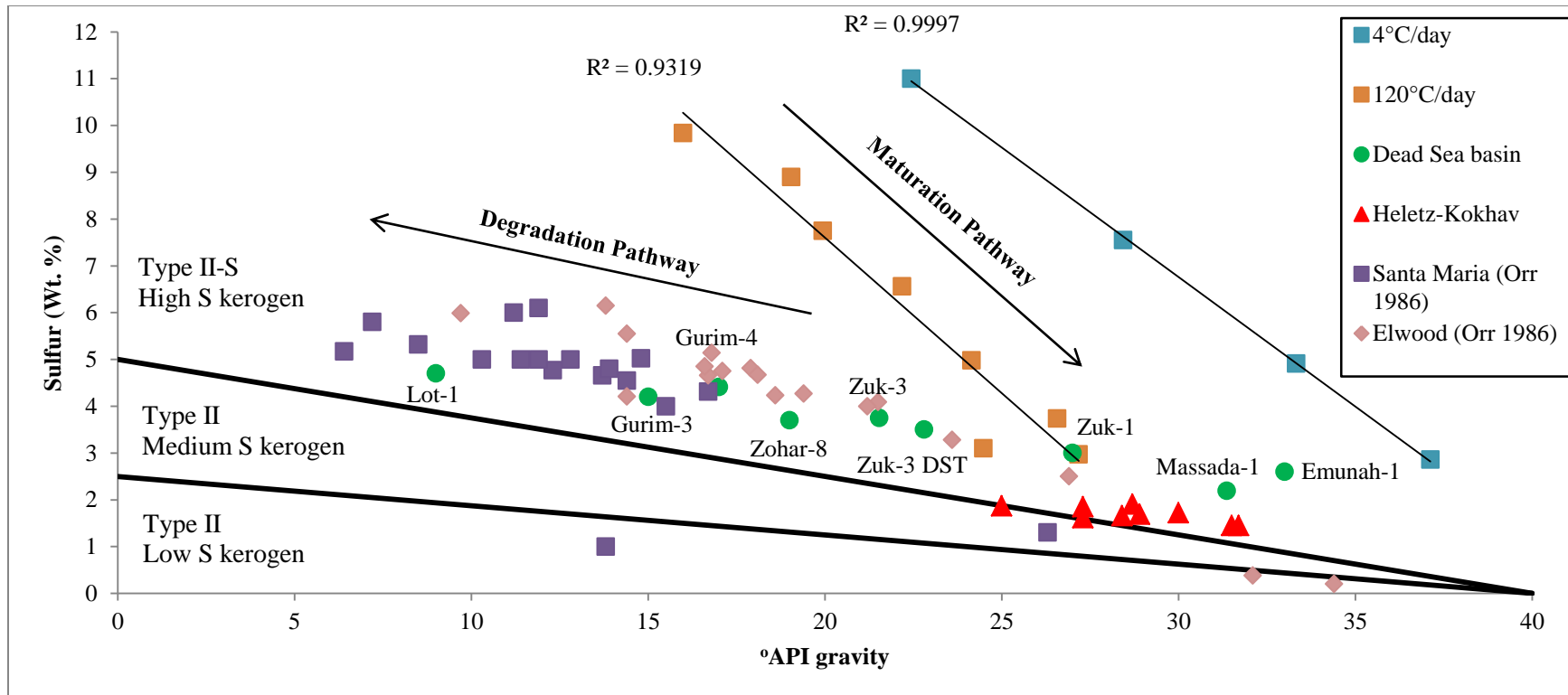


Figure 25. The relation of sulfur (wt. %) to °API gravity of oils. Boundary lines are from Orr (2001). Oil sample data from Heletz-Kokhav fields taken from a database provided by the Department of Energy (National Institute for Petroleum and Energy Research, 1995). Data of oils from the Santa Maria basin in California is from Orr (1986). Red triangles represent oils produced at Helez and Kokhav fields of the coastal plain in Israel. Green circles represent oils produced at the Dead Sea basin. Black lines represent linear trend lines, the R^2 values are 0.9997 for 4°C/day gradient and 0.9319 for 120°C/day gradient in the Aderet experiments. Error bars are smaller than the symbols

5.1.2. Pyrolysis oils viscosity

Baskin and Peters (1992) showed that viscosity of oils decreases with increasing level of maturity. In the Aderet experiment an overall decrease of viscosity with increasing thermal maturity was observed yet the variation of viscosity during the experiment is irregular (Figure 9). The relation of alkyl-thiophenes to kinematic viscosity is irregular as well for most of the experiments length (Figure 26). The only part of the experiments where a distinctive relation between alkyl thiophene content and kinematic viscosity was observed is in the three lowest viscosity samples of the low heating gradient experiment where the alkyl-thiophene content is decreasing gradually with decreasing viscosity. In the high heating gradient experiment at the viscosities range 3.5-2.5 cSt the alkyl-thiophenes concentration is kept constant (within error). The irregular relation of kinematic viscosity to alkyl-thiophene content was also observed in the low heating gradient experiment where the alkyl-thiophene content changes rapidly from 42.87 mg/g_{oil} to 69.51 mg/g_{oil} with viscosity changing by less than 0.1 cSt.

These observations suggest that alkyl-thiophenes may play a role in determining the kinematic viscosity of oil produced by pyrolysis as was observed for several high maturity samples of the low heating gradient experiment, but the alkyl-thiophenes content and the thermal maturity of the oil cannot account for the variation of the kinematic viscosity during the entire duration of the experiments and especially in the low maturity samples. Therefore, for the majority of the oil samples analyzed, the variation of oil viscosity cannot be addressed by the level of thermal maturity or alkyl-thiophenes content alone.

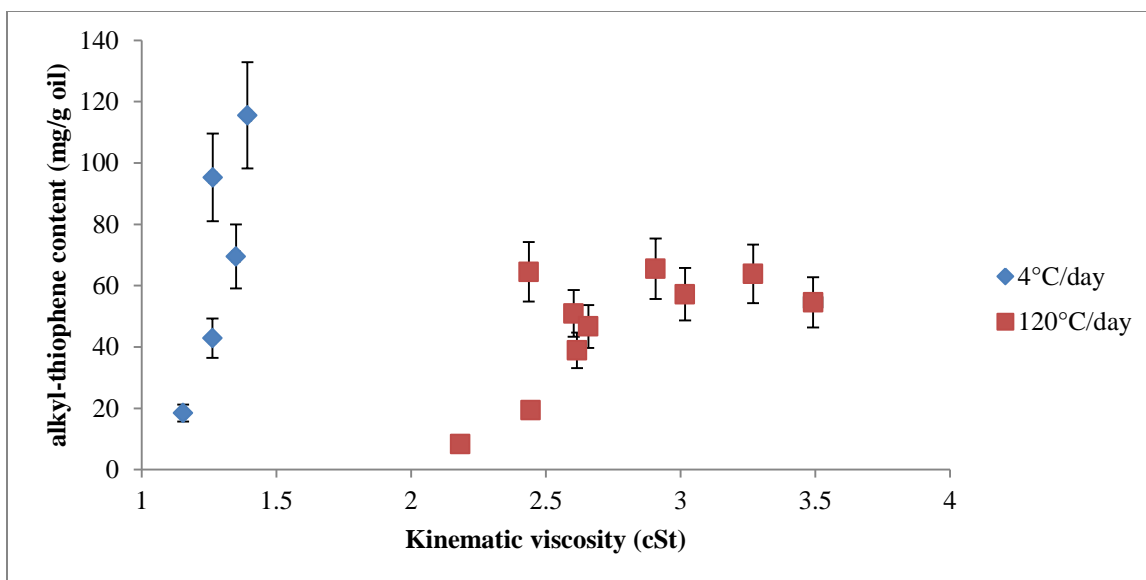


Figure 26. The change of alkyl-thiophenes content (mg/g oil) against kinematic viscosity (cSt) for the Aderet experiment at different heating gradients (4°C/day and 120°C/day). Data of the 120°C/day experiment alkyl-thiophenes concentration is from Amrani et al., in preparation. Error bars are smaller than the symbols.

Figure 27 shows the relation of kinematic viscosity to API gravity in naturally occurring, high sulfur ($S > 0.5\%$; Baskin and Jones, 1993) oils of the California coast. The presented data set is an extended version of the data presented by Baskin and Peters (1992). Also, on the same plot are oils of the Dead Sea basin, Heletz - Kokhav field and the Aderet experiment oils. Clearly, naturally-occurring oils follow a distinct trend of viscosity decrease with API gravity increase. The oils of the Dead Sea basin and those of the coastal plain behave similarly to the California high sulfur oils.

When compared to naturally-occurring oils, the Aderet oils have distinctively lower viscosities in the whole range of API gravities because they are middle range distillates with very little asphaltenes and resins. The difference in viscosities reaches two orders of magnitude in the low API gravity oils. Values of the same order of magnitude are only reached at high API gravities. This difference is most likely the outcome of the oil collection method during pyrolysis experiments: oil is collected by distillation where the distillation temperature is the reactor temperature at time of collection. The operational temperatures of the reactor are not high enough to distill high boiling point compounds of the asphaltene group. This leads to a condition where produced oils have lower

asphaltene content during the experiment. In general, asphaltenes are the heaviest components of oil and have very high viscosity in the range of 100,000 cSt (Luo & Gu, 2007). Asphaltenes are known to have a major effect on the viscosity and are the probable cause for the noted difference between distillation pyrolysis and naturally-occurring oils.

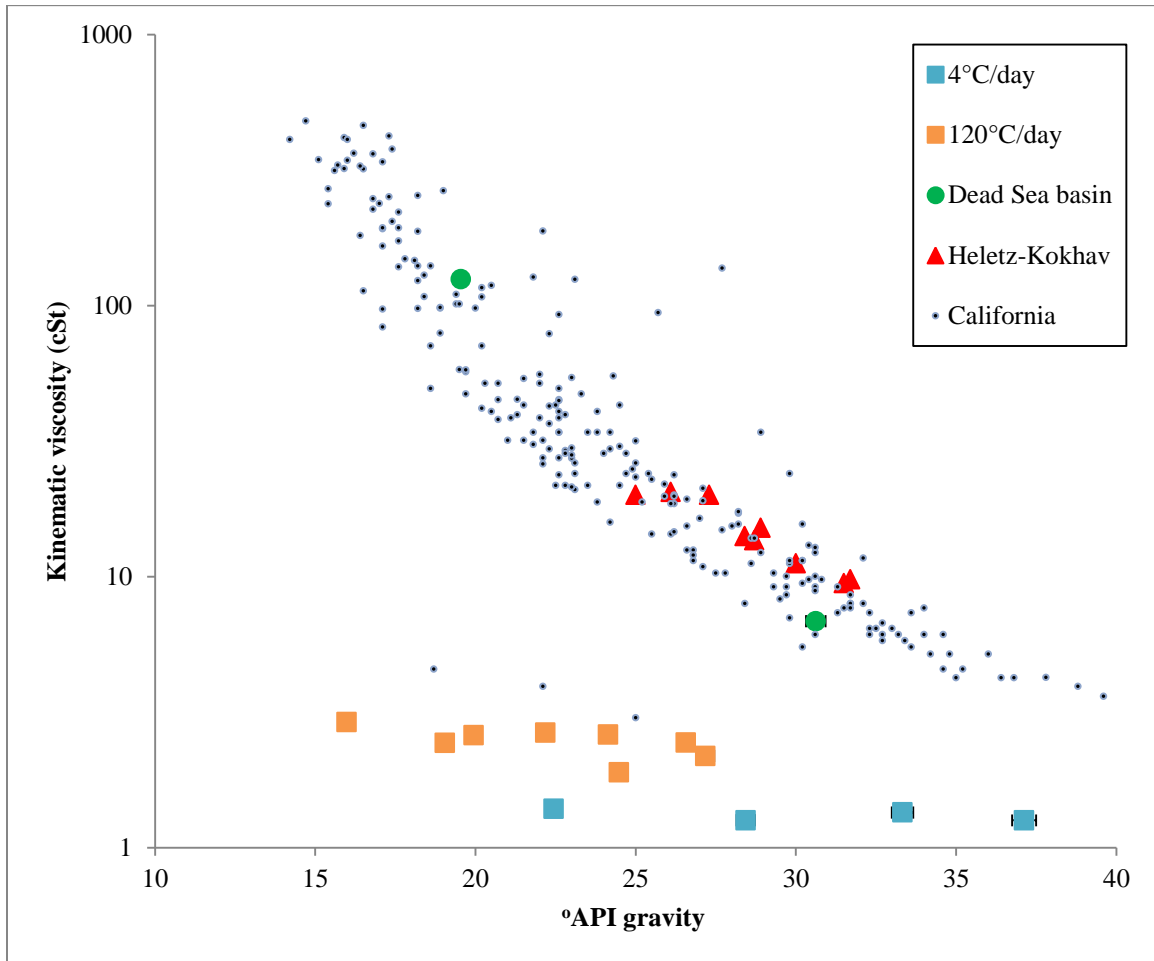


Figure 27. The relation of kinematic viscosity (cSt) (Logarithmic scale) to API gravity (°) of oils. Oil sample data from Heletz and Kokhav fields and California taken from a database provided by the Department of Energy (National Institute for Petroleum and Energy Research, 1995). Black dots represent oils produced in California with sulfur content higher the 0.5%. Red triangles represent oils produced at Helez and Kokhav fields. Green circles represent oils produced at the Dead Sea basin. Orange and turquoise squares represent the Aderet oils produced by pyrolysis.

5.2. Evolution of sulfur species

5.2.1. In oil

The evolution of the studied sulfur species in the oil can be divided into two processes: The first is the alkyl-thiophenes “window” which spans from the start of the experiments at %Ro equ. = 0.43 and reaches its end at %Ro equ. = 1.16-1.95 (depends on the heating gradient). The second is the benzothiophene window which initiates at the start of the experiments and lasts until the end of the experiments. These two processes run parallel and have stages of concentration increase and decrease yet the concentrations of the two groups are different with the alkyl-thiophenes concentration being significantly higher than that of the benzothiophenes. The peak of alkyl-thiophene window is reached at %Ro equ. = 0.74-0.78 in the low gradient experiments and at %Ro equ. = 0.65 in the high gradient experiment.

In contrast to the analyzed groups of thiophenes, the total sulfur content of the oil has a trend of decrease from the start of the experiments to their end. If the analyzed groups of thiophenes had a major influence on the total sulfur content of the oil we would expect to see variation of total sulfur content that is similar to the analyzed thiophene groups. The dissimilarity between the trends indicates that total decrease of sulfur content cannot be explained by the formation and decomposition of the analyzed sulfur species alone.

These observations suggest there must be a different, more abundant or sulfur-rich group of compounds within the oil that dictate the total sulfur content. The fact that it was not observed on the GC-MS chromatograms suggest these groups are either unresolved by the detector or have a retention time below 7 minutes and were therefore missed during the solvent delay.

An attempt to compare the sulfur speciation of pyrolysis oil to that of naturally-occurring oil was proven to be unsuccessful. No alkyl- or benzothiophenes were detected in the naturally-occurring oils. In fact, the only thiophenes detected were dibenzothiophenes and their alkyl forms. This gap of sulfur speciation is most likely due to the difference between pyrolysis distillation and natural-sourcing of oil as alkyl-thiophenes are unstable over geological time. Another factor affecting the sulfur

speciation gap can be the major difference in time-temperature relation between the laboratory where the high heating gradients and short time period of experiments aid the preservation of sulfur species that are unstable under natural conditions in the field where heating gradient is order of magnitude of lower and time periods are in the scale of millions of years rather than months. In addition, the gap can be attributed to facies difference between the Shfela basin and the Dead Sea basin as was suggested for various oils derived from the Monterey formation by Waldo (1991).

5.2.2. In bitumen

The sulfur content of the bitumen is dictated by the sulfur content of its two components: Maltene and Asphaltene. Figure 17 presents the relation of the bitumen, asphaltene and maltene sulfur content against the level of thermal maturation. In the low maturity range (%Ro equ. = 0.32- 0.78) the majority of the sulfur is in the asphaltene fraction. At %Ro equ. = 1.07 the bitumen's sulfur content is identical to that of his maltene and asphaltene fractions. This decrease of sulfur content is explained by preferential loss of sulfur by cracking of weak sulfur bonds and release of volatile sulfur compounds that are removed to the oil fraction and as H₂S that is released from the pyrolysis system. At the maturities range of %Ro equ. = 1.07-1.57 the bitumen sulfur content is increasing, indicating that from this stage the bitumen is losing more carbon compared to sulfur. Baskin and Peters (1992) observed a similar trend and attributed it to a stage where the easily removed sulfur species had been removed from the bitumen and the more difficult to remove sulfur species are remaining in the bitumen fraction. This hypothesis is supported by the relative increase of the aromatic fraction in the final bitumen sample. The aromatic fraction contains the benzo- and dibenzothiophenes that tend to concentrate in the bitumen. The concentration of all benzo- and dibenzothiophenes analyzed is increasing in the bitumen during the transfer from %Ro equ. = 1.07 to 1.57. Again this supports the mechanism proposed by Baskin and Peters (1992).

The behavior of the alkyl-thiophenes group is identical to their behavior in the oil phase: Increase at low thermal maturities (%Ro equ. = 0.32- 0.78), peak at %Ro equ. = 0.78 and then a decrease of concentration to a constant value. Similar behavior of the

alkyl-thiophenes was observed in bitumen extracted in flash pyrolysis experiments of the Kimmeridge formation kerogen performed by Eglinton et al., (1990). They referred the constant alkyl-thiophenes content at high maturities to a condition where the loss of alkenes from the bitumen is high enough to keep the relative concentration of alkyl-thiophenes constant. The benzothiophenes appear to behave similarly to the oil phase until %Ro equ. = 1.07 where it reaches a minimum concentration. Instead of a gradual decrease with increasing thermal maturity the concentration is rapidly increasing. A similar trend of bimodal distribution of benzothiophenes concentration was observed by Di Primio (1995) in pyrolysis products of Italian carbonate source rock and by Santamaria et al. (1998) in Tithonian source rock from Sureste Basin in Mexico.

5.3. Maturation of the organic matter

5.3.1. Correlation of T_{max} to Easy $R_0\%$

Correlation of different thermal maturity parameters is a useful tool in basin modeling. Among the most popular maturation parameters are the RockEval T_{max} parameter and optical vitrinite reflectance (Peters et al., 2005). If a source rock sample is not available for direct measurement of thermal maturity one has to estimate the maturity by other means which include molecular maturity markers in available hydrocarbons and modeling of the thermal maturity based on the time-temperature relation during the rock period of maturation (Waples, 1981). Among the most extensively used thermal maturity parameters is the Easy $R_0\%$ model (Sweeney and Burnham, 1990).

The Zoharim experiment provides a unique opportunity to correlate the Easy $R_0\%$ model to the RockEval T_{max} parameter for a type IIS kerogen containing source rock over a wide range of thermal maturities (Figure 28).

The main assumption behind the proposed correlation is that the increase of T_{max} versus modeled %Ro is linear between data points. The correlation displays a good agreement between anhydrous pyrolysis of Ghareb source rock to the hydrous pyrolysis of the same source rock (Amrani et al., 2005). Samples of the La-Luna formation which contain type IIS kerogen are in good agreement with the trend for both lab pyrolysis

experiments (Burnham et al., 1992) and vitrinite reflectance measured on naturally occurring mature source rock (Zumberge, 1984).

An attempt to compare measured vitrinite reflectance (%Ro) from the Monterey formation and Tithonian source rock from Sureste Basin in Mexico (Santamaria et al., 1998) to the modeled trend has only partial success in the T_{max} range of 430-460 °C. Samples with very high T_{max} (>500°C) such as the Aderet experiment residual rock samples and two of samples in Burnham et al. (1992) dataset do not fit the correlation at all. To conclude, the proposed correlation between T_{max} and EasyRo% provides good results in the T_{max} range of 405-450 °C or EasyRo% range of 0.3-1.2.

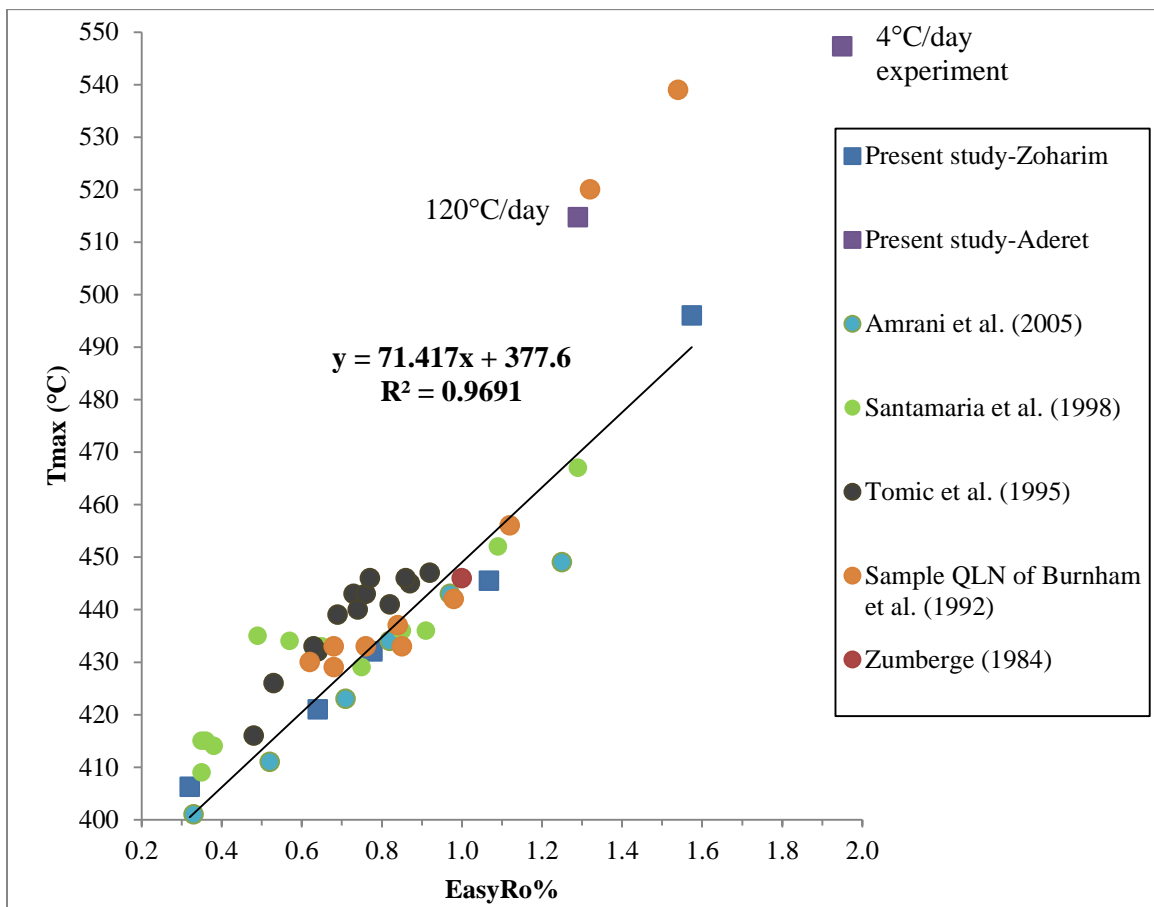


Figure 28. Correlation between the modeled %EasyRo to measured T_{max} (°C) for the type IIS kerogen. Gradient labels refer to the two Aderet experiments. The solid black line represents a linear regression: T_{max} (°C) = 71.417 • (EasyRo %) + 377.6. Correlation coefficient: $R^2=0.9691$.

5.3.2. Early maturation of the organic matter

Early generation of oil from sulfur-rich kerogens has been noted by several studies in the past (Orr 1986; Sinninghe Damsté and de Leeuw 1990; Baskin and Peters 1992). The only maturity values for the start of the oil window of type IIS kerogen was proposed by Baskin and Peters (1992) who defined the oil window to start at %Ro of 0.3-0.35 for the Israeli oil shale and at T_{\max} of 410°C for the Monterey formation source rock.

By utilizing the correlation of EasyRo% model to the RockEval T_{\max} as described above (5.3.1) it is possible to define the start of the oil window for the Israeli oil shale at T_{\max} 412-414°C or EasyRo% of 0.43-0.52. The peak of the oil window is reached at T_{\max} 439-449°C or EasyRo% of 0.86-1.0. The end of the oil window was not reached at any of the experiments performed and oil was produced at very high T_{\max} range of 470-516°C or EasyRo% of 1.42-1.95.

The ranges described above are in good agreement with those proposed by Baskin and Peters (1992) for both start of the oil window and peak of oil window.

It is worth noting that the start and peak of the oil window in the anhydrous pyrolysis experiments of Zoharim and Aderet agree with start and peak observed in several works (Baskin and Peters (1992), Burnham et al., (1992) and Amrani et al., (2005)) in which hydrous pyrolysis of different type IIS source rock was performed. The most important work for this discussion is Amrani et al., (2005) since they have used the Ghareb formation source rock for the pyrolysis experiments but performed hydrous pyrolysis. The similar start and peak of the oil window for different types of pyrolysis methods, reactor and time-temperature heating programs suggests that the kinetics of petroleum generation for a type IIS kerogen are not affected by type of pyrolysis.

When compared to traditional definition of the oil window such as that proposed by Peters and Cassa (1994) for kerogen types I and II the concept of early maturation is emphasized: the start of oil window for the type IIS kerogen has T_{\max} of ~20°C lower than that proposed by Peters and Cassa (1994).

The peak of the oil window as defined by Peters and Cassa (1994) is at T_{\max} of 445-450°C. This range is very close to that suggested for the type IIS kerogen, thus suggesting the oil window of the type IIS kerogen starts early and spans a broader range of thermal maturities.

5.3.3. Molecular maturity and environment of deposition parameters

In their work Hughes et al., (1995) proposed the use of DBT/PHE vs. Pr/Ph plot as a method for establishing the lithology and environment of deposition of a crude oil. The reasoning for the coupling of DBT/PHE and Pr/Ph ratios lies in the fact that Pr/Ph ratio is known to be sensitive to the environment of deposition of a source and DBT/PHE ratio is known to be dependent on the lithology of source rock (Chakhmakchev and Suzuki, 1995a).

All of the hydrocarbon samples used in this study are known to be sourced from the Ghareb formation source rock yet the DBT/PHE vs. Pr/Ph plot suggests the samples are from source rocks deposited under various conditions (Figure 29). Moreover, the majority of the samples are far from region 1A and 1B which are attributed to marine carbonate source rock such as the Ghareb formation. It seems that the significant scatter of the results on the DBT/PHE vs. Pr/Ph plot is mainly due to the variation of Pr/Ph ratio. The DBT/PHE ratios values of all samples are within the expected range for marine carbonates deposited under reducing conditions such as the Ghareb formation.

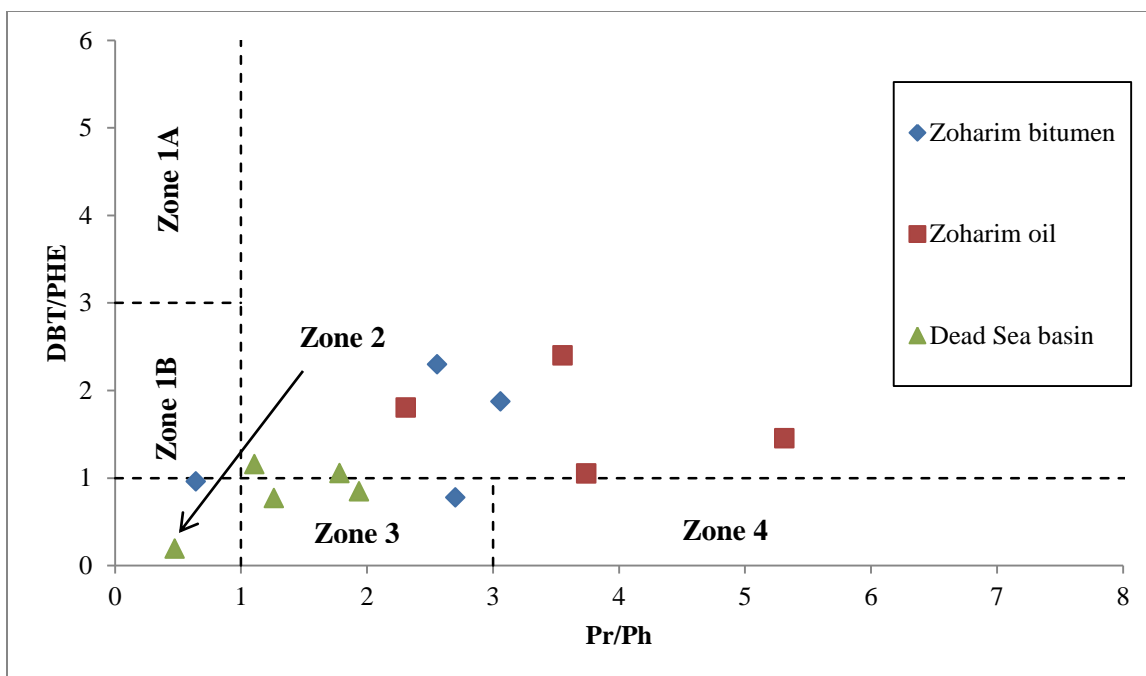


Figure 29. The relation of DBT/PHE ratio to Pr/Ph ratio for hydrocarbon samples that have originated from the Ghareb source rock. Border lines between various zones are after Hughes et al., (1995).

An additional method for determining the environment of deposition suggested by Hughes et al., (1995) is the relation of DBT/PHE ratio to the sulfur content of the oil (wt. %). When applied to the hydrocarbon samples in this study (Figure 30) the hydrocarbon samples are divided between group 3 and a region where Hughes et al., (1995) did not observe any samples. The group 3 region was suggested to host the sulfide-rich oils such as those sourced from the Monterey formation and Rozel point. The group 2 region was suggested to host thiophene-rich oils such as those from all Middle Eastern samples. The distilled pyrolysis oils and bitumens of Zoharim are clearly thiophene-rich yet none of them fits the group 2 region. Additionally, the Dead Sea basin oils sourced from the Ghareb formation are suggested to be of sulfide-rich type.

These observations suggest that the use of DBT/PHE vs. Pr/Ph or S% plots is limited to naturally occurring-oils where it should be used cautiously.

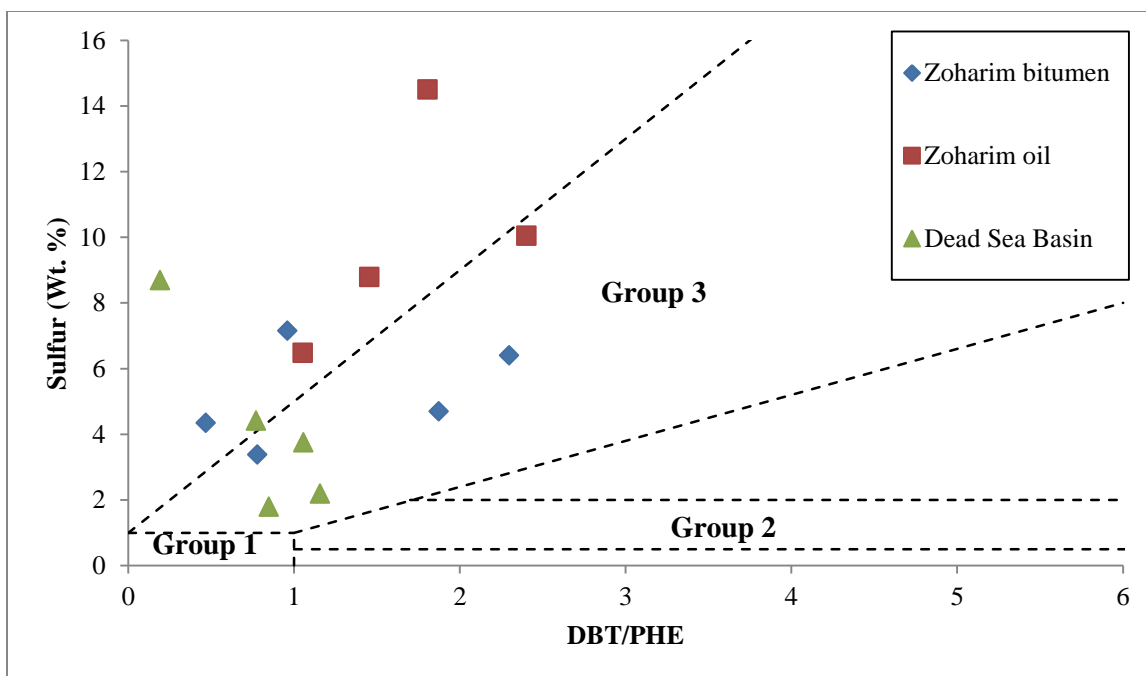


Figure 30. The relation of sulfur content (wt. %) to DBT/PHE ratio for hydrocarbon samples that have originated from the Ghareb source rock. Border lines of the various groups are after Hughes et al., (1995).

The ratios of DBT/phenanthrene and MDBT's/MP's were used for maturity assessment of the various samples of hydrocarbons. Both ratios decreased with increasing thermal maturity for bitumen and oil of Zoharim experiment. The DBT and MDBT's concentration in the bitumen increased with increasing thermal maturity during the entire duration of the experiment (Figure 22). The combination of both observations indicates the phenanthrene and methyl phenanthrenes concentrations are increasing at a greater rate than that of the benzothiophenes during thermal maturation. The application of DBT/phenanthrene and MDBT's/MP's ratios as maturity parameters is limited to their use for a set of oils or bitumens derived from the same source rock where they can be used to arrange the samples according to their level of maturity. When this rule is applied to the Dead Sea basin oils it provides a conflicting result- the DBT/Phenanthrene ratio is decreasing from Emunah oil to Heimar asphalt while the MDBT/MP's ratio is increasing for the same arrangement. The Dead Sea basin samples are known to be degraded to some extent (Tannenbaum, 1983; Rullkötter et al., 1985). Hydrocarbon samples that have been water washed are prone to the removal of DBT compared to phenanthrene because

it is more water soluble (Hughes et al., 1995). It is likely that the observed trend of DBT/Phenanthrene and MDBT's/MP's ratios for the Dead Sea basin oils is the result of degradation and therefore these ratios can be applied in cases where degradation is absent or where the study aims to monitor the degree of degradation in a specific sample.

The BT's/DBT's parameter calculated for the bitumen showed a trend of initial decrease from the starting value followed by a sharp increase to peak value and is then decline until the end of experiments (Figure 31). This trend seems to depend on the BT's concentration as the DBT's concentration is only increasing during the entire duration of the experiments. The observed trend is unlike that observed by Santamaria et al., (1998); their observed trend is a decrease of the BT's/DBT's parameter during the whole length of the experiment. The difference between both works might lie in a facies difference between the Ghareb formation and the Tithonian source rock from Sureste Basin in Mexico. The Dead Sea basin oils do not contain BT and therefore the use of this ratio for maturity analysis of the basin's oils is not possible.

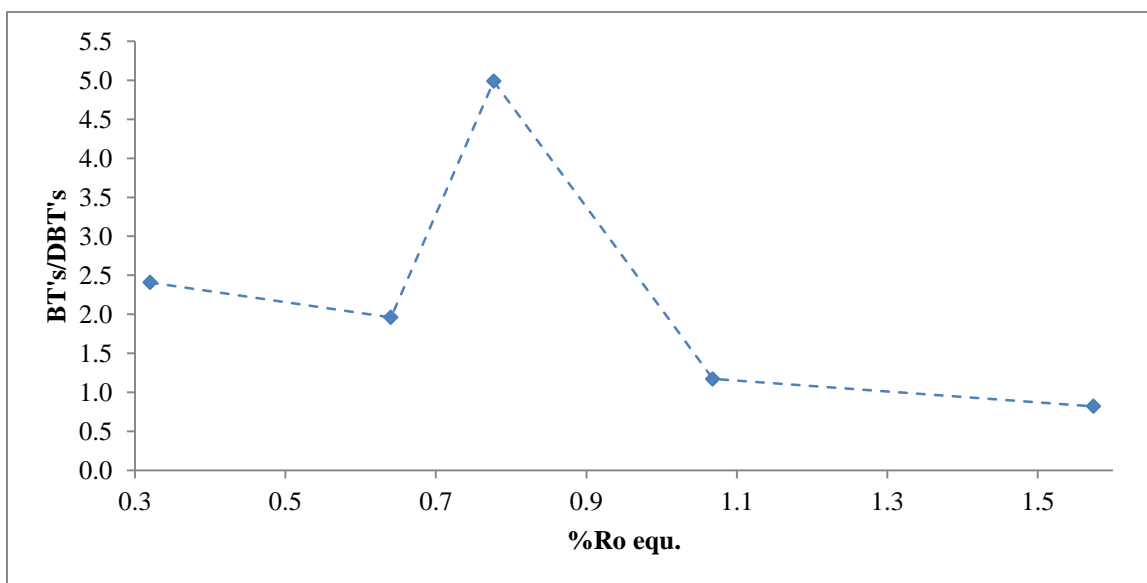


Figure 31. The relation of BT's/DBT's ratio as a function of thermal maturation (%Ro equ.) for the Zoharim experiments bitumens.

The methyl phenanthrene ratio (MPR) calculated from the Zoharim experiments showed the opposite relation to thermal maturity from that described by Radke (1988).

This observation makes the MPR parameter useless for bitumens and oils produced by pyrolysis.

The MPR calculated for the Dead Sea basin oils ranges from 1.28 to 1.52 thus suggesting the oils are from a mature - very mature source rock. This observation contradicts the findings of Rullkötter et al., (1985) who used the MPI 1 index and other molecular parameters and established levels of maturity that are below %Ro = 1.0 for all samples analyzed from the Dead Sea basin.

It is worth noting that the MPR parameter was proposed originally for coals that contain type III kerogen. Possibly the incompatibility of the MPR with other kerogens is the reason for the inverse trend observed in the pyrolysis experiments and the high values calculated for the Dead Sea basin hydrocarbons.

In contrast, the methyl phenanthrene index (MPI 1) and methyl dibenzothiophene ratio (MDR) parameters produced calculated vitrinite reflectance trends that are in agreement with those proposed by Radke (1988) for all samples except the unheated sample (%Ro equ.=0.32).

The calculated vitrinite reflectance based on MPI 1 is overestimated compared to the modeled vitrinite reflectance by the EasyR_O% model. The calculated vitrinite reflectance and T_{max} based on MDR are both underestimated compared to modeled vitrinite reflectance by the EasyR_O% and measured RockEval T_{max} for all samples except the unheated and Ex41 samples (%Ro equ = 0.32 and 0.64 respectively).

The correlation between T_{max} to MDR proposed by Radke (1988) enables the comparison of the Zoharim oil and bitumen to other type IIS oils from the literature (Figure 33). Clearly the rate at which the MDR parameter is increasing in the Zoharim experiments with respect to T_{max} is much higher than that observed by other works. Also, the Zoharim samples present a crescent-like trend (Figure 32) unlike the correlations suggested by Radke (1988) or other type IIS oils results. It appears that at the low levels of thermal maturity the MDR ratio is actually decreasing rather than increasing with maturation; this trend is observed for both the oil and bitumen of Zoharim and for the Aderet high gradient experiment. The trend of MDR decrease continues until %Ro equ. = 0.64 - 0.77 where it reverses and leads to an increase of the MDR value until the end of the experiments. Also, the initial, final and minimal value of the MDR that dictate the

magnitude of the crescent-like shape seems to be affected by the heating gradient implied in the pyrolysis with high gradient “shifting” the crescent shape to the right on Figure 32.

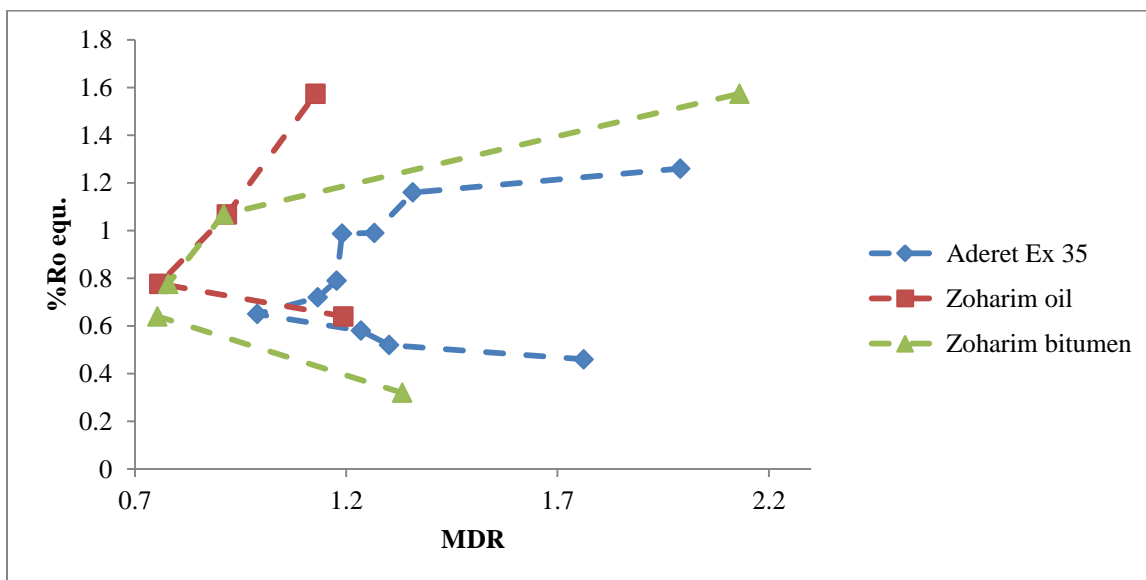


Figure 32. The relation of %Ro equ. to MDR of the hydrocarbons produced in the pyrolysis experiments of Aderet Ex35 and Zoharim. A crescent- like trend is observed.

As was noted previously, one of the striking differences between the genesis of pyrolysis oils compared to naturally-occurring oils is the difference in heating gradient which is orders of magnitude higher in the lab than that in the field. The MDR values of the pyrolysis hydrocarbons combined with the very high heating gradient applied suggest that the conversion of 1-MDBT to 4-MDBT in the pyrolysis oil and bitumen is a process affected mainly by time rather than temperature. A similar effect was observed for samples of the Posidonia shale formation that experienced abnormally high thermal gradients due to heating by magmatic intrusions (Radke and Willsch., 1994). If in fact such a kinetic effect takes place, it will lead to high T_{max} values being observed at MDR values much lower than expected for naturally-occurring samples. In addition, the MDR value of oil or bitumen is highly dependent on the distribution of the MDBT isomers in the original source rock- thus making it dependent on the lithology of the source rock. Differences of source rock lithology of the various oils compared in Figure 33 may also account for the different trends observed.

The calculated vitrinite reflectance based on MPI and MDR for the naturally-occurring oils from the Dead Sea basin produced a wide range of maturities that generally agree with the levels of maturity proposed by Rullkötter et al., (1985) for Dead Sea basin oils. The calculated T_{\max} based on the MDR parameter provides a range of 434-438°C for the Dead Sea oils, meaning they were generated from the Ghareb formation just below the peak of the oil window (439-449°C).

The Heimar asphalt sample has very low calculated vitrinite reflectance based on MDR parameter, probably due to degradation of methyl dibenzothiophenes by either biological processes or water washing. The calculated vitrinite reflectance based on MPI is within the range calculated by Rullkötter et al., (1985) for asphalt from the same seep. The difference between the MPI and MDR results noted for this sample suggests that the MPI parameter is particularly useful for samples that have been degraded.

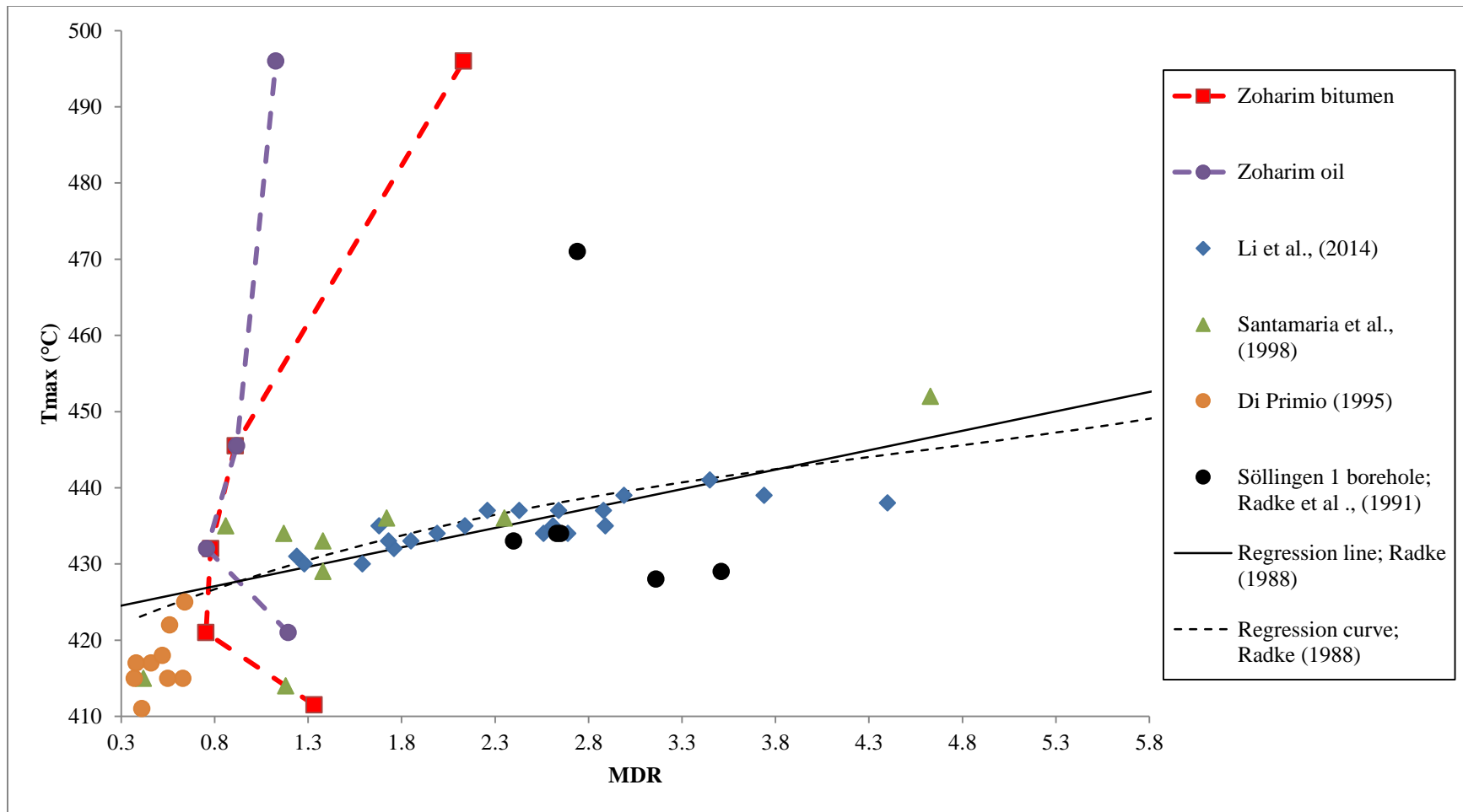


Figure 33. The relation of T_{max} (°C) to MDR of various hydrocarbons. Red squares represent Zoharim bitumen, Purple circles represent Zoharim oil. Solid black line and dashed black curve represent relations of MDR to T_{max} proposed by Radke (1988)

6. Conclusions

The Aderet and Zoharim experiments demonstrated that oil distilled from the sulfur-rich kerogen in Israeli oil shale by means of semi-open anhydrous pyrolysis has exceptionally high sulfur content that declines during maturation. An attempt to describe the decrease of sulfur in the oil by variations in thiophene groups was proven to be ineffective.

The viscosity of the produced oils does not exhibit a distinctive relation to the alkyl-thiophene content as was hypothesized. In fact, the variation of the oil viscosity could not be fully explained by any parameter analyzed in this study. The density of the oil was found to be mainly affected by the *n*-alkanes content because the *n*-alkanes do not contain sulfur atoms. A comparison of the pyrolysis oils to naturally-occurring oils that originated from the same source rock presented similar trends of variation in oil viscosity and density but with a different order of magnitude. The much lower viscosity in the distilled pyrolysis oils is believed to be due to the absence of asphaltenes.

The evolution of sulfur species in the Zoharim oil and bitumen showed some resemblance to other oils that originated from type IIS kerogens by natural genesis or laboratory pyrolysis. Comparison to the Dead Sea basin oils that originated from the same source rock was impossible due to different distribution of sulfur species in the oils.

This observation suggests the different mechanism of petroleum formation between natural and laboratory conditions have a significant effect on the distribution of sulfur species.

Thermal modeling of the experiments by using the EASY% R_O model proved to be a valuable tool that can be used for the prediction of the physical and chemical properties of pyrolysis oils. The correlation of EASY% R_O to Rock-eval T_{max} provides a tool for relating pyrolysis experiments to other studies.

The Zoharim and Aderet experiments support the concept of early maturation in sulfur-rich kerogens of type IIS. The oil window of the type IIS kerogen starts earlier than other kerogens, peaks at a value similar to type II kerogen, and continues expelling oil at high maturities. This conclusion is significant for thermal maturity modeling of basins where petroleum generation is from type IIS kerogens.

An attempt to determine the level of maturity of produced oil and bitumen by molecular means was partially successful. Some of the produced trends were in accordance with other studies yet the rates of isomerization in pyrolysis experiments where the oils are produced by distillation seem to differ from those occurring under natural time-temperature conditions.

The application of molecular parameters for the determination of source rock lithology and environment of deposition has produced poor results and therefore its application for pyrolysis oils should be further investigated.

Future research should aim at performing large scale hydrous-pyrolysis of the Shfela basin oil shale for producing sufficient amounts of oil to analyze their physical properties. This would allow comparison of hydrous-pyrolysis oils to the results of this study and to naturally-occurring oils of the Dead Sea basin and possibly the Golan Heights basin.

7. References

- Abed, A. M., Arouri, K. R., & Boreham, C. J. (2005). Source rock potential of the phosphorite–bituminous chalk-marl sequence in Jordan. *22*, 413-425.
- Aizenshtat, Z., & Amrani, A. (2004). Significance of $\delta^{34}\text{S}$ and evaluation of its imprint on sedimentary organic matter: I. The role of reduced sulfur species in the diagenetic stage: A conceptual review. In R. J. Hill, *Geochemical Investigations in Earth and Space Science: A Tribute to Issac R. Kaplan* (pp. 15-33). Amsterdam: Elsevier.
- Amrani, A., Dror, G., Said-Ahmed, W., Feinstein, S., & Reznik, I. (2014). The distribution and S isotope values of individual organic sulfur compounds during pyrolysis experiments of thermally immature kerogen. *Israel geological society conference 2014*.
- Amrani, A., Lewan, M. D., & Aizenshtat, Z. (2005). Stable sulfur isotope partitioning during simulated petroleum formation as determined by hydrous pyrolysis of Ghareb Limestone, Israel. *Geochimica et Cosmochimica Acta*, *69*(22), 5317–5331.
- Baskin, D. K., & Jones, R. W. (1993). Prediction of oil gravity prior to drill-stem testing in Monterey formation reservoirs, offshore California. *American Association of Petroleum Geologists Bulletin*, *77*, 1479-1487.
- Baskin, D. K., & Peters, K. E. (1992). Early generation characteristics of a sulfur-rich Monterey kerogen. *American Association of Petroleum Geologists Bulletin*, *76*, 1-13.
- Bastow, T. P., van Aarssen, B. G., & Lang, D. (2007). Rapid small-scale separation of saturate, aromatic and polar components in petroleum. *Organic Geochemistry*, *38*, 1235–1250.
- Behar, F., Beaumont, V., & De B. Penteadó, H. (2001). Rock-Eval 6 Technology: Performances and Developments. *Oil & Gas Science and Technology*, *56*(2), 111-134.
- Behl, Richard J.; (1999). Since Bramlette (1946): The Miocene Monterey Formation of California revisited. In E. M. Moors, D. Sloan, & D. L. Stout, *Classic Cordilleran*

- Concepts: A view from California* (pp. 301-313). Boulder, Colorado: Geological Society of America.
- Bein, A., & Sofer, Z. (1987). Origin of Oils in Helez Region, Israel- Implications for Exploration in the Eastern Mediterranean. *AAPG bulletin*, 71(1), 65-75.
- Beydoun, Z. R., Futyan, A. R., & Jawzi, A. H. (1994, April). Jordan Revisited: Hydrocarbons Habitat and Potential. *Journal of Petroleum Geology*, 17(2), 177-194.
- Bou Daher, S., Nader, F. H., Müller, C., & Littke, R. (2015). Geochemical and petrographic characterization of Campanian-Lower Maastrichtian calcareous petroleum source rocks of Hasbayya, South Lebanon. *Marine and Petroleum Geology*(64), 304-323.
- Burg, A., & Gersman, R. (2016). Hydrogeology and geochemistry of low-permeability oil-shales – Case study from HaShfela sub-basin, Israel. *Journal of Hydrology*(540), 1105-1121.
- Burg, A., Bartov, Y., Gersman, R., Dror, Y., & Rosental, A. (2010). *Summary Report of Beit-Guvrin & Aderet survey wells hydro-geological findings*. IEI/1/2010.
- Burnham, A. K., Braun, R. J., Sweeney, J. J., Reynolds, J. G., Vallejos, C., & Talukbar, S. (1992). *Kinetic Modeling of Petroleum Formation in the Maracaibo Basin*. Oklahoma: U.S. Department of Energy.
- Chakhmakhchev, A., & Suzuki, N. (1995a). Saturate biomarkers and aromatic sulfur compounds in oils and condensates from different source rock lithologies of Kazakhstan, Japan and Russia. *Organic Geochemistry*, 24(4), 289-299.
- Chakhmakhchev, A., Suzuki, M., & Takayama, K. (1997). Distribution of alkylated dibenzothiophenes in petroleum as a tool for maturity assessments. *Organic Geochemistry*, 26(7), 483-490.
- Connan, J., & Nissenbaum, A. (2004). The organic geochemistry of the Hasbeya asphalt (Lebanon): comparison with asphalts from the Dead Sea area and Iraq. *Organic Geochemistry*(35), 775-789.
- di Primio, R. (1995). *The generation and migration of sulphur-rich petroleums in a low-maturity carbonate source rock sequence from Italy*. Institute of Petroleum and Organic Geochemistry (ICG-4). Julich: University of Cologne.

- Eglinton, T. I., Sinninghe Damste, J. S., Kohnen, M. E., De Leeuw, J. W., Larter, S. R., & Patience, R. L. (1990). Analysis of Maturity-Related Changes in the Organic Sulfur Composition of Kergoens by Flash Pyrolysis-Gas Chromatography. In W. L. Orr, C. M. White, & J. M. Comstock (Ed.), *Geochemistry of Sulfur in Fossil Fuels* (pp. 529-565). Washington: American Chemical Society.
- Gardosh, M. A., & Tannenbaum, E. (2014). The Petroleum Systems of Israel. In L. Marlow, C. Kendall, & L. Yose, *Petroleum Systems of the Tethyan Region: AAPG memoir 106* (pp. 179-216). A: AAPG.
- Gersman, R., Bartov, Y., & Rozenthal, A. (2012). *Summary Report of Zoharim survey well hydro-geological findings*. IEI/3/2012.
- Heller- Kallai, L., Esterson, G., Aizenshtat, Z., & Pismen, M. (1984). Mineral reactions and pyrolysis of Israeli oil shale. *Journal of Analytical and Applied Pyrolysis*, 6, 375-389.
- Huang, H., & Pearson, M. J. (1999). Source rock palaeoenvironments and controls on the distribution of dibenzothiophenes in lacustrine crude oils, Bohai Bay Basin, eastern China. *Organic Geochemistry*, 30, 1455-1470.
- Hughes, W. B., Holba, A. G., & Dzou, L. I. (1995). The ratios of dibenzothiophene to phenanthrene and pristane to phytane as indicators of depositional environment and lithology of petroleum source rocks. *Geochimica et Cosmochimica Acta*, 59(17), 3581-3598.
- Koopmans, M. P., Carson, F. C., Sinninghe Damste, J. S., & Lewan, M. D. (1998). Biomarker generation from Type II-S kerogens in claystone and limestone during hydrous and anhydrous pyrolysis. *Organic Geochemistry*, 29(5-7), 1395-1402.
- Koopmans, M. P., Rijpstra, W. C., De Leeuw, J. W., Lewan, M. D., & Sinninghe Damste, J. S. (1998). Artificial maturation of an immature sulfur- and organic matter-rich limestone from the Ghareb Formation, Jordan. *Organic Geochemistry*, 28(7-8), 503-521.
- Lafargue, E., Marquis, F., & Pillot, D. (1998). Rock-Eval 6 Applications in Hydrocarbon Exploration, Production, and Soil Contamination Studies. *Oil & Gas Science and Technology*, 53(4), 421-437.

- Lewan, M. D., & Henry, A. A. (1999). *Gas:Oil Ratios for Source Rocks Containing Type-I, -II, -IIS, and -III Kerogens as Determined by Hydrous Pyrolysis*. U.S. Geological Survey,.
- Li, M., Wang, T.-G., Shi, S., Liu, K., & Ellis, G. S. (2014a). Benzo[b]naphthothiophenes and alkyl dibenzothiophenes: Molecular tracers for oil migration distances. *Marine and Petroleum Geology*, *57*, 403-417.
- Li, M., Wang, T.-G., Shi, S., Zhu, L., & Fang, R. (2014b). Oil maturity assessment using maturity indicators based on methylated dibenzothiophenes. *Petroleum Science*, *11*, 234-246.
- Luning, S., & Kuss, J. (2014). Petroleum Geology of Jordan. In L. Marlow, C. Kendall, & L. Yose, *Petroleum systems of the Tethyan region* (pp. 217-239). AAPG Memoir 106.
- Luo, P., & Gu, Y. (2007, May). Effects of asphaltene content on the heavy oil viscosity at different temperatures. *Fuel*, *86*(7-8), 1069-1078.
- Meilijson, A., Ashkenzai-Polivoda, S., Rob-Yankovich, L., Illner, P., Alsenz, H., Speijer, R. P., et al. (2014). Chronostratigraphy of the Upper Cretaceous high productivity sequence of the southern Tethys, Israel. *Cretaceous Research*(50), 187-213.
- Minster, T. (2009). *Oil Shale Deposits in Israel*. Jerusalem: Geological Survey of Israel.
- Minster, T., Nathan, Y., & Raveh, A. (1992). Carbon and sulfur relationships in marine Senonian organic-rich, iron-poor sediments from Israel — A case study. *Chemical Geology*, *97*, 145-161.
- National Institute for Petroleum and Energy Research*. (1995). (Crude Oil Analysis Database: Department of Energy) Retrieved 10 2015, from <http://www.netl.doe.gov/research/oil-and-gas/software/databases>
- Nissenbaum, A., & Aizenshtat, Z. (1975). Geochemical Studies on Ozokerite from the Dead Sea Area. *Chemical Geology*, *16*, 121-127.
- Nissenbaum, A., & Goldberg, M. (1980). Asphalts, heavy oils, ozocerite and gases in the Dead Sea Basin. *Organic Geochemistry*, *2*, 167-180.
- Orr, W. L. (1986). Kerogen/asphaltene/sulfur relationships in sulfur-rich Monterey oils. *Organic Geochemistry*, *10*, 499-516.

- Orr, W. L. (2001). Evaluating kerogen sulfur content from crude oil properties: cooperative Monterey organic geochemistry study. In C. M. Isaacs, & J. Rullkötter, *The Monterey Formation: From rocks to molecules* (pp. 348-367). New York: Columbia University Press.
- Peters, K. E., & Cassa, M. R. (1994). Applied Source Rock Geochemistry. In L. B. Magoon, & W. G. Dow, *The Petroleum System- From source to Trap* (pp. 93-120). Tulsa: The American Association of Petroleum Geologists.
- Peters, K. E., Walters, C. C., & Moldowan, J. M. (2005). *The Biomarker Guide* (Vol. 1). Cambridge, UK: Cambridge Univ. Press.
- Price, L. C. (1980). Crude Oil Degradation and an Explanation of the Depth Rule. *Chemical Geology*, 28, 1-30.
- Radke, M., Welte, D. H., & Willsch, H. (1991). Distribution of alkylated aromatic hydrocarbons and dibenzothiophenes in rocks of the Upper Rhine Graben. *Chemical Geology*, 93, 325-341.
- Radke, M. (1988, August). Application of aromatic compounds as maturity indicators in source rocks and crude oils. *Marine and Petroleum Geology*, 5, 224-236.
- Radke, M., & Willsch, H. (1994). Extractable alkyl-dibenzothiophenes in Posidonia Shale (Toarcian) source rocks: Relationship of yields to petroleum formation and expulsion. *Geochimica et Cosmochimica Acta*, 58(23), 5223-5244.
- Rullkötter, J., Spiro, B., & Nissenbaum, A. (1985). Biological marker characteristics of oils and asphalts from carbonate source rocks in a rapidly subsiding graben, Dead Sea, Israel. *Geochimica et Cosmochimica Acta*, 49, 1357-1370.
- Ryan, R. C., Fowler, T. D., Beer, G. L., & Nair, V. (2010). Shell's In Situ Conversion Process—From Laboratory to Field Pilots. In O. e. Oguniola, *In Oil Shale: A Solution to the Liquid Fuel Dilemma* (pp. 161-183). Washington, DC: ACS Symposium Series; American Chemical Society.
- Santamaria-Orozco, D., Horsfield, B., Di Priomio, R., & Welte, D. H. (1998). Influence of maturity on distributions of benzo- and dibenzothiophenes in Tithonian source rocks and crude oils, Sonda de Campeche, Mexico. *Organic Geochemistry*, 28(7-8), 423-439.

- Schneider-Mor, A., Alsenz, H., Ashckenazi-Polivoda, S., Illner, P., Abramovich, S., Feinstein, S., et al. (2012). Paleooceanographic reconstruction of the late Cretaceous oil shale of the Negev, Israel: Integration of geochemical, and stable isotope records of the organic matter. *Palaeogeography, Palaeoclimatology, Palaeoecology*, 319-320, 46-57.
- Shirav, M., & Ginzburg, D. (1983). Geochemistry of Israeli Oil Shales. In A. C. Society, *Geochemistry and Chemistry of Oil Shales* (pp. 85-97). ACS.
- Sinninghe Damste, J. S., & de Leeuw, J. W. (1990). Analysis, structure and geochemical significance of organically-bound sulphur in the geosphere: State of the art and future research. *Organic Geochemistry*, 16(4-6), 1077-1101.
- Spiro, B., Dinur, D., & Aizenshtat, Z. (1983a). Evaluation of source, environments of deposition and diagenesis of some israeli "oil shales" — N-Alkanes, fatty acids, tetrapyrroles and kerogen. *Chemical Geology*, 39, 189-214.
- Spiro, B., Welte, D. H., Rullkotter, J., & Schaefer, R. G. (1983b). Asphalts, Oils and Bituminous Rocks from the Dead Sea Area- A Geochemical Correlation Study. *The American Association of Petroleum Geologists Bulletin*, 67(7), 1163-1175.
- Sweeney, J. J., & Burnham, K. A. (1990, October). Evaluation of a Simple Model of Vitrinite Reflectance Based on Chemical Kinetics. *American Association of Petroleum Geologists Bulletin*, 74(10), 1559-1570.
- Tannenbaum, E., & Aizenshtat, Z. (1985). Formation of immature asphalt from organic-rich carbonate rock- I. Geochemical correlation. *Organic Geochemistry*, 8(2), 181-192.
- Tannenbaum, E. (1983). *Researches in the Geochemistry of Oils and Asphalts in the Dead Sea Area*. Jerusalem: The Hebrew University Jerusalem.
- Tannenbaum, E., & Aizenshtat, Z. (1984). Formation of immature asphalt from organic-rich carbonate rocks—II. Correlation of maturation indicators. *Organic Geochemistry*, 6, 503-511.
- Tippee, B. (2001). Worldwide Look at Reserves and Production. In B. Tippee, *International Petroleum Encyclopedia* (pp. 296-324). PennWell Corporation.
- Tissot, B. P., & Welte, D. H. (1984). *Petroleum Formation and Occurrence* (2nd ed.). Berlin: Springer- Verlag.

- Tomić, J., Behar, F., Vandenbroucke, M., & Tang, Y. (1995). Artificial maturation of Monterey kerogen (Type II-S) in a closed system and comparison with Type II kerogen: implications on the fate of sulfur. *Organic Geochemistry*, 23(7), 647–660.
- Waldo, G. S., Carlson, R. M., Moldowan, M. J., Peters, K. E., & Penner-Hahn, J. E. (1991). Sulfur speciation in heavy petroleums: Information from X-ray absorption near edge structure. *Geochimica et Cosmochimica Acta*, 55, 801-814.
- Waples, D. (1981). Time and Temperature as Factors in Oil Generation. In D. Waples, & J. Goodrich (Ed.), *Organic Geochemistry for Exploration Geologists* (pp. 95-104). Minneapolis, Minnesota: Burgess Publishing Company.
- Winter, Y. E. (1988). *Geochemical aspects for the Hor Hahar phosphate field*. Ben Gurion University of the Negev, Geological department. Beer Sheva: Ben Gurion University of the Negev.
- Yoffe, O., Wohlfarth, A., Nathan, Y., Cohen, S., & Minster, T. (2007). Oil shale fueled FBC power plant – Ash deposits and fouling problems. *Fuel*, 86, 2714–2727.
- Zerah Oil and Gas Exploration LP. (2006). *Periodic Report*. Company periodic report, Tel Aviv.
- Zumberge, J. E. (1984). Source Rock of the La Luna formation (Upper Cretaceous) in the Middle Magdalena Valley, Colombia. In J. G. Palacas, *Petroleum Geochemistry and Source Rock Potential of Carbonate Rocks* (pp. 127-135). Tulsa: American Association of Petroleum Geologists.

8. Appendix

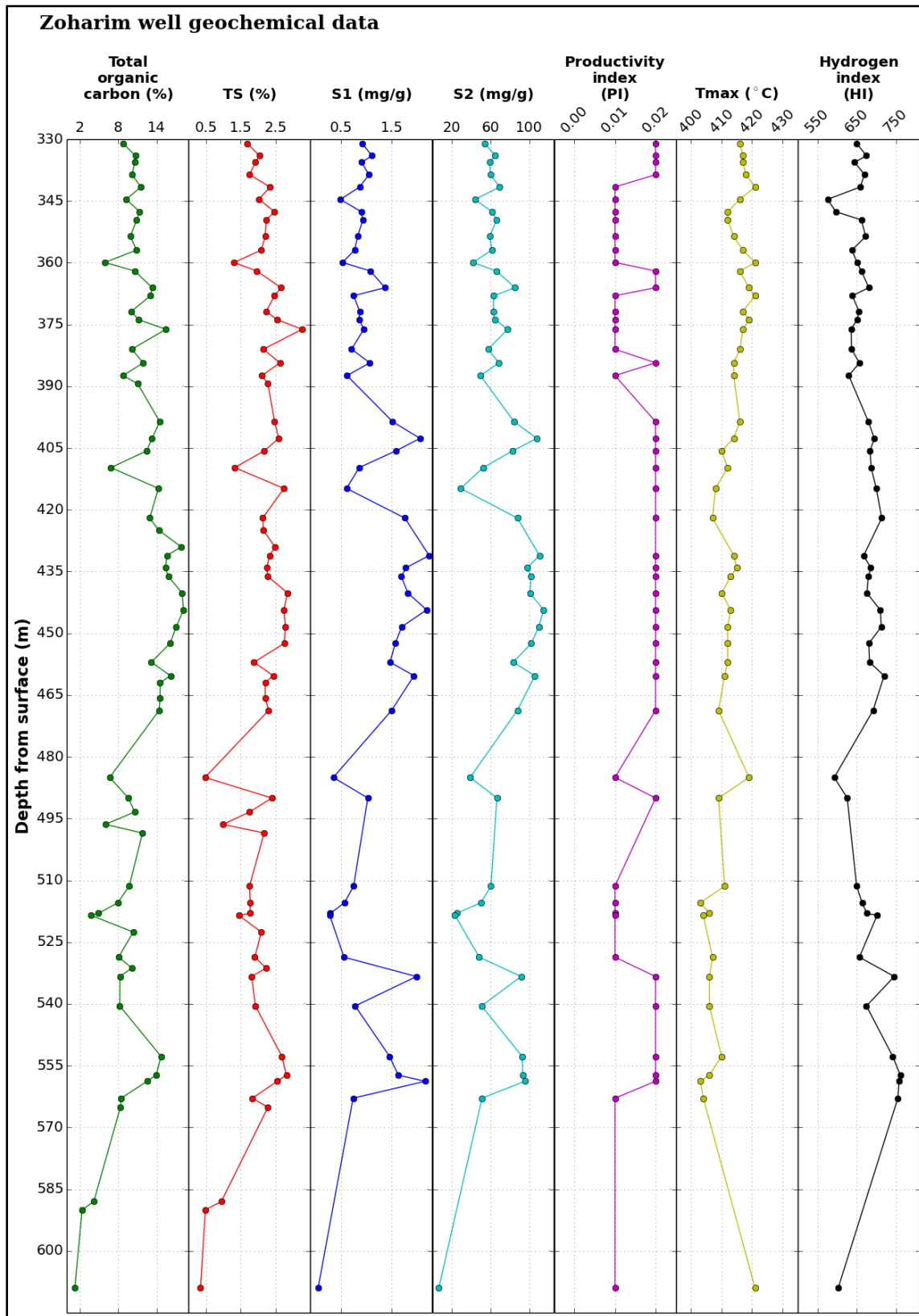
Appendix I- Well sections for Aderet and Zoharim boreholes

| Group | Formation | Depth (m) | Lithological Description |
|--------------------|--------------------------------|---|--|
| Avedat group | Tzora formation, Adulam member | 14 m | Brown soil with fragments of white chalk |
| | | 50 | Alternating chalk, yellow marl, white limestone, chert and siliceous limestone Presence of pyrite, manganese and limonite |
| Mount Scopus group | Taqiye formation | 140 m | |
| | | 200 | Grey plastic clay, marl, chalk horizons. Rich with pyrite. Slight bituminous smell. |
| | | 300 | |
| | Ghareb formation | 313 m | |
| | | 350 | Hard, black- brown bituminous chalk with marl and clay horizons Presence of fossil fragments and phosphate at the base |
| | | 450 | |
| Mishash formation | 515 m | | |
| | 550 | Hard, black- brown bituminous chalk with marl and clay horizons Presence of fossil fragments and phosphate | |
| | 600 | Alternating chert and siliceous chalk: 556 m – 561.7 m Hard, grey, calcareous, siliceous bituminous chalk | |
| Menuha fm. | 627 m | Light grey, hard bituminous chalk | |
| | 631 | Light grey, hard chalk Slight bituminous smell | |

Appendix 1.1 - Lithological well log for Zoharim wellbore. After Gersman et al., 2012.

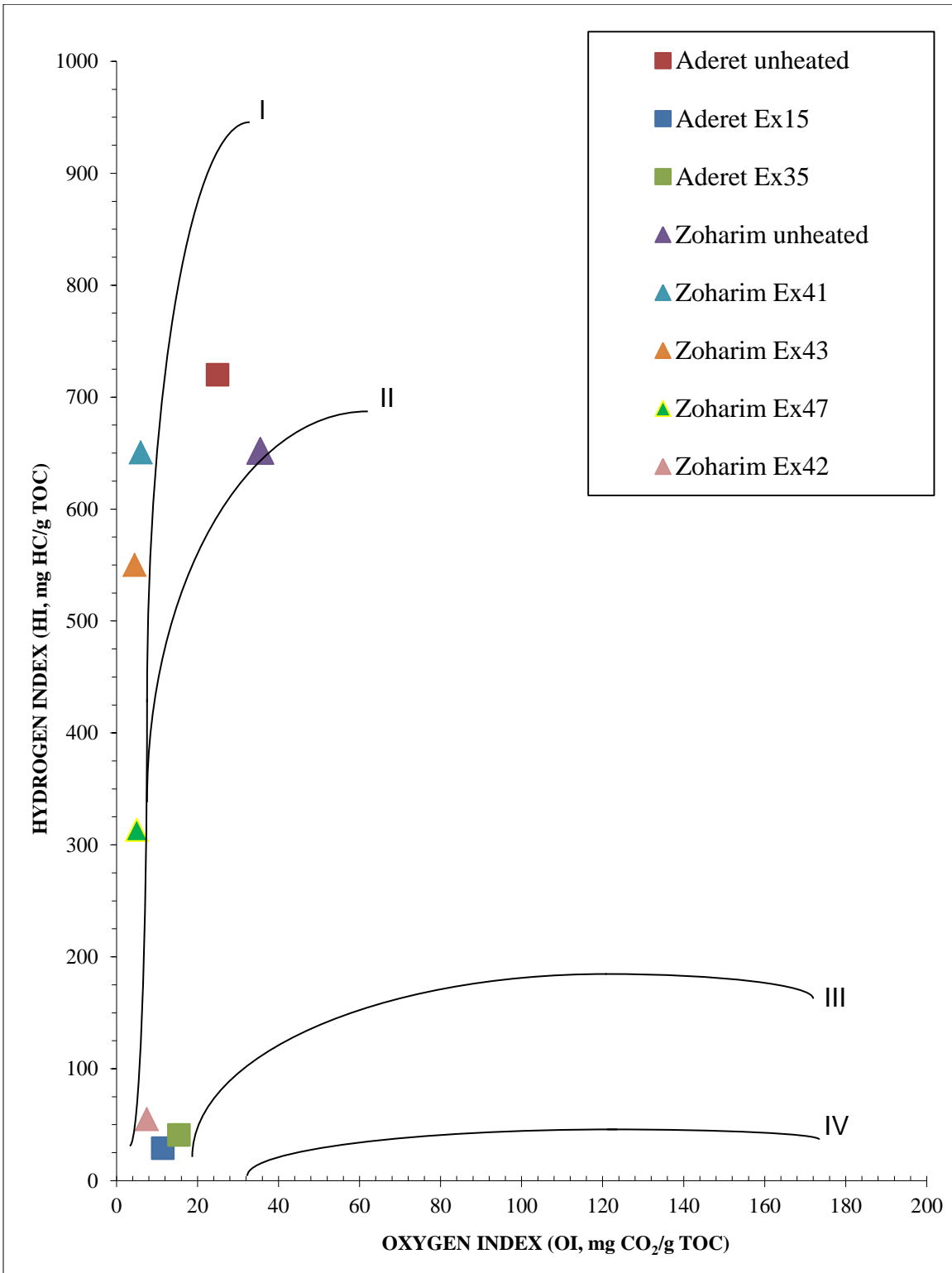
| Group | Formation | Depth (m) | Lithological Description | Paleontological Age (Depth of analyzed sample) |
|--------------------|--|---|---|--|
| Avedat group | Adulam formation | | 8.5 m White chalk and red soil | |
| Mount Scopus group | Taqiye formation | 50 | Alternating white chalk, yellow limestone, grey marl, some chert, limonite stains and dotting of iron oxide. | Upper Paleocene-Lower Eocene P6-a (51 m) |
| | | 100 | Grey plastic marl with alternations of grey chalk. Layer of limestone at 75.5-77m that contains chert chips. Appearance of pyrite through the section. | Upper Paleocene-Lower Eocene P6 (72 m) |
| | | 150 | Alternation chalk, marl and grey limestone. Appearance of few chert chips. | Middle Paleocene P2-3 (198 m) |
| | | 200 | Grey, plastic marl and marly clay. Alternations with few layers of grey chalk (mostly at the top of the section). Appearance of pyrite through the section. Weak bituminous smell at the clay. | |
| | Ghareb formation | 250 | Alternations of brown bituminous chalk, grey marly chalk and grey mal. | Middle to Upper Maastrichtian (252 m) |
| | | 300 | Massive brown-black bituminous chalk, partially coarse bedded, abundance of large fossils, no fractures, some phosphate. From 342m- areas with appearance of thin marl layers within the bituminous chalk. Fractures with skid marks and secondary calcite at 367.6-368.0 m. Additional fractures at 387m and 392.7m. Fine bedding at 447-458m. | |
| | | 400 | | Non diagnost (400,416,420 m) |
| | | 450 | | Maastrichtian (430 m) |
| | Mishash formation | 460 m | | Non diagnost (451,460 m) |
| | | 500 | Bituminous chalk with alternating thin marl horizons. | Campanian (480 m) |
| 529.8 m | | Massive, very dark bituminous chalk. Abundance of fossils. Phosphate at the base. | | |
| 550 | Alternating chert, bituminous chalk and phosphate. | Lower Campanian (585,590 m) | | |
| 600 | Massive, brown-grey, bituminous chalk. Phosphate and large fossils present at the top. Amount of organic matter declines with depth. | | | |

Appendix 1.2 - Lithological well log for Aderet wellbore. After Burg et al., 2010.



Appendix 1.3 - Geochemical well log for Zoharim borehole.

Appendix II- Pseudo-Van-Krevelen plot



Appendix 2.1 - Pseudo-Van-Krevelen plot. Squares represent Aderet rock samples.

Triangles represent Zoharim rock samples.

Appendix III- Selected GC-MS chromatograms

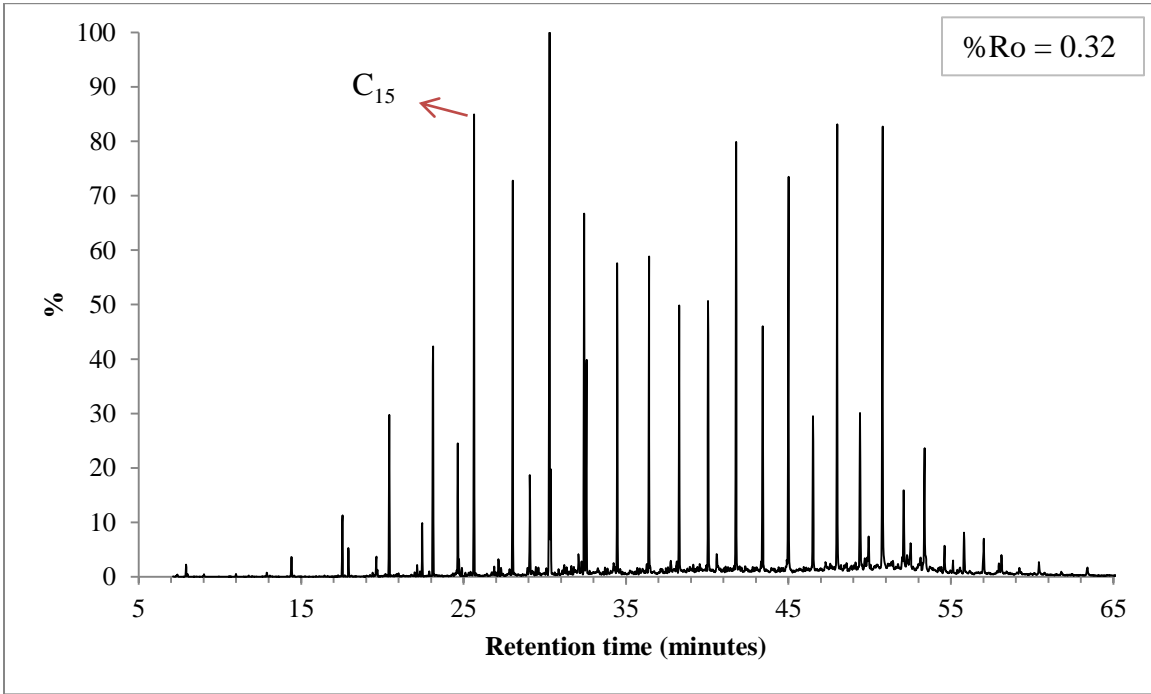


Figure 34. Chromatogram of the n-alkanes ($m/z=57.10$) in the unheated sample (%Ro equ. = 0.32)

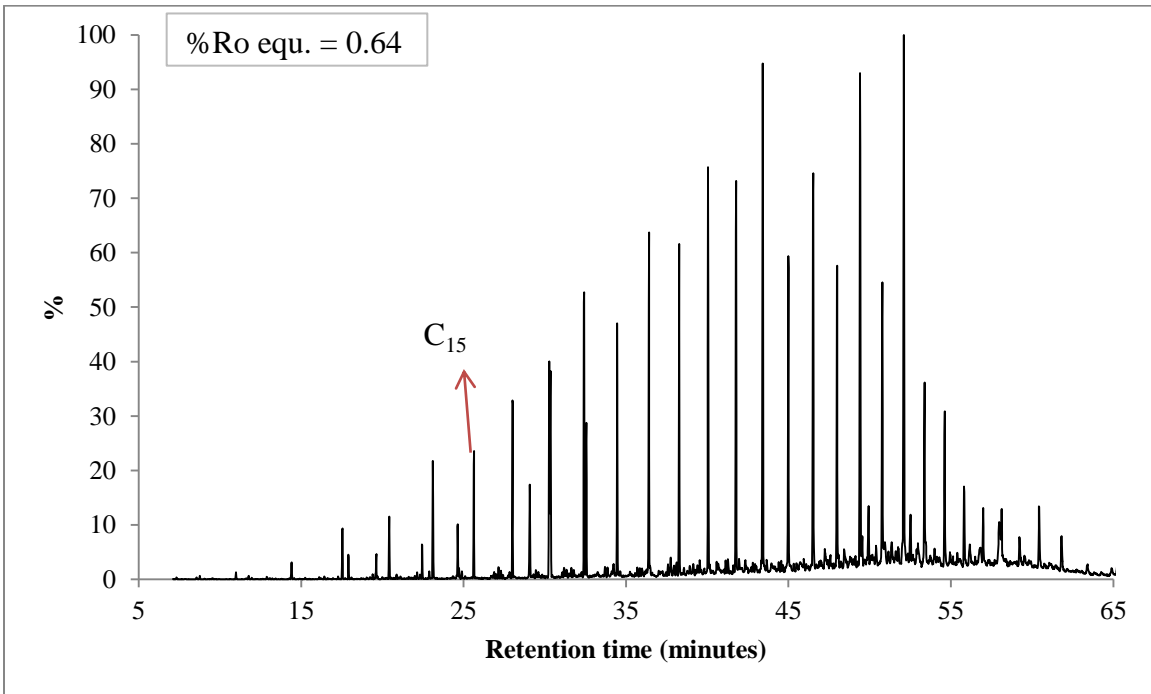


Figure 35. Chromatogram of the n-alkanes ($m/z=57.10$) in the Ex41 bitumen (%Ro equ. = 0.64)

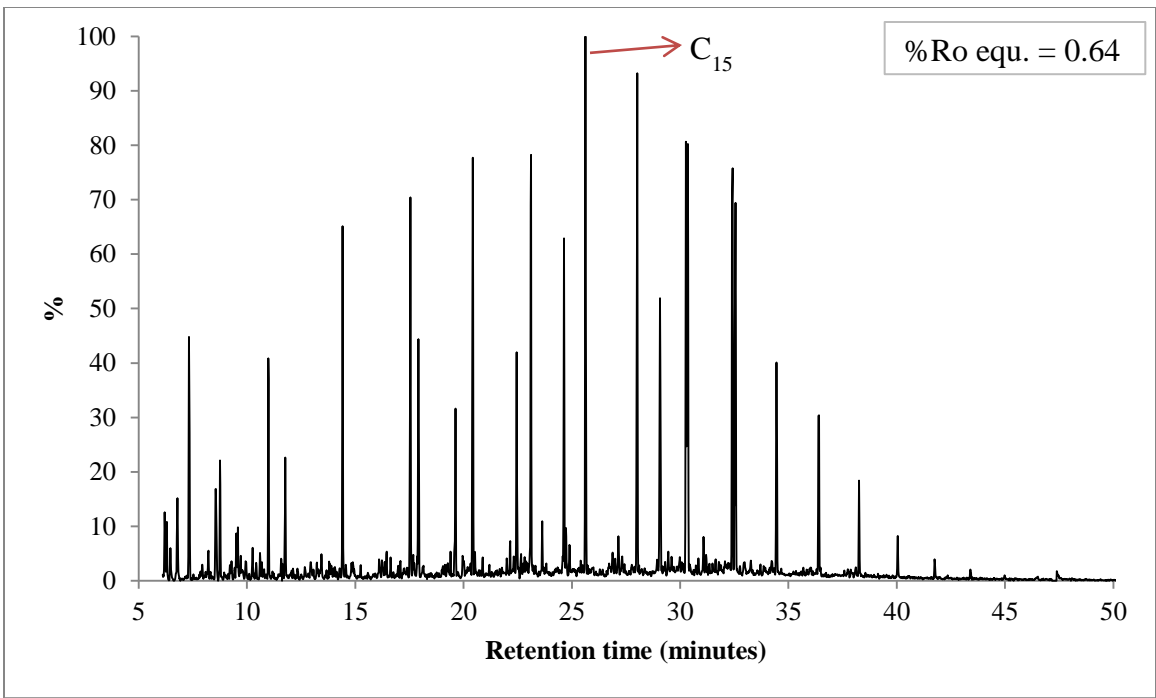


Figure 36. Chromatogram of the n-alkanes ($m/z=57.10$) in the Ex41 oil (%Ro equ. = 0.64)

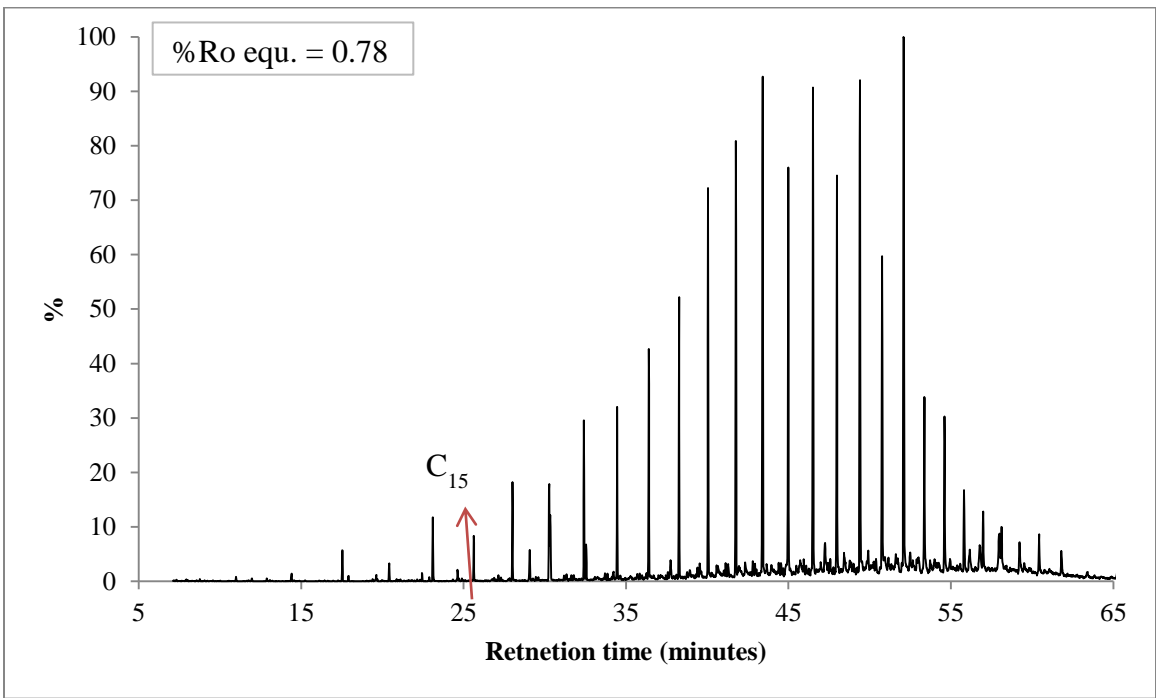


Figure 37. Chromatogram of the n-alkanes ($m/z=57.10$) in the Ex43 bitumen (%Ro equ. = 0.78)

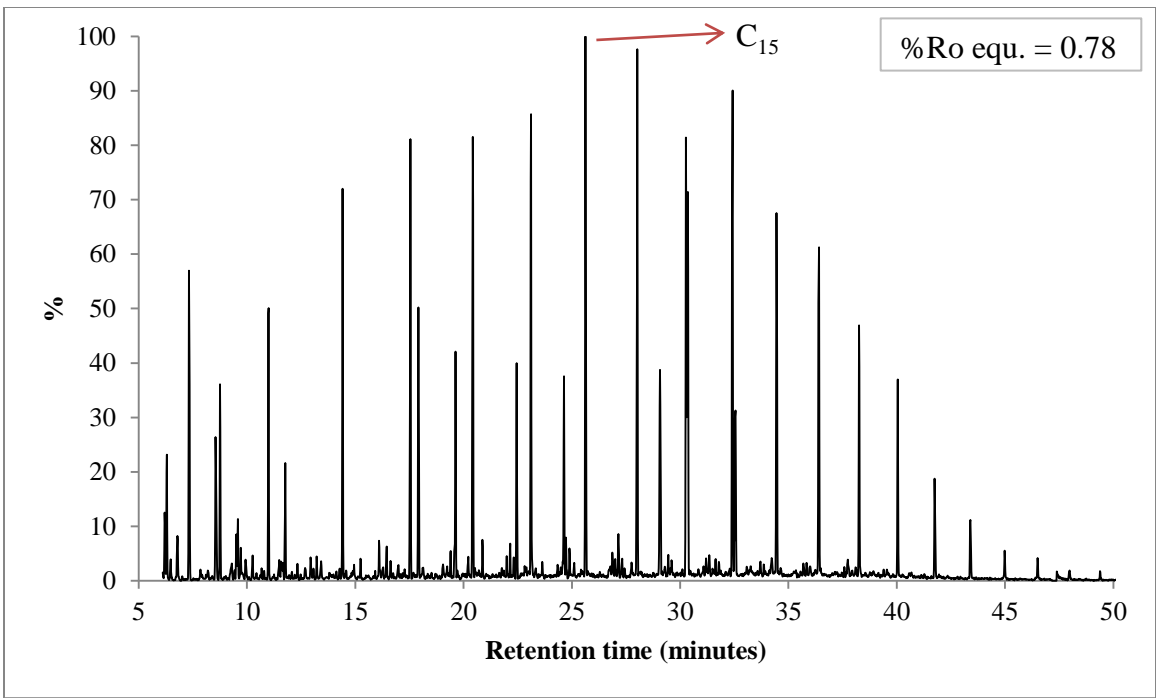


Figure 38. Chromatogram of the n-alkanes ($m/z=57.10$) in the Ex43 oil (%Ro equ. = 0.78)

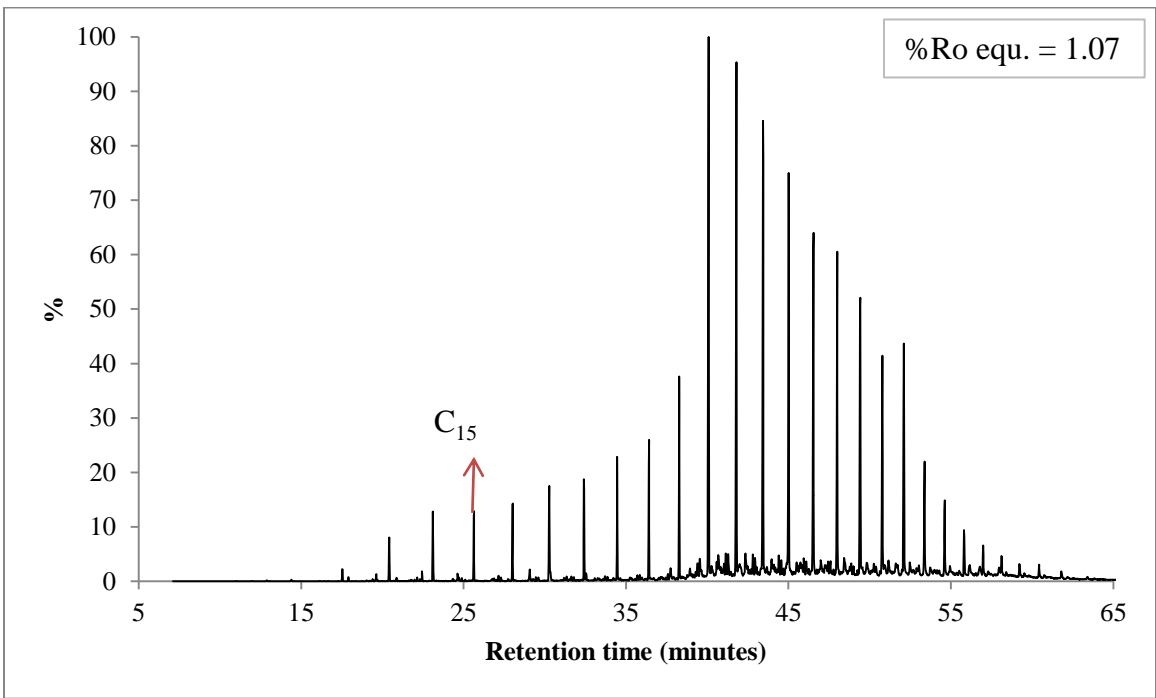


Figure 39. Chromatogram of the n-alkanes ($m/z=57.10$) in the Ex47 bitumen (%Ro equ. = 1.07)

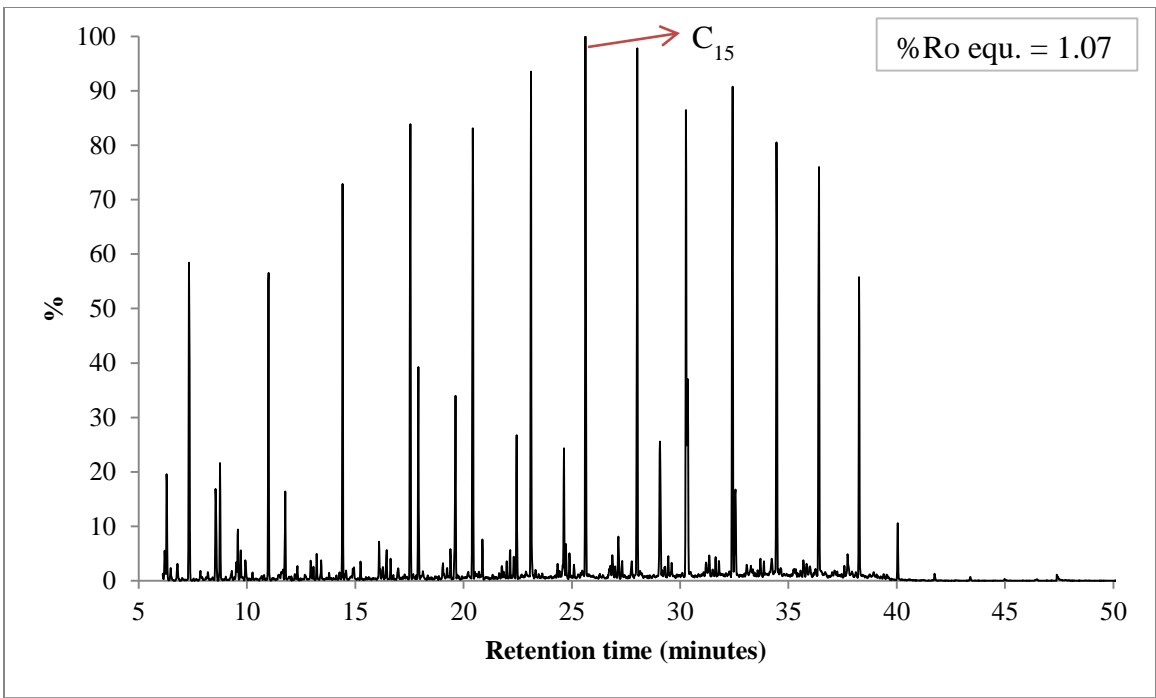


Figure 40. Chromatogram of the n-alkanes ($m/z=57.10$) in the Ex47 oil (%Ro equ. = 1.07)

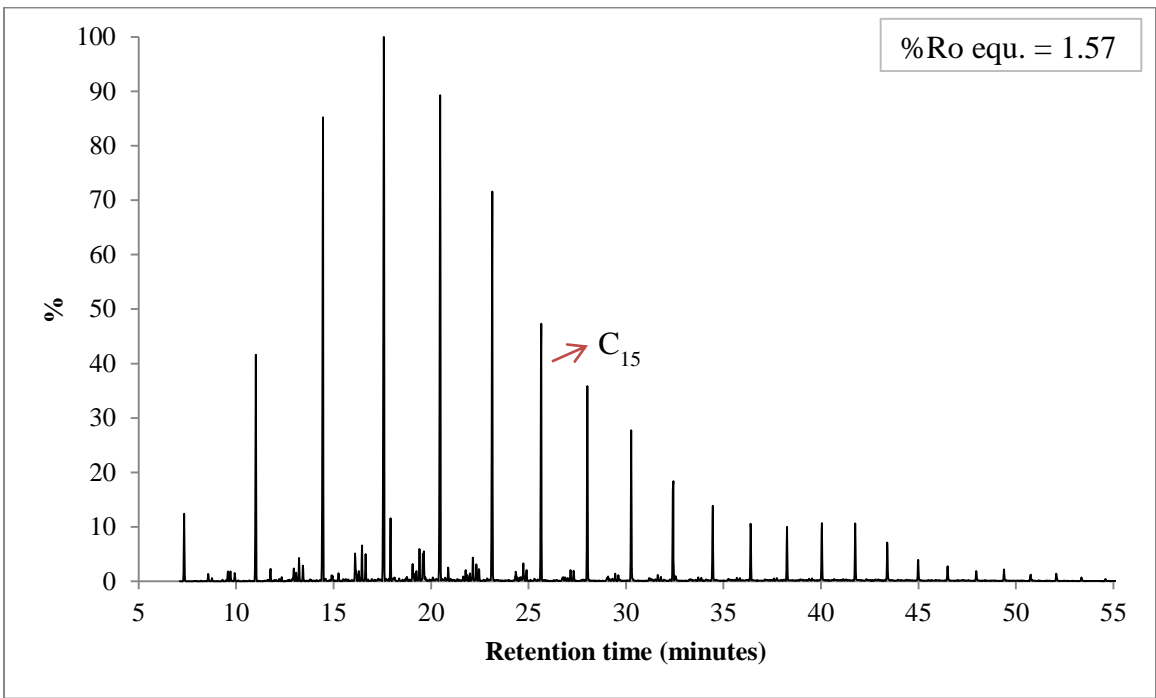


Figure 41. Chromatogram of the n-alkanes ($m/z=57.10$) in the Ex42 bitumen (%Ro equ. = 1.57)

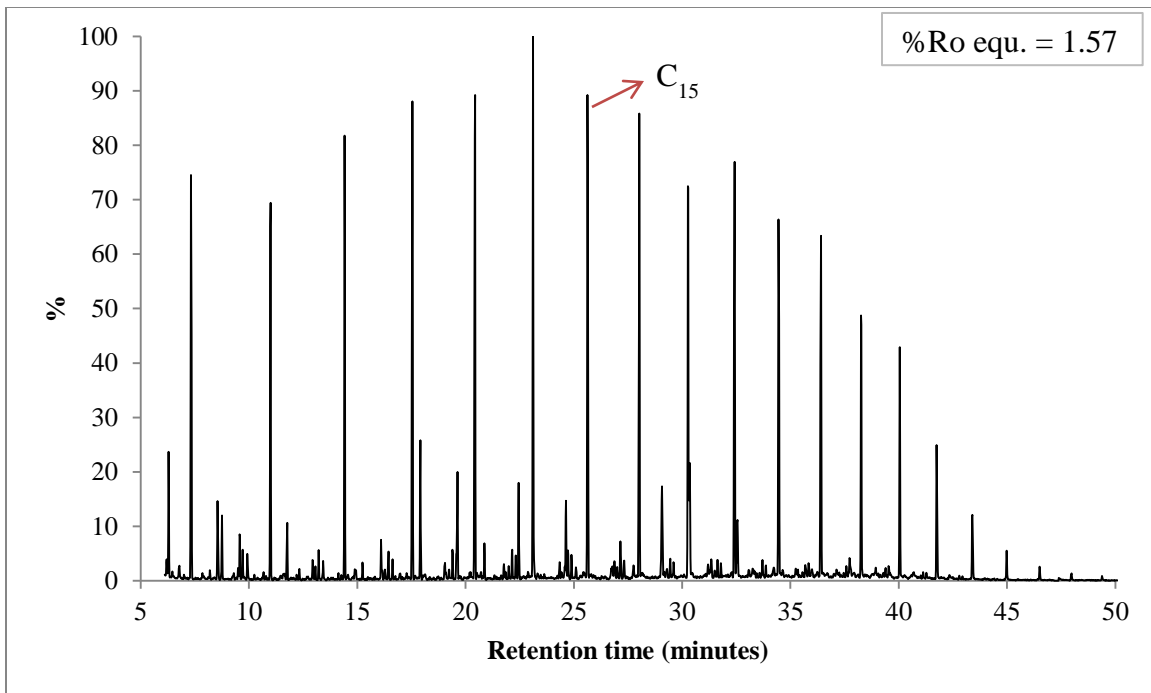


Figure 42. Chromatogram of the n-alkanes ($m/z=57.10$) in the Ex42 oil (%Ro equ. = 1.57)

Appendix IV- Density and Sulfur content of Dead Sea basin and Coastal Plain oils

| Sample name | Sulfur Wt. % | Source of data | API gravity | Source of data |
|---------------------------|--------------|--|-------------|--|
| Emunah 1 | 2.2 | This study | 31.4 | This study |
| Zuk Tamrur 3 | 3.75 | | 21.5 | |
| Gurim 4 | 4.4 | | 17 | Tepee (2001) |
| Zuk Tamrur 1 | 3.0 | | 27 | Tannenbaum (1983) |
| Lot-1 | 4.7 | 9 | | |
| Massada-1 | 2.6 | 33 | | |
| Zohar-8 | 3.7 | 19 | | |
| Gurim 3 | 4.2 | (Zerah Oil and Gas Exploration LP, 2006) | 15 | Nissenbaum and Goldberg (1980) |
| Zuk Tamrur 3 (DST sample) | 3.5 | | 22.8 | (Zerah Oil and Gas Exploration LP, 2006) |
| Heletz A | 1.45 | (National Institute for Petroleum and Energy Research, 1995) | 31.7 | (National Institute for Petroleum and Energy Research, 1995) |
| Heletz K | 1.72 | | 30 | |
| Heletz 32 (Dolomite) | 1.66 | | 28.4 | |
| Kokhav (Dolomite) | 1.87 | | 25 | |
| Kokhav (Sand Helez W) | 1.91 | | 28.7 | |
| Kokhav (Sand Kokhav B) | 1.69 | | 28.9 | |
| Heletz-Kokhav | 1.45 | | 31.5 | |
| Heletz-Kokhav | 1.62 | | 27.3 | |
| Heletz-Kokhav | 1.85 | | 27.3 | |

Appendix V- Density results for Aderet oils

| Sample name | %Ro equivalent | Density at 40°C | Density at 15.5°C | API gravity (°) |
|-------------|----------------|-----------------|-------------------|-----------------|
| Ex15 L5 | 0.74 | 0.896 | 0.918 | 22.4 |
| Ex15 L6 | 0.86 | 0.858 | 0.884 | 28.4 |
| Ex15 L7 | 1.13 | 0.839 | 0.858 | 33.3 |
| Ex15 L8 | 1.30 | 0.808 | 0.838 | 37.1 |
| Ex35 L5 | 0.58 | 0.930 | 0.959 | 16.0 |
| Ex35 L6 | 0.65 | 0.926 | 0.939 | 19.0 |
| Ex35 L7 | 0.72 | 0.909 | 0.933 | 19.9 |
| Ex35 L8 | 0.79 | 0.909 | 0.920 | 22.2 |
| Ex35 L9 | 0.87 | 0.884 | 0.908 | 24.1 |
| Ex35 L10 | 0.99 | 0.881 | 0.894 | 26.6 |
| Ex35 L11 | 1.16 | 0.865 | 0.891 | 27.2 |
| Ex35 L12 | 1.29 | 0.889 | 0.906 | 24.5 |

Appendix VI- Spreadsheet version of the EASY%Ro model (After Sweeney and Burnham, 1990)

| Stage | Time (days) | Time (seconds) | Temperature (°C) | Temperature (°K) | Heating rate (°C/Sec) | Total conversion sum | Ro% | log(Ro%) |
|-------------|-------------|----------------|------------------|------------------|-----------------------|----------------------|------|----------|
| Start | 0 | 0 | 25 | 298.15 | | 0 | 0.20 | -0.69 |
| Pre-heating | 1 | 86400 | 200 | 473.15 | 0.002025463 | 0.058857462 | 0.25 | -0.60 |
| L3 | 26.75 | 2311200 | 251.5 | 524.65 | 2.31481E-05 | 0.254715955 | 0.52 | -0.29 |
| L4 | 33.5 | 2894400 | 265 | 538.15 | 2.31481E-05 | 0.276006966 | 0.56 | -0.25 |
| L5 | 49.5 | 4276800 | 297 | 570.15 | 2.31481E-05 | 0.35093484 | 0.74 | -0.13 |
| L6 | 60.25 | 5205600 | 318.5 | 591.65 | 2.31481E-05 | 0.392572924 | 0.86 | -0.06 |
| L7 | 73.25 | 6328800 | 344.5 | 617.65 | 2.31481E-05 | 0.465863185 | 1.13 | 0.05 |
| L8 | 81.5 | 7041600 | 361 | 634.15 | 2.31481E-05 | 0.502894857 | 1.30 | 0.11 |
| L9 | 100.5 | 8683200 | 399 | 672.15 | 2.31481E-05 | 0.612954047 | 1.95 | 0.29 |

- The values presented in this spreadsheet are for a maturity modeling of Aderet Ex15 oils.
- Stage, time and temperature columns are filled in according to the experimental conditions. The calculation of other columns is as described below (equations 1-11):

$$1) \text{ Heating rate } \left(\frac{^{\circ}\text{C}}{\text{Sec}} \right) = \frac{(\text{Temperature at step}_{i+1}) - (\text{Temperature at Step}_i)}{(\text{Time at step}_{i+1}) - (\text{Time at Step}_i)}$$

$$2) \text{ Total conversion sum (TCS)} = \sum_{i=a}^v \text{column}_a$$

$$3) R_o \% = e^{(-1.6 + 3.7 \cdot TCS)}$$

| | | |
|--|-------------|--|
| Pre-exponential factor (A) (constant) | 1.00E+13 | sec ⁻¹ |
| R (kcal/K*mol) (constant) | 0.001987204 | kcal K ⁻¹ mol ⁻¹ |

| | a | b | c | d | E | Columns f- u | v |
|------------------------------------|------------|-------------|------------|-------------|-------------|--------------|----------------|
| Weights (constants) | 0.03 | 0.03 | 0.04 | 0.04 | 0.05 | | 0.01 |
| E(kcal/mol) (constants) | 34 | 36 | 38 | 40 | 42 | | 72 |
| E/R | 17109.4655 | 18115.90465 | 19122.3438 | 20128.78295 | 21135.22209 | | 36231. 8093 |

| | |
|---------------------------------|----------|
| a₁ (constant) | 2.334733 |
| a₂ (constant) | 0.250621 |
| b₁ (constant) | 3.330657 |
| b₂ (constant) | 1.681534 |

$$4) \frac{E}{R} = \frac{E_i \left(\frac{\text{Kcal}}{\text{mol}} \right)}{R \left(\frac{\text{Kcal}}{\text{K} \cdot \text{mol}} \right)}$$

| E_a/RT_j | E_b/RT_j | Columns E_c/RT_j to E_i/RT_j | E_u/RT_j | E_v/RT_j |
|-------------|-------------|-------------------------------------|-------------|-------------|
| 57.38542849 | 60.76104193 | | 118.1464704 | 121.5220839 |
| 36.16076404 | 38.28786781 | | 74.44863184 | 76.57573561 |
| 32.6111989 | 34.52950472 | | 67.14070363 | 69.05900944 |
| 31.79311624 | 33.66329955 | | 65.45641579 | 67.3265991 |
| 30.00870912 | 31.7739273 | | 61.78263642 | 63.54785461 |
| 28.91822108 | 30.61929291 | | 59.537514 | 61.23858583 |
| 27.70090748 | 29.33037263 | | 57.03128011 | 58.66074525 |
| 26.98015533 | 28.56722329 | | 55.54737863 | 57.13444659 |
| 25.45483226 | 26.95217534 | | 52.4070076 | 53.90435067 |

$$5) \frac{E_i}{RT_j} = \frac{E_i \left(\frac{Kcal}{mol} \right)}{R \left(\frac{Kcal}{^\circ K \cdot mol} \right) \cdot \text{Temperature at stage } i \text{ (} ^\circ K \text{)}}$$

| I_{aj} | I_{bj} | Columns I_{cj} to I_{dj} | I_{uj} | I_{vj} |
|-------------|-------------|------------------------------|-------------|-------------|
| 5.99394E-12 | 1.93926E-13 | | 1.21061E-38 | 4.0267E-40 |
| 0.024474435 | 0.002762291 | | 2.87016E-19 | 3.32796E-20 |
| 1.041677962 | 0.144906172 | | 5.25155E-16 | 7.50359E-17 |
| 2.480251406 | 0.362058539 | | 2.97529E-15 | 4.46087E-16 |
| 16.5280941 | 2.680174412 | | 1.31368E-13 | 2.18768E-14 |
| 52.84802575 | 9.138502693 | | 1.33416E-12 | 2.36904E-13 |
| 194.0554784 | 36.05186218 | | 1.78004E-11 | 3.39553E-12 |
| 419.883289 | 81.39154068 | | 8.26822E-11 | 1.64556E-11 |
| 2160.113189 | 458.1170803 | | 2.14272E-09 | 4.66505E-10 |

$$6) I_{ij} = \left(\text{Temperature at stage } i \text{ (}^\circ\text{K)} \right) \cdot A \left(\frac{1}{\text{sec}} \right) \cdot e^{\left(-\frac{E_i}{RT_j} \right) \cdot \left(1 - \frac{\left(\frac{E_i}{RT_j} \right)^2 + a_1 \cdot \left(\frac{E_i}{RT_j} \right) + a_2}{\left(\frac{E_i}{RT_j} \right)^2 + b_1 \cdot \left(\frac{E_i}{RT_j} \right) + b_2} \right)}$$

| Δ_{aj} | Δ_{bj} | Columns Δ_{cj} to Δ_{ij} | Δ_{uj} | Δ_{vj} |
|---------------|---------------|--|---------------|---------------|
| 0 | 0 | | 0 | 0 |
| 12.08337796 | 1.363782297 | | 1.41704E-16 | 1.64306E-17 |
| 43943.19241 | 6140.615693 | | 2.26743E-11 | 3.24011E-12 |
| 62146.37278 | 9380.982234 | | 1.05846E-10 | 1.60294E-11 |
| 606866.8045 | 100142.6057 | | 5.54657E-09 | 9.25807E-10 |
| 1569021.047 | 278999.7817 | | 5.19605E-08 | 9.28918E-09 |
| 6100161.956 | 1162657.13 | | 7.1134E-07 | 1.36453E-07 |
| 9755761.415 | 1958674.111 | | 2.8029E-06 | 5.64195E-07 |
| 75177931.66 | 16274543.31 | | 8.89937E-05 | 1.94421E-05 |

$$7) \Delta_{ij} = \frac{(I_{ij \text{ of stage } i+1} - I_{ij \text{ of stage } i})}{\text{Heating rate at stage } i+1}$$

| ω_a/ω_{0a} | ω_b/ω_{0b} | Columns ω_c/ω_{0c} to ω_t/ω_{0t} | ω_u/ω_{0u} | ω_v/ω_{0v} |
|------------------------|------------------------|---|------------------------|------------------------|
| 0 | 0 | | 0 | 0 |
| 1 | 0.7443 | | 0 | 0 |
| 1 | 1 | | 2.26743E-11 | 3.24007E-12 |
| 1 | 1 | | 1.05846E-10 | 1.60294E-11 |
| 1 | 1 | | 5.54657E-09 | 9.25807E-10 |
| 1 | 1 | | 5.19605E-08 | 9.28918E-09 |
| 1 | 1 | | 7.11339E-07 | 1.36453E-07 |
| 1 | 1 | | 2.80289E-06 | 5.64194E-07 |
| 1 | 1 | | 8.89897E-05 | 1.94419E-05 |

$$8) \frac{\omega_i}{\omega_{0i}} = 1 - e^{(-\Delta_{ij})}$$

| AA | BB | Columns CC to TT | UU | VV |
|-----------|-----------|---------------------|-------------|-------------|
| 0 | 0 | | 0 | 0 |
| 0.03 | 0.02 | | 2.22045E-18 | 0 |
| 0.03 | 0.03 | | 4.53486E-13 | 3.24007E-14 |
| 0.03 | 0.03 | | 2.11692E-12 | 1.60294E-13 |
| 0.03 | 0.03 | | 1.10931E-10 | 9.25807E-12 |
| 0.03 | 0.03 | | 1.03921E-09 | 9.28918E-11 |
| 0.03 | 0.03 | | 1.42268E-08 | 1.36453E-09 |
| 0.03 | 0.03 | | 5.60579E-08 | 5.64194E-09 |
| 0.03 | 0.03 | | 1.77979E-06 | 1.94419E-07 |

9) *If $\Delta_{ij} < 10^{-20}$ then column II = 0*

10) *If $\Delta_{ij} > 220$ then column II = weight(constant)i*

11) *if $10^{-20} < \Delta_{ij} < 220$ then column II = $1 - e^{-\Delta_{ij}}$*

תקציר

פרויקט זה הוקדש לחקר תכונות הנפט הראשוני המופק מחדך פצלי השמן של תצורת רארב. במסגרת הפרויקט נדגמו פצלי שמן מקידוחי "אדרת" ו "זוהרים" באגן השפלה. דוגמאות הסלע חוממו במערכת פירוליזה פתוחה למחצה תוך איסוף הנפט המתקבל בתהליך. בנוסף נבחנו 5 דוגמאות של פחמימנים ממקור טבעי מאיזור ים המלח שמקורם הוא בפצלי השמן של תצורת רארב. בעבור נפטים שהתקבלו בפירוליזה נבדקו הפרמטרים הבאים: צמיגות, צפיפות, תכולת גפרית, תכולת אלקיל-טיופנים, תכולת בנזוטיופנים ותכולת אלקאנים רוויים ישרי שרשרת. סלעים שאריתיים מתהליך הפירוליזה נבדקו בRockEval כדי לקבוע את דרגת המטורציה שלהם, נבדקה תכולת הגפרית של הסלעים ובנוסף מוצא מתוך דוגמאות הסלע כלל הביטומן על ידי סוקסלט. דוגמאות הפחמימנים הטבעיים מים המלח ודוגמאות הביטומן שמוצא מהסלע השאריתי נבדקו לתכולת גפרית ואז הופרדו לפרקציות הרכב עיקרית אשר מתוכן הפרקציות הרוויה והארומטית נבדקו בגז כרומטוגרף עם גלאי ספקטרומטר מסה כדי לקבוע את תכולת אלקיל-טיופנים, תכולת בנזוטיופנים, תכולת דיבנזוטיופנים, תכולת אלקאנים רוויים ישרי שרשרת ואת תפוצת הביומרקרים בדוגמאות. נמצא שנפטים שהתקבלו בפירוליזה הם בעלי תכולת גפרית גבוהה מאוד (עד 19% משקלי) בדוגמאות מדרגות המטורציה הנמוכות. לא נמצא קשר מובהק בין צמיגות הנפט לבין תכולת האלקיל-טיופנים שלהם. נמצא התאמה טובה בין צפיפות דוגמאות הנפט לבין תכולת האלקאנים ישרי השרשרת בנפט. ניסיון להשוות בין נפטים המתקבלים בפירוליזה לבין דוגמאות נפט ממקור טבעי שפצלי השמן של תצורת רארב הם סלע המקור שלהם הראה דימיון מסויים בעיקר בתכונות הפיזיקליות של הנפט. השוואה של יחסי הביומרקרים בין שני קבוצות הנפט (תוצר פירוליזה וטבעי) הראתה פיזור גדול של התוצאות בקביעת דרגת המטורציה וסביבת ההשקעה של סלע המקור. תצפיות אלה מצביעות על הבדלים משמעותיים בין שני קבוצות נפט שנוצרו מאותו סלע מקור. יתכן כי מקור ההבדלים נובע בהבדל בין גרדיאנט חימום פצלי השמן במעבדה אל מול גרדיאנט החימום בתנאים טבעיים.

בוצעה קורולציה בין מודל הבגרות הטרמלית $EASY\%R_o$ לבין פרמטר T_{max} שנמדד על דוגמאות הסלע השאריתי, הקורולציה מאפשרת השוואה של תוצאות הניסויים בעבודה הנוכחית לעבודות בספרות. בחינה של שינוי דרגת המטורציה לאורך ניסויי הפירוליזה הציגה בצורה מובהקת תחילת התבגרות מוקדמת של החומר האורגני, תצפית זו נמצאה בהתאמה טובה עם תצפיות מעבודות קודמות.

אוניברסיטת בן - גוריון בנגב
הפקולטה למדעי הטבע
המחלקה למדעי הגיאולוגיה והסביבה

חיבור זה מהווה חלק מהדרישות לקבלת התואר "מוסמך למדעי הטבע" (M.Sc.)

חקר הנפט הראשוני המופק מפצלי השמן
הישראליים

מאת : איליה קוטוזוב
בהנחיית : דוקטור אלכסי קמישני
פרופסור הרולד ויניגר
דוקטור אלון עמרני

תאריך 6/9/2017

תאריך 03.09.2017

תאריך 03/09/2017

תאריך 6/9/2017


תאריך 28.08.2017

חתימת הסטודנט : 

חתימת המנחה : 

חתימת המנחה : 

חתימת המנחה : 

חתימת יו"ר הועדה המחלקתית : 

אוניברסיטת בן - גוריון בנגב
הפקולטה למדעי הטבע
המחלקה למדעי הגיאולוגיה והסביבה

חקר הנפט הראשוני המופק מפצלי השמן הישראליים

חיבור זה מהווה חלק מהדרישות לקבלת התואר "מוסמך למדעי הטבע" (M.Sc.)

מאת: איליה קוטוזוב

<ספטמבר, 2017>

<אב, תשע"ז>